UNIVERSIDAD DE LA FRONTERA

Facultad de Ingeniería y Ciencias
Programa Doctorado y Magíster en Recursos Naturales

PROJECTING THE IMPACT OF CLIMATE CHANGE ON CENTRAL SOUTHERN CHILE: A CASE STUDY FOR ARAUCANIA REGION ON WINTER WHEAT

TESIS PARA OPTAR AL GRADO DE DOCTOR
EN CIENCIAS DE RECURSOS NATURALES

RAÚL ORREGO VERDUGO

TEMUCO-CHILE
2014

PROJECTING THE IMPACT OF CLIMATE CHANGE ON CENTRAL SOUTHERN CHILE: A CASE STUDY FOR ARAUCANIA REGION ON WINTER WHEAT

Esta tesis fue realizada bajo la supervisión del Director de Tesis, Dr. ÁNDRES AVILA BARRERA, Departamento de Ingeniería Matemática, Universidad de La Frontera y ha sido aprobada por los miembros de la comisión examinadora

RAÚL ORREGO VERDUGO

Dr. ÁNDRES ÁVILA BARRERA

DIRECTOR PROGRAMA DE POSTGRADO EN CIENCIAS DE RECURSOS NATURALES

Dr. FRANCISCO MATUS

Dr. FRANCISCO MEZA

Dr. RODRIGO ABARCA DEL RÍO

DIRECCIÓN DE POSTGRADO UNIVERSIDAD DE LA FRONTERA

Dr. LUIS MORALES SALINAS

Dr. MIREN ALBERDI

“You can't build a peaceful world on empty stomachs”
Norman Borlaug

“No habrá paz en el mundo mientras haya estómagos vacíos ”
Norman Borlaug

Agradecimientos/Ackowledgements

No es sencillo resumir en unas breves líneas todos los momentos preciosos, consejos, palabras de aliento, vivencias, y en definitiva todo aquello que ha hecho este andar un proceso de un enorme crecimiento académico y personal. Son muchas las personas que me han acompañado en este largo y fructífero camino que ha sido la realización de este doctorado, y cada una de ellas, a su manera, me ha hecho crecer y aprender. De hecho, no soy el mismo. Me lo dijo una vez mi tutor, uno no puede pasar por un doctorado y ser la misma persona, y es cierto, se crece y madura mucho, y lo más importante, se pierde el miedo a ese crecimiento. En este sentido agradezco a todos los que me han acompañado en este camino, aventura y peregrinación: A mi familia global, tanto a mi familia consanguínea como a la que me adoptó acá en Temuco, a mis amigos y a mis profesores. A todos ellos, ¡gracias por todo lo vivido! Also, my grateful thanks to Dr. Huade Guan and the Ground Water Group (Flinders University) for all good moments and friendship.

Pese a que son muchas las personas a las que agradezco, En esta dedicatoria quisiera destacar algunos en particular.

En primer lugar quisiera agradecer al Dr. Luis Morales Salinas, la persona con la que entré al mundo de la ciencia, y quien ya se ha ido convirtiendo en un gran amigo. El es el responsable de que haya estudiado el doctorado, y es la persona que me entregó las primeras armas para blandirme en el terreno que me estoy desarrollando. En términos metafóricos, él es de quien aprendí el oficio. O si se quiere, el arte.

En segundo lugar a mi tutor, al Dr. Andrés Ávila Barrera, la persona de quien he aprendido el significado de un proceso doctoral, y con quien he compartido más de alguna significativa conversación en este, y otros temas. Agradezco de él también su paciencia y ayuda en mi aprendizaje del inglés. También a quien comenzó siendo mi tutor, el Dr Franciasco Matus Baeza, quien tuvo la valentía de acompañarme con un tema distinto a lo que se hace en el Programa, y me enseñó muchos de los valores que son propios de un doctor. En términos de la metáfora que acá construyo, de ellos aprendí la profesión.

En tercer lugar agradecer al Dr. Rodrigo Abarca del Río, la persona que me apoyó en la última parte de mi investigación. Con el pude concretar la tesis, además de ser mi interlocutor en lo respecto a la temática que desarrollo. Continuando con la metáfora, de él aprendí el trabajo.

También agradezco a las personas que me colaboraron con la revisión y chequeo del inglés del texto. De esta manera, my gratefoul to María Eugenia Osses and to Carolina Armijo.

Finalmente, debo agradecer el financiamiento otorgado en primera instancia por la dirección de postgrado de la Universidad de la Frontera a través de su beca de Mantención para doctorado, y a la beca CONICYT para doctorados nacionales, que me financió los últimos dos años del Doctorado. También a la beca de Término de Tesis también de la dirección de postgrado de la Universidad de la Frontera, que financió parte de la pasantía realizada en la Universidad de Flinders. Agradezco también al proyecto FONDEF DO6I 1100 "Sistema de Soporte de Decisiones Para Cultivos Tradicionales Basados en Integración SIG y Estaciones Meteorológicas", que permitió la obtención de los datos para la validación del modelo de cultivos, y al programa de Doctorado en Ciencias de los Recursos Naturales, que financió mi mantención durante la pasantía realizada en la Universidad de Flinders.

Summary

It is expected that climate change will modify crop yield with important consequences on food security in the next 100 years. An important step for mitigating these impacts is to project crop responses under the expected climate change conditions. This can be conducted by using climate models that simulate the future atmospheric status, based on greenhouse gas concentrations. These simulations have been summarized by the International Panel of Climate Change (IPCC), providing climate projections considering several scenarios for crop modeling. T his projected climate databases have been used as input in crop models to project yield responses under climate change conditions.

Climate and crop models show important uncertainties that need to be addressed to achieve reliable projections. One of their main limitations is the difference between large scale climate model outputs (~300 km), and the climate input required by crop simulation models (< 1 km). Downscaling techniques have been developed for solving this problem. This technique has been used for generating mesoscale climate datasets (~ 25-50 km) commonly used in climate change and crop response researches. However, there are few studies evaluating the scale effect on the crop model reliability. In fact, optimal climate grid cell size (*i.e.* the maximal pixel representing the spatial crop variability) is an unsolved problem.

A dynamical downscaling (PRECIS, Providing Regional Climates for Impact Studies) from an Atmospheric and Oceanic Global Climate Model (HadCM3), Departamento de Geofísica, Universidad de Chile (DGF) computed a mesoscale (25 km) database for A2 (850 ppm of CO_2 eq and 3°C forth year 2100), B2 (621 ppm of CO_2 eq, and 1°C for the year 2100) and baseline (1961-1991) from IPCC scenarios along all the Chilean continental territory. This database (hereafter DGF-PRECIS) was created for developing climate change public policies. Although it is an important progress for mitigating climate change impact, it has not been compared with *insitu* data.

In this thesis, we performed high resolution simulations (1 km) for winter wheat (*Triticum aestivum* L) in Araucanía region (37°- 40° S and 71°-74° W) under the most severe IPCC A2 scenario. To achieve this, we first validate DGF-PRECIS by comparing the baseline projection (1961-1991) with *insitu* data (56 metrorological stations) and latter DGF-PRECIS database was corrected and downscaled. CERES-DSSAT model was used with downscaled dataset for projecting the crop response. Additionally, we propose an optimal climate grid cell size based on downscaling and crop simulation, where complex and flat topography zones were studied.

In Chapter 1, we give a General Introduction where the problem is addressed. In Chapter 2 we show a theoretical framework of the current knowledge of climate change impact by crop simulation models using climate models as input data (hereafter climate-crop-models, CCM). The broad implication of our findings is that theoretical downscaling

techniques can be proposed for correcting differences of scales between CCM and high resolution crop models (< 1 km grid).

In Chapter 3, we compare the baseline DGF-PRECIS rainfall projection with in situ rainfall records (56 meteorological stations) located in Araucanía region to correct and validate the climate projection (A2 and B2 scenarios) at 25 km grid. Since one of the main climate drivers in Chile is ENSO, we also asses these effects comparing DGF-PRECIS database with the time span where the phenomenon occurs. The result shows that DGF-PRECIS underestimates the precipitation rate during the La Niña and El Niño phases. In the the neutral phase of ENSO, it presents a more extreme cycle (dryer summer and rainier winter). Based on these results, we corrected DGF-PRECIS with empirical coefficients for southern regions. To understand this error, we compare the DGF-PRECIS database with whole continental Chilean territory rainfall. However, there is an important lack of historical records (1961-1991) to perform this validation. To increase the rainfall density data distribution on the Chilean continental territory, a global mesoescale rainfall database, (50 km) was obtained from Global Precipitation Climate Centre (GPCC). GPCC was validated by comparing *in-situ* meteorological records (12,240) spread all over the continental Chilean territory. As the difference between GPCC and in situ data was < 10 %, we concluded that the GPCC database can be used to validate the DGF-PRECIS database in all continental Chilean territory. DGF-PRECIS database reproduced well the rainfall pattern from central to southern Regions (56-30º S) under neutral conditions of ENSO influence. However, in the northern regions (17°-30°S), DGF-PRECIS database showed unacceptable errors (>30%). This was explained based on climatic pattern influenced by stationary Pacific Anticyclone in northern Chile.

In Chapter 4, the corrected DFG-PRECIS database was downscaled to obtain a high resolution rainfall grid (1 km) using a topography model (Precipitation Characterization with Auto-Searched Orographic and Atmospheric, PCASOA). The downscaling was performed over the Araucanía Region and allowed the analysis of climate pattern that cannot be observed using mesoscale climate model. In general, our results indicated an increase of the orographic effect (*i.e.* rainfall shade) and delay in the dry season in the northern region.

In Chapter 5 we show the winter wheat crop projection for A2 scenario (between year 2070 and 2100) and yield response. We computed high resolution downscaled dataset (CERES crop model, DSSAT). The result indicated a high spatial and temporal variability. The projected crop yield increased in 52.5% over the base line (1961-1991). According to simulation results, sowing time is modify, May instead of April in wet zones and March instead of April on dry zones.

In Chapter 6, we performed a spatial analysis to evaluate the impact of high resolution downscaling climate on crop yield simulation response. We propose an optimal climate grid cells size using semivarograms technique including topographic effects. The optimal climate grid cell size in complexity topography zones (hilly side, low mountain ranges) was < 7 km and > 25 km in flat intermediate depression and costal zones.

Finally, a general discussion and concluding remarks is presented in Chapter 7. Our main conclusion suggests the corrected DGF-PRECIS database is an important input of climate information for adapting new public policies for future scenarios. Downscaling based on topographic techniques improved the climate projection compared with *insitu* data. Our projected crop response showed important differences at complex topography zone compared with flat agricultural land. It seems possible to use semivariograms techniques for determining the optimal climate grid cells resolution for crop modeling porpuses.

Several challenges persist for achieving climate change adaptation. Further research is needed to understand climate cycles, such as ENSO and Antarctic Oscillation, genetic plant adaptation and soil-plant-climate interactions. The tools developed in this thesis may contribute to frame new scenario projections, particularly for southern Chile.

Índice / Contents

Chapter 1
General Introduction

1. General Introduction

Climate is one of the main concerns in agriculture (Hansen *et al*., 2006; Betts, 2005). Several climate-crop problems such as drought and frost, extemporaneous rains, and extreme events are more frequent (Beniston *et al*., 2007). All these phenomena are associated to high probability with the global climate change (IPCC, 2007; 2013). Although there is a controversy about the importance of greenhouse effect on the current climate change, global warming is a phenomenon well supported by scientific evidences (IPCC 2001; 2007; 2013). Climate change will modify crop yield responses implying important consequences on food security (Porter y Semenov, 2005; Rosenzweig and Parry, 1994; Thomson *et al*., 2005). Also, climate change will increase frequency of extreme event, decrease water supply, and increase pest and plant diseases (IPCC, 2001; 2007).

To mitigate agriculture damage produced by climate change (or even benefit from the new climate condition) the first step is climate projection through climate models. Climate projection helps to design management practices such as: selecting climate-fitted plants, choosing the best date and location for planting, and implementing safe agricultural mitigation measurements. However, climate models have several biases, for example climate forecast. For this reason the term "climate projection" instead of "climate forecast" is used in this thesis (IPCC, 2007; Räisänen, 2007).

Climate models are based on physical laws, such as: energy, momentum and mass (water) conservation, Navier-Stokes flow laws, and hydrostatical equations, among others. These models use partial differential equations solved by numerical methods (Zorita, 2000; Gutierrez y Pond, 2006), which are called Atmospheric and Oceanic Global Climate Models (AOGCM) to simulate the oceanic and atmosphere dynamics at global scale (*i.e.* the whole Earth). They are originally used for forecasting short-term meteorological conditions (Räisänen, 2007). However, through some simplifications, they are adapted for long-term climate simulations. These are: discretization of spatial values in low resolution "boxcells" (about 200-300 km of surface grid size), using of idealized years (*i.e,* 12 month of 30 days), parameterization schemes for sub-grid process simulation (Räisänen, 2007), and linked with nested models for simulating dynamical processes, which are "constant" under short-term simulation, such as atmosphere CO_2 concentration, land-use, and ice cover (IPCC 2007).

Climate models are the base of crop yield projections. Therefore, the first step is to develop a reliable climate projection, which should be validated using *in-situ* data. Since future data are not available, we cannot directly validate them. On the other hand, climate models generate low resolution grid dataset, and climate records are punctual observations, which do not always represent the entire cell. For solving these problems, indirect validation methods have been developed, which are based on several models (ensemble) (Christensen *et al.,* 2007) and/or the comparison between climate projection with current or past values (hindcast) (Beniston *et al.,* 2007).

For assessing the climate change impacts, we require to understand the current climate patterns and identify their main drivers and source of variability. For Chile, one of the main climate drivers is El Niño-South Oscillation (ENSO) phenomenon (Kiladis and Val Loon, 1988; Guevara-Díaz, 2008). ENSO involves two components: El Niño current, and the southern oscillation. El Niño is a warm current which move from the North Australia to central Chile when the easterly Alisios winds are weakened. Southern oscillation is a temporal pattern of pressure differences measured in Darwin (Australia, 12º 27' S, 130º 50'W) and Papetee (Tahiti, 17º 32' S, 140º 34'W). Both phenomena affect the Pacific Anticyclone, the main barrier to the fronts, which produce the rain in southern and central Chile (Montecinos and Aceituno, 2003). Therefore, for projecting the climate change impacts, we should describe the current spatial and temporal climate patterns, and including ENSO variation could be an interesting way. This description is used for giving a geophysical base of observed changes. Since, ENSO is not explicit computed in climate models (Vidale *et al.*, 2003), it is expected that ENSO impact on climate variability projection, but not in the mean of the projection. This has not been evaluated. These analyses should consider both synoptic (*i.e.* country) and local (*i.e.* specific work domain for example, the Araucanía Region-Chile) view points.

The use of climate models output used as input in crop model is a very common strategy for assessing crop performance under climate change conditions (Tan and Shibasaky, 2003; White *et al*., 2011; Soussana *et al*., 2010). This approach presents several advantages with respect to other approximations such as: Ricardian Analysis, projection based on historical time series, or *in-situ* experimental approaches. Climate-crop simulations are precise and relatively easy to adapt to new scenarios and to changes on the conceptual framework. The crop simulation models are used by several researches in relation to the climate change. Thus, several studies use Decision Support System for Agro Technology Transfer (DSSAT) crop models (*e.g.* Orrego *et al*., 2014; Meza *et al*., 2008; Long *et al*., 2006; Jones and Thornton, 2003), EPIC model (Erosion Productivity Impact Calculator) (Prya and Shibasaki, 2001), and other specific models (Semenov, 2007) for assessing the climate change on crop systems. The simulations are mainly performed in cereals, such as Wheat (*Triticum aestivum* L.) (Orrego *et al*., 2014; Semenov, 2007; Tomsom *et al*., 2005) and Maize (*Zea mays* L) (Meza *et al*., 2008; Jones and Thornton, 2003). Besides, studies in Soybean (*Glycine max* [L.] Merr) has been performed (Grimm and Natori, 2006; Tan and Shibasaki, 2003). Most of these studies show the detrimental effects for adapting the crop system to new conditions.

One of the main problems for using the climate model outputs as input for crop modeling is that both, climate and crop models, are at different spatial scales (Baron *et al*., 2005; Mearns *et al*., 2003). Most crop models are designed for performing simulations without spatial dimensions or for small areas when they are linked with the Geographical Information System (GIS). In both cases, climate inputs are local. On the other hand, AOGCM outputs are about 300 km grids, which are inadequate for crop modeling. In fact, there are important differences between global and local climate projections affecting crop modeling. Mearns *et al*. (2003) reported a decrease of about 25% in winter rains from models with 400 km to 50 km in the South Great Lake States (USA), which was translated into changes about 30 % in crop yield. Similar differences were also reported by Baron *et al*. (2005) in West Africa, and Tsvetsinskaya (2003) in Southern USA. The scale problem is

critical when complex topography areas are simulated. In fact, it occurs in our work domain in Chilean southern regions. For example, in Angol city (37°48′S 72°43′O) two meteorological stations located 3 km apart from each other showed differences up to 34% in annual average precipitation. Moreover, complex topography is the main land cover in many countries associated with poverty and low agricultural productivity. Complex topography also generates microclimates, which produce high valuable crops.

To improve AOGCM resolution, numerical techniques, called downscaling, have been developed (Wilby *et al*., 2004; Hewitson and Crame, 1996). Downscaling is used in many researchs related to climate change (*e.g.* Bergström *et al.*, 2001; Hanssen-Bauer *et al.*, 2005), but only a few studies have covered South America. The main examples are "CREAS" (Regional Climate Change Scenarios for South America) in Argentina, Uruguay and Brazil (Marengo and Ambrizzi, 2006), "Variabilidad Climática para el Siglo XXI" ("Climate Variability for 21th century") in Chile (Fuenzalida *et al.*, 2006), and Misra *et al*. (2003)'s work in the zone located between 30°N and 40°S. Chilean database was created by Departamento Geofísica, Universidad de Chile (DGF) through downscaling of Hadley Centre Coupled Model (HadCM3) outputs generated for the Third Assessment Report of IPCC (TAR, IPCC, 2001). DGF nested the atmospheric model called Providing Regional Climates for Impact Studies (PRECIS) (Fuenzalida *et al.*, 2006) into HadCM3 for generating a complete climate database. This database (hereafter DGF-PRECIS) involved projection on the baseline data between 1961 and 1991 together with A2 (severe, i.e. high CO_2 which is about 850 ppm and global temperature increasing about 3°C at 2100) and B2 (moderate, i.e. high CO_2 which is about 621 ppm and global temperature increasing about 1°C at 2100) scenarios for 2070 and 2100 at 0.25º resolution (25 km grid). These projections showed a temperature increase across Chilean area, along with a decreasing rainfall in Northern and Central zones (18º - 30º S and 30º - 40º S, respectively). The reduction in rainfall increased the evapotranspiration and lowered the summer snow reserves representing a significant decrease in the 'water supply'.

Downscaling is a step forward in climate change research. However, few crop projections have been obtained with downscaling techniques. Semenov (2007) worked in UK using wheat crop as target vegetation with a 10 km size grid. In this work they used the UKCIP (The United Kingdom program for climate change adaptation) climate dataset, which was downscaled by a topoclimate regression and interpolation with irregular triangulation network algorithm. Zhang *et al* (2005) worked in Oklahoma using HadCM3 projection downscaled by likelihood curves to site-specific records. On the other hand, when we perform a downscaling for modeling the crop yield, we are defining a spatial working scale. Thus, it poses the question: *what is the optimum climate grid cell size that represents crop yield variability if the soil properties remain constant*? This question is not solved yet.

In this thesis, we generate a general description of the rainfall pattern in both whole Chile (17º to 56ºS and 70º to74º W) and Araucania Region (37º to 40º S and 71º to 74º W). Using this description, we validated and corrected the DGF-PRECIS dataset by downscaling techniques to generate a high resolution (1 km) rainfall dataset for Araucania Region. Based on this rainfall dataset, we projected key Chilean crop yields such as winter wheat, assessing the impact of climate change of them. Finally we assess the impact of the

downscaling on the crop model proposing a methodology for defining the optimal grid cell size.

This thesis is divided into seven chapters with four manuscripts in preparation for publication, one submitted and one published paper. In Chapter 1 we gave a general introduction. In Chapter 2, we presented a theoretical framework of the current knowledge about the impact of climate change and how assessing it by climate and crop models. In Chapter 3, we validated the DGE-PRECIS for Araucanía Region using *in-situ* records, and also including a validation for the whole Chilean territory that was required to understand the local model biases. In Chapter 4 we performed a downscaling technique which we applied in the Araucanía Region for a high resolution (1 km of grid size) climate dataset. In Chapter 5, we showed the crop projection made by corrected climate projection linked with CERES crop model (DSSAT). In Chapter 6 we performed a spatial analysis for measuring the effect of downscaling on the crop simulation model for an optimal climate grid cell size. Finally, a general discussion and the main conclusions are presented in Chapter 7.

1.1 Hypothesis of the thesis

Downscaling of climate models to high resolution (1 km) output significantly improves the performance of crop models than direct use of mesoscale climate model dataset in crop modeling.

1.2 The goals were:

1.2.1 Generate and validate a high resolution (1 km) climatic database for baseline between 1961 and 1991 using DGF-PRECIS database downscaled using PCASOA model in Araucanía Region (coordinates),

1.2.2 To generate a high resolution climatic database for future conditions A2 scenario of IPCC using corrected DGF-PRECIS database and PCASOA model.

1.2.3 To estimate the climate change effect on winter wheat crop based on high resolution climate projections under A2 scenarios of IPCC.

1.2.4 To measure the impact of spatial downscaling on crop modeling and define an optimal climate grid cell size to estimate the impact of climate on crop yield under different topographic complexity.

Chapter 2

Assessing the impact of climate change on agriculture through climate models coupled with crop simulation: Importance of downscaling

Orrego, Raúl[1]. Ávila Andrés[1,2] and Matus, Francisco[1,3]

Paper draft

[1] Scientific and Technological Bioresource Nucleus, Universidad de La Frontera, Chile

[2] Centro de Modelación y Computación Científica, Universidad de La Frontera, Chile

[3] Departamento de Ciencias Químicas, Universidad de La Frontera, Chile

2. Assessing the impact of climate change through climate models coupled with crop simulation: Importance of downscaling

Abstract

Climate change implies important consequences on food security. Several authors have evaluated these effects using climate models linked with crop model called in this chapter climate crop modeling (CCM) approach. CCM is based on the Atmospheric and oceanic general circulation models (AOGCM), which simulates the state of the atmosphere and the ocean for the whole Earth based on physical laws. Although CCM measures the impact of climate changes on crop responses, it does not consider key issues of crop projections. One of the main issues is the difference between AOGCM output scale and the scale requirement of crop modeling. These differences are critical in complex topography areas, which are crucial for small farmers in many countries. Topography complexity generates microclimate conditions associated with important agronomic activities influenced by aspect, slope, and soil water retention. The aim of this review is to give a theoretical framework of current knowledge about the climate change impact assessed by linking the outputs of climate models as input for crop simulation models. Downscaling and related technique are discussed. We conclude that downscaling techniques are the best tools for correcting the scale differences between climate and crop models.

Key Words: *Climate projection, crop model, downscaling*

2.1. Introduction

More before in 500,000 years, the concentration of atmospheric CO_2 had reached the highest point at 400 ppm observed today (IPCC, 2013; 2007; 2001). In addition, the observed temperature has increased since Industrial Revolution affecting all the climate system. (IPCC, 2013; 2007; 2001). Both, climate and CO_2 concentration are the main factors that impact the crop response (Murungan *et al.*, 2012, Hansen *et al*., 2006; Long *et al.*, 2006; Betts, 2005), in fact factors such as rainfall, solar radiation and temperature are the most important drivers on crop yield responses and food quality (Porter y Semenov, 2005; Thomson *et al*., 2005; Rosenzweig y Parry, 1994). Thus, climate change adaptation is one of the main challenges for sustaining the food security.

Knowledge of crop response and growing pattern under climate change scenarios will allow us to mitigate the negative effects by changing cultivars, identifying input requirements, and evaluating agronomic measurements to counteract deleterious effects and to improve crop adaptation to the new conditions. To understand crops response under climate change, several techniques have been proposed. There aresummarized in Table 2.1. All these methods are based on a sequence step, which combine climate scenarios associated with crop response (Figure 2.1).

Table 2.1. *Methods used for assessing the impact of climate change on crop responses*

Methods	**Description**	**Advantages**	**Disadvantages**	**Reference**
Ricardian analysis	Multiple regression among climate values and economical outputs (land values or profitability)	-does not need specific model	- High error	Gbetibouo and Hassen, 2005
		- can be used for future scenarios	-Does not consider CO_2 effects	
In-situ experimental approach	Established essays assessing plants under expected controlled conditions	-Precise outputs (measurement)	-Specific outputs (controlled condition. Also expensive to generate new conditions) - Expensive	Dijkstra *et al.,* 2010
		- can be used for future scenario		
Climate-crop current trends	Research trends in the last years climate/crop behavior	-Precise outputs (measurement)	- Cannot be used for future scenario	Lobell and Field, 2007
		- Do not need specific model	-Do not consider CO_2 effects	
Climate-crop models	Simulate current and future crop behavior using a crop model and climate model outputs	-Precise output (but not a measure)	-Specific outputs (but easy to generate new conditions)	Paruelo and Salas, 1993
		- Can be used for future scenario		

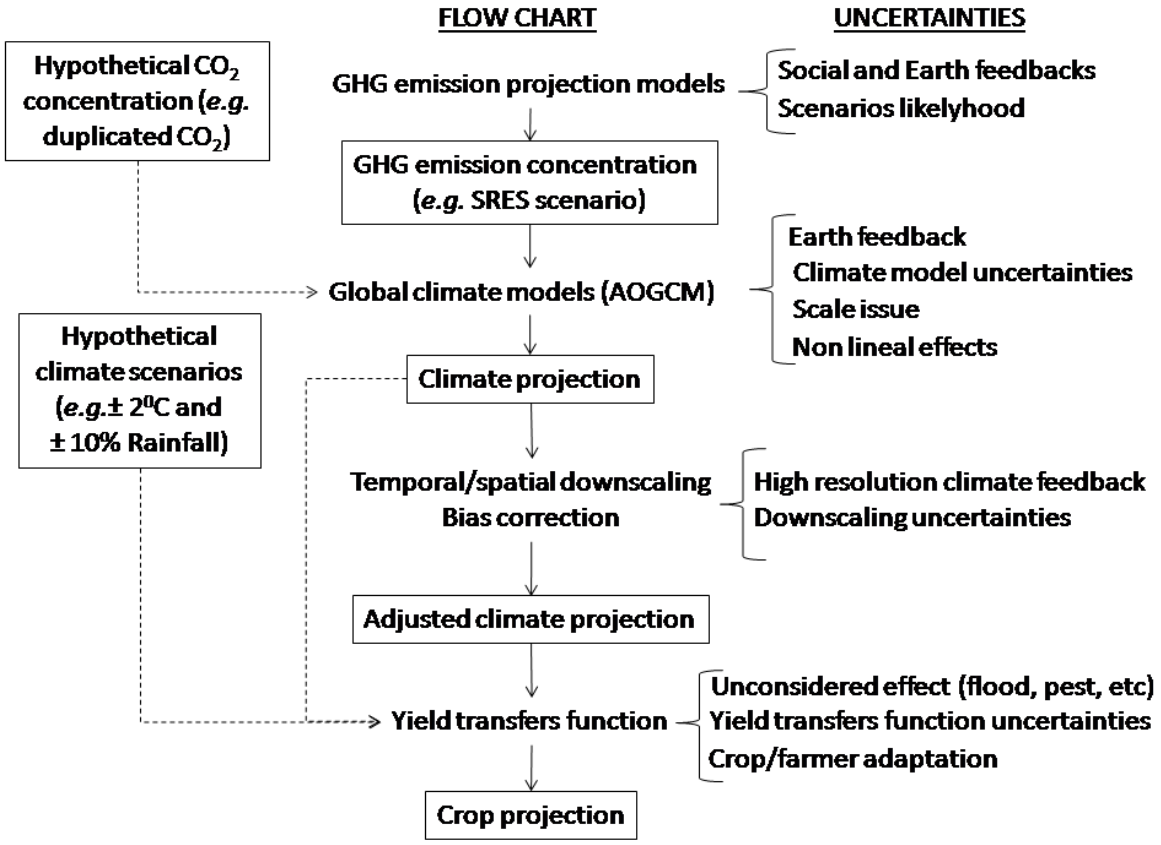

Figure 2.1. *Flow charts for developing crop projections (arrows) and their uncertainties (brackets). In the Flow chart inbox text main input data, free text main process, and dotted lines show other commonly used ways.*

Climate model output used as crop modeling input (CCM) approach is one of the most used techniques for assessing the impact of climate change on crop response (Lee, 2011; Challinor *et al.,* 2009; Thomson *et al*., 2005; Paruelo and Salas, 1993). First, CCM results are precise and relatively easy to adapt to new changes on the conceptual framework. Moreover, this strategy *a*lso allows us to evaluate the countermeasure for adapting crops to new conditions. CCM has been used at both, global (Betts, 2005; Parry *et al.*, 2004; Tan and Shibasaki, 2003) and local scale (Lee, 2011; Semenov, 2007), and it can be run under several climate conditions (White *et al.*, 2011). This approach is supported on three key issues: (i) crop simulation, (ii) climate projection, and (iii) adjusted climate projection (mainly by fitting the scale).

Climate projection considers assumptions, conceptualizations, and climate model strategies used to estimate the effect of greenhouse gases on climate system. Several models have been developed for projecting climate change conditions, but they should face some problems such as future emissions, high resolution boundary condition, validation model projection, and the complexity of atmospheric simulation (Räisänen, 2007).In fact, several authors recommend the word "climate projection" (*i.e.* the goal is that the simulated values represent the mean and distribution of the real values) instead of climate forecast

(*i.e.* the goal is that the simulated values are close to the real values). Thus, long term climate modeling produces an expected climate condition at a possible long-term scenario, which is not the typical climate forecast, but it is a precise referential projection (IPCC, 2007).

Adjusting climate projection is the first step for improving the climate input by correcting the produced temporal and spatial bias (Wilk, 1992; Semenov and Barrow, 1997; Ines and Hansen 2006). Climate projection bias could affect significantly the crop projection. Lobell (2013) measured this impact using a statistical global crop. He concluded that temperature bias produces a slight change, but rainfall bias produces about 30% error. On the other hand, low spatial resolution (200-300 km) output database from climate models are commonly reduced to a high resolution (e.g. 50 km) grid (Challinor *et al.*, 2009; Hansen *et al*., 2006) which affect the simulated crop response. For example, Mearns *et al*. (2003) reported 25% decreases in winter rains from models of 400 km to 50 km in the South Great Lake States (USA). This was translated in 30 % of crop yield decrease. Similar differences were also reported by Mearns *et al*., (2003) in other places of USA, Baron *et al*. (2005) in West Africa, and Tsvetsinskaya (2003) in Southern USA. On the other hand, the scale problem is more difficult when complex topography areas are simulated producing microclimate and inherent spatial variability.

In this review we examine the CCM approach for assessing the climate change impact on agriculture. We address the scale problem and downscaling techniques as a possible solution. This improvement allows a better understand the problems including climate projection in complex topography land. This review is divided into six sections. In the first section we discuss the main concepts to understand the crop modeling identifying uncertainties attached to the model output projections. In the second section we review the main issues related to climate projection identifying their uncertainties for the crop response. In the third and fourth section we defined the scale problem and we proposed downscaling techniques. Finally, in the sixth section we present the main conclusions and future prospects for CCM approach.

2.2. Crop models and climate crop models

Crop simulation is the process of translating climate projection into agriculture terms through crop models. Crop models are mathematical tools combining mechanistic and empirical equations to simulate the main plant processes (Villalobos, 2002). These models appeared in the early 1970's with De Witt's works reviewed by Van Ittersum, *et al*. (2003). Besides, there are some studies funded by the intelligence services of the USA contributing to predict agricultural production in the USSR farms (Villalobos *et al*., 2002). Crop models used weather variables (photosinthetically active solar radiation, precipitation, temperatures, and wind speed when use Penman Monteith model for simulating the evapotranspiration), soil physical and chemical properties, and plant ecophysiological parameters to predict crop yield response (Brinsson *et al*., 2003).

Crop models is originally performed mainly for a specific zone, but the main models allow linking the crop model output with Geographical Information System (GIS)

for representing the crop spatial variability. Batchelor *et al*., (2002) defined three strategies for linking the crop models with GIS: (i) defining homogeneous cells and modeling each cluster, (ii) applying point-based models on imagery derived zones within a field, and iii) combining point-based models with spatial water balance. Three strategies are commonly used with advantages and disadvantages. The first strategy is easier than the other two, but it cannot represent the relationship between near zones (spatial autocorrelation). The *second* and third strategies represent autocorrelation, but require many complex spatial measurements. Nowadays, remote sensing tools obtain spatial data to use the later strategies.

The crop models allow a systemic evaluation of weather variables on crop response, but some empirical parameters inside the model structure must be measured *in-situ* and tuned. On the other hand, there are also changes under fixed conditions, changing from short-term to long-term crop simulation *e.g.* crop managements, crop varieties, pest, and genetic coefficients, (Challinor *et al*., 2009). Soussana *et al*. (2010) claimed CCM must be based on the experience in for issues: (i) role of extreme climatic events, (ii) interactions between abiotic factors and elevated CO_2, (iii) the genetic variability for plants to CO_2 and temperature response, (iv) the interaction with biotic factors, and (v) the effect on harvest quality.

Climate change impact the crops system in two ways: 2.1) It produces changes on climate conditions and 2.2) it increases the CO_2 concentration in the atmosphere (Chartzoulakis and Psarras, 2005; Olsen and Bindi, 2002; Lawlor and Michel, 1991; Huntingford *et al*., 2005). The main effects of these changes are detailed as follow.

2.2.1 Changes on Climate condition

The main effect of climate change is the temperature increases since preindustrial time (IPCC, 2007). Temperature accelerates plant growth rates speeding up phenological stages (Petrie and Sadras, 2008; Wolfe *et al*., 2005; Spark *et al*., 2005). In addition, it implies a carbon fixation decrease during this period, which may affect negatively the quality and quantity of crop yield (Hu *et al*., 2005). A fast developing process can produce an overlap between sensitive periods (flowering or some stages of fruit growth) under adverse weather conditions (Semenov, 2007; Meza *et al*., 2008). However, Zhang *et al* (2008) proposed that the relationship between temperature and phenology is non-stationary, which could mitigate this effect. Although the increase of temperature decreases the number of frost-days (Liu *et al*., 2008; Nemani *et al*., 2001), several authors propose that the early bud-break will also increase frost damage (Augspurger, 2009; Nemani *et al*., 2001).

Another negative effect on high atmospheric temperature is the failure to reach vernalization in the cereal crops, which ensures the normal growth of the plant and flowering. Seed germination and pollen viability are also negative impacted (Vara-Prasad et al., 2006). Temperature can produce indirect effects on crops. Some examples are: pest and

diseases (Chakraborty and Newton, 2011; Yamamura et al., 2006; Cerri et al., 2007), water reserves, changes in nutrient cycling, and evapotranspiration increase (Brouder, 2008; Fisher et al., 2007)

Climate change modifies precipitation regimes with high spatial variability. Also, they show larger errors than temperature errors. The main effects are: high disease risk by high rainfall and temperature (Jara *et al*., 2013; Alexandrov and Hoogenboom, 2000), germination rate decrease by changes of soil water content (Sayar et al., 2008; Rounsevell and Reay, 2009), increases of photosynthesis rate by high soil water content reserves (Rounsevell and Reay, 2009), water stress in critical phenological stages by low rainfall (Lobell et al., 2007), flower drop by extemporaneous rainfall, altered polinitation (Cock et al., 2013), seed germination before harvest (Grupta et al., 2009), and yield quality losses by high humidity (e.g. cracking in cherry). On the other hand, flood and drought produce important crop production damage (Lobell and Burke, 2008; Rosenzweig et al., 2002), hence extreme event is an important issue for assessing the effect of climate change on crop systems (Soussana et al., 2010; Lobell and Burke, 2008).

2.2.2 Changes of atmospheric CO_2 concentration

Increases in atmospheric CO_2 concentration stimulate photosynthesis (Amthor, 2001) although this is not necessarily translated into productivity (Fuhrer, 2003). In addition, if the plant metabolizes more carbon, water and nutrients requirements are increased as well. Therefore, this phenomenon only temporally improves crop growth (Lobell and Field, 2008; Gitay *et al*., 2001). This concept is called CO_2 fertilization (Long *et al*., 2006; Thomsom *et al*., 2005).

Decrease in stomatal conductance (*i.e.* a numerical measure of the maximum rate of passage of either water vapor or carbon dioxide through the stomata) is another effect of CO_2 (Drake *et al*., 1997). However, this is often mitigated by the availability of water and changes on the leaf area index (Olesen and Bindi, 2002). A CO_2 increase can also mitigate the effect of temperature on the phenological development (Centritto *et al*., 1999; Sparks *et al*., 2005; Reyes-Fox *et al*, 2014), but the main crop models do not include this effect. Several authors have pointed out that an increase in CO_2 concentration produces: (i) an increase on nitrogen uptake (Fangmeier *et al*., 1999; Prior *et al*., 1998) (ii) a decrease on nutrients-use efficiency (Drake *et al*., 1997), (iii) an increase of evapotranspiration rate (Tognetti *et al*., 2001), and (iv) a decrease in grain protein content of cereals (Tomsom *et al*., 2005). In this way, one of the most important challenges is to predict the impact of climate change on nitrogen, carbon, and water cycles inside the plant by an integral perspective (Morgan *et al.*, 2011), such as the studies on grassland with free air CO_2 enrichment (FACE technology) (Dijkstra *et al.*, 2010). Although the simulation is useful for assessing the effects of CO_2 on the plant response, Long *et al*. (2006) argued that the effects are overestimated. The main reason is that crop models are tuned in "enclosure experiments". However, Ziska and Bunce (2007) compared “enclosure experiments” with others based on FACE technology obtaining similar results. Figure 2.2 presents an overview of the effects of climate change and the atmospheric CO_2 increase on crop yield

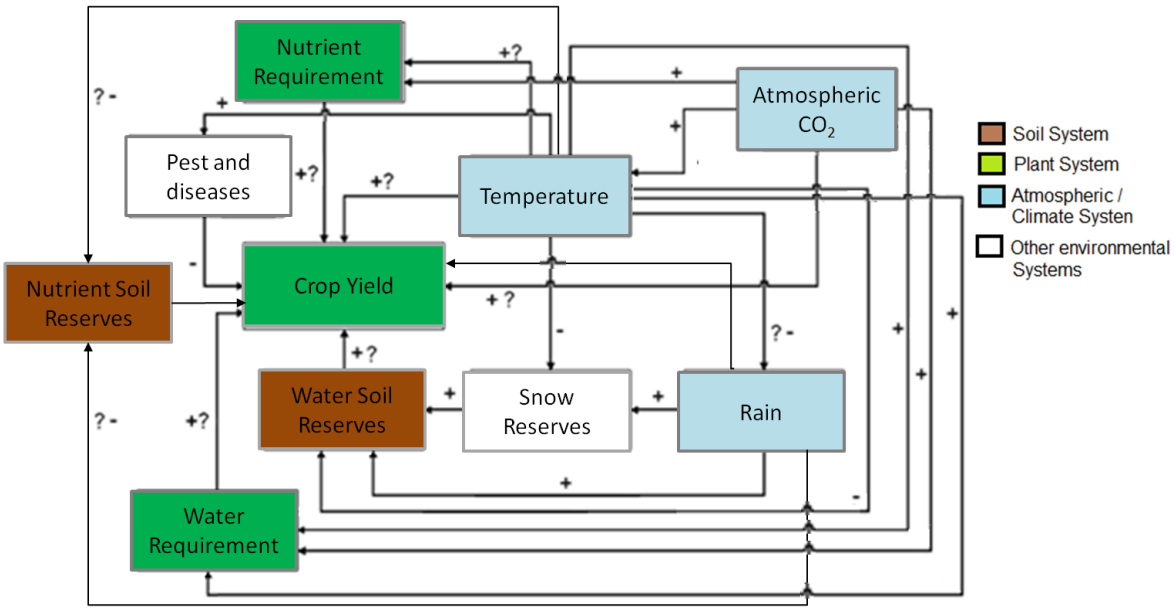

Figure 2.2.*Relational diagram representing the effects of climate changes (increases in atmospheric CO_2 and temperatures) in agriculture. We denoted a positive feedback by +,negative feedback by –, and no effect by 0. Elusive feedbacks are denoted by question mark.*

The crop models must consider both, the effect of meteorological conditions and the effect of atmospheric CO_2 increase. Today, photosynthesis oriented models are suitable for this purpose and one of the most wodly used is DSSAT (Decision Support System for Agro Technology Transfer) developed by IBSNAT (International Benchmark Sites Network for Technology Transfer) (Jones *et al*., 2003). DSSAT is a decision support tool containing several models such as CERES (mainly for cereals) and CROPGRO (mainly for legumes). There are also studies based on EPIC model (Erosion Productivity Impact Calculator) (Prya and Shibasaki, 2001). The simulations are mainly performed in cereals, for wheat (*Triticum aestivum L*.) (Semenov, 2007; Tomsom *et al*., 2005), maize (*Zea mays L*) (Meza *et al*., 2008; Jones and Thornton, 2003) and soybean (*Glycine max L. Merr*) (Grima and Natori, 2006; Tan and Shibasaki 2003). The climate change impacts on agriculture projected by CCM are inherently uncertain. For solving these uncertainties, Asseng *et al* (2013) proposes to use multi-model simulation. They perform a meta-analysis, including recent wheat yield simulation. They observed significant differences among them, which are reduced when the models are fully calibrated. In this way, in 2012 started the Agricultural Model Intercomparison and Improvement Project (AgMIP) conducting a series of activities to support integrated climate change impact assessments for agricultural systems (Rosenzweig *et al*., 2013).

In South America, crop simulations have been performed mainly on maize (Meza *et al*., 2008; Jones and Thornton, 2003). They are based on HadCM models (Meza *et al*., 2008; Paruelo and Salas, 1993) and ECHAM models (Grimm and Natori, 2006). The output of these studies is at continental scale and they project a decrease in the crop yield response. The reduction occurs in almost all countries, except for Chile and Ecuador (Table

2.2). These results should be considered with caution because they did not consider varieties used in Chile, Brazil, Mexico, and Argentina (Jones and Thornton, 2003).

Table 2.2.*Climate change impact on maize yields in different South American countries. (Adapted from Jones and Thornton, 2003)*

Country	Productive area* (Km^2)	Measured current yield* ($Kg\ ha^{-1}$)	Modeled current yield** ($Kg\ ha^{-1}$)	Modeled future yield*** ($Kg\ ha^{-1}$)	Country variation future yield**** (Ton)
Argentina	28,000	5,500	1,189	1,065	-347,200
Belice	180	2,111	1,380	1,032	-6264
Bolivia	3,061	2,214	1,278	1,088	-58,162
Brazil	128,190	3,237	1,377	1,032	-4,422,558
Chile	826	9,431	2,600	3,470	71,820
Colombia	5,800	1,828	1,492	1,404	-51,040
Costa Rica	130	1,731	1,781	1,581	-2600
Ecuador	4,596	1,398	1,538	1,539	460
El Salvador	2,627	2,165	1,781	1,556	-59,106
Guatemala	6,350	1,575	1,853	1,778	-47,625
Guyana	26	1,192	2,349	1,735	-1596
Honduras	3,650	1,370	1,611	1,350	-95,265
Mexico	76,800	2,500	1,555	1,440	-883,200
Nicaragua	2,750	989	1,670	1,375	-81,125
Panama	600	1,250	1,306	1,068	-14,280
Paraguay	3,700	2,432	1,187	1,156	-11,470
Peru	5,239	2,707	1,574	1,527	-24,623
Puerto Rico	5,4	1,870	1,293	1,029	-143
Suriname	0.2	2,000	827	740	-2
Uruguay	425	1,522	1,413	1,386	-1,148
Venezuela	4,500	2,667	1,323	967	-569,563

** Based on FAO record (year 2000)*

*** Based on base-line HadCM2 simulation (averages between 1961-1991)*

**** Based on HadCM2 simulation performed by Cullen (1993) for the year 2055*

***** Variation computing by the differences between modeled current yields minus modeled future yield times by productive size*

2.3. Climate projection

Several simulation models were developed to project future climatic conditions considering the concentration of greenhouse gases and ocean dynamics (IPCC, 2007; Cohen 1990; Gates, 1985). These models are called atmospheric and oceanic general circulation models (AOGCM) (Houghton *et al*., 1997). Nowadays, AOGCM-outputs generate databases, which are used as meteorological crop model input for evaluating the effect of climate change on agriculture. The AOGCM are very similar to the models used in meteorological forecasting adapted by the explicit consideration of radiative forcing due to greenhouse

gases. Radiative forcing is a quantification of the impact of greenhouse gases by computing their impact in the energy balance in the atmosphere (IPCC 2001).

Although both kinds of models are based on the same physical laws, long-term prediction is complex since the output presents more uncertainties by assumptions and simplifications (Räisänen, 2007). AOGCM outputs represent trends with precision, but they do not necessarily represent the accurate value. AOGCM are based on air flows generated by solar radiation differential warming on the earth surface (Mechoso and Arakahua, 2003). These flows result in many processes simulated from the laws of gases, the Navier-Stokes equations (fluid dynamics), the equations of thermodynamics, and balances of mass, energy and momentum. For solving these equations, a 3-D grid space division (boxcells) is built. The equations are solved at each cell by numerical methods (Anderson, 2003). Due to the complexity of these equations, AOGCM must assume the atmosphere at hydrostatic equilibrium (Anderson, 2003; Gutierrez and Pond, 2006; Zorita, 2000). Both, the ocean and atmospheric models increase the error associated with numerical diffusion, *i.e.* the error accumulated by rounding numbers and selected approximations of solutions during computations. Several models include a correction motor called flow adjustment (Gordon *et al.*, 2000; Zorita, 2000). Thus, the flow energy for all computed interactions by the ocean and atmosphere models is independently corrected for the outputs (Zorita, 2000). Finally, AOGCM cannot explicitly model several phenomena at world scale such as cloud formation and rainfall. This problem is indirectly solved by functions of different modeled climatic outputs through parameterization (Gutierrez and Pond, 2006; IPCC, 1997; Zorita, 2000).

Nowadays, there is a global system to generate dataset for obtaining input for AOGCM (Rodell *et al*., 2004). Several databases were developed that combine models and historical dataset for validating forecasts. These datasets are called reanalysis and they are: NCEP-NCAR (Kalnay *et al.*, 1996), JRA-25 (Onogy *et al*., 2007), MERRA (Bosilovich *et al*., 2006), and the ECMWF (ERA-40) (Uppala *et al.*, 2005). Database output generated by AOGCM models include the main meteorological variables such as temperature, solar radiation, air humidity, precipitation, barometric pressure, components of wind vector among others (Russo and Zack, 1997). Some of the most commonly used models are listed in Table 2.3.

Table 2.3 *Main AOGCM used in climate change research*

Model	Affiliation group	Country	References
IPSL-CM4	Institute Pierre Simon Laplace	France	Valcke *et al.,* 2004
ECHAM5	Max Planck Institute	Germany	Roeckner *et al.,* 2003
CNRM-CM3	Centre National de Recherches Météorologiques	France	Déqué and Piedelievre, 1995
EGMAM	Freie Universität Berlin	Germany	Legutke and Voss, 1999
HadGEM1	Met Office	U.K.	Johns *et al.,* 2006
HadCM3	Hadley Centre	U.K.	Gordon *et al.,* 2000
BCM2	Bjerknes Centre for Climate Research	Norway	Furevik *et al.,* 2003
GFDL-CDG1	Geophysical Fluid Dynamics Laboratory	U.S.A.	Gordon and Stern, 1982
NCAR-CCM3	National Centre for Atmospheric Research (NCAR)	U.S.A	Bonan, 1996
CGCM3	Canadian Centre for Climate Modeling and Analysis (CCCMA)	Canada	Flato eta al., 2000
CSIRO-AOGCM	Commonwealth Scientific and Industrial Research Organization (CSIRO)	Australia	Kowalczyk *et al.,* 1994

The AOGCM outputs can be linked with crop models for projecting plant growth under climate change conditions. However, there are two key issues that should be considered when using AOGCM projection on crop simulations: climate change scenarios, and the working scale.

2.3.1 Climate Change Scenarios

The definition of climate change scenarios is based on estimations of future emissions of greenhouse gases and "negative radiative forcing", such as SO_2 and aerosols (IPCC, 2007; Lamb, 1987). These values are measures in CO_2 equivalent (CO_2 eq), which is the radiative forcing produced by 1 ppm of CO_2. The prospective scenarios were built by simulating the economic and social impacts focused on growing population, environmental policies, technological growth, social equality, and globalization. There were several involved assumptions to determine global change scenarios described in the Special Report of Emission Scenarios (SRES, 2000). Thus six scenarios are proposed. Sorted based on the final expected warming they are: A1F1, A2, A1B, B2, A1T, and B1. There are differences about 6°C between A1F1 (the most extreme scenario) and B1 (Figure 2.3). Scenario selection is the first source of uncertainties, which are not associated with occurrence likelihood (Collins, 2007). Indeed, we do not know which scenario will be the right one in the future, but they help to develop public policies. Finally, we notice that several studies use only scenarios representing an extreme condition of high impact. The most of them use A2 for representing a severe (i.e., 850ppm of CO_2 eq and global temperature increasing about 3°C at 2100) impact and B2 for representing a moderate (621 ppm of CO_2 eq and

global temperature increasing about 1°Cat 2100) impact (*e.g.* Fuenzalida, 2006, Marengo and Ambrizzi, 2006)

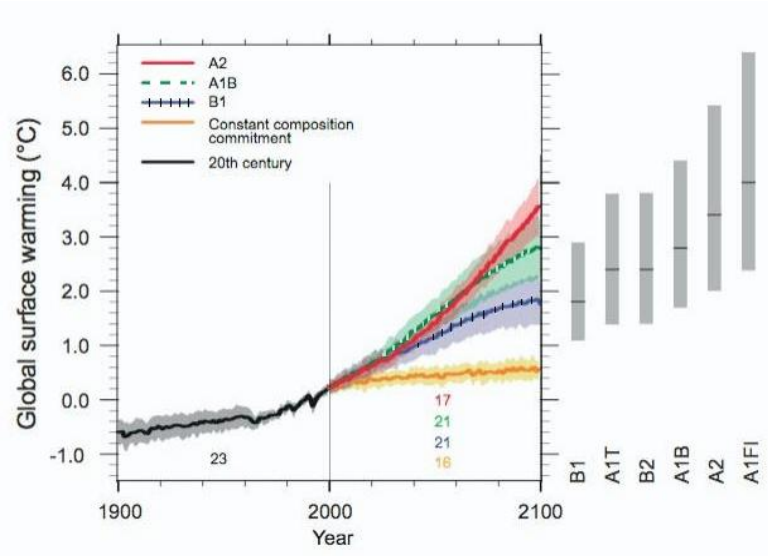

Figure 2.3.*Temperature changes projected by AOGCM (IPCC, 2007) for each SRES scenario. Shaded region show the "probable ranges". The gray bars on the right represent* year *2100 temperatures considering the ranges (bars), and the averages (dark line inside the bar).*

These scenarios supported the projection generated in the Third Assessment report (TAR) and the Assessment Report 4 (AR4)developed by IPCC, and used for many countries for guiding public policies and adaptation countermeasures (IPCC 2007; 2001).

SERES scenarios are not the unique used in the climate change researches. Before TAR scenarios, they used the so called IS92 scenarios (there are 6 from "a" to "f" sorted from most severe to less severe). Also, the last IPCC report (Assessment Report 5, so called AR5) propose improves new scenarios. These scenarios are based on a new concept: the "Representative Concentration Pathways" (RCP), *i.e.* patterns representing the expected GHG temporal behavior (IPCC, 2013). The main scenarios are summarized in the Table 2.4.

Table 2.4. *Scenarios used in the AR5 IPCC projection (adapted from Van Vuuren et al., 2011)*

Scenario	Description	Severity
RCP8.5	Rising radiative forcing pathway leading to 8.5 Wm^{-2} (~1370 ppm CO_2 eq) by 2100.	Extreme
RCP 6.0	Stabilization without overshoot pathway to 6 Wm^{-2} (~850 ppm CO_2 eq) at stabilization after 2100	High (equivalent to A2)
RCP 4.5	Stabilization without overshoot pathway to 4.5 Wm^{-2} (~650 ppm CO_2 eq) at stabilization after 2100	Medium (equivalent to B2)
RCP 2.6	Peak in radiative forcing at ~3 Wm^{-2} (~490 ppm CO_2 eq) before 2100 and then decline (the selected pathway declines to 2.6 Wm^{-2} by 2100).	Low

2.3.2 Climate Model Uncertainties

Although the equations that model the atmospheric-ocean circulation are well identified and boundary conditions are also obtained with high precision on a global-scale (Collins; 2007; Räisänen, 2007), the models have an associated error due to parameterizations, numerical diffusion, assumptions, and simplifications used in the simulations. In addition, this effect increases by atmospheric chaotic behavior (Baize, 2003; Smite, 2003). However, this effect does not restrict their worldwide use (Bonan, 1996; Flato *et al*., 2000; Valcke *et al*., 2004).

The AOGCM differs in their climate projections (Allen *et al*., 2000; Weaver and Weirs, 2000) (Figure 2.4). These differences are explained by programming architecture (for instance, grid size, numerical schemes, parameterization of physical processes), together with differences in the nesting models (*e.g.* carbon balance, dynamics of aerosols, ice-cover) (Gutierrez and Pond, 2006). These differences were investigated using probabilistic scenarios. However, there are few examples for constructing scenarios based on these techniques (Wilks and Wilby, 1999). The Commission of the European Union called Climate Change and Environmental Risks Unit generates scenarios based on the combination of the main European models developing the emblematic 'Ensemble Project' (Morse, 2007).

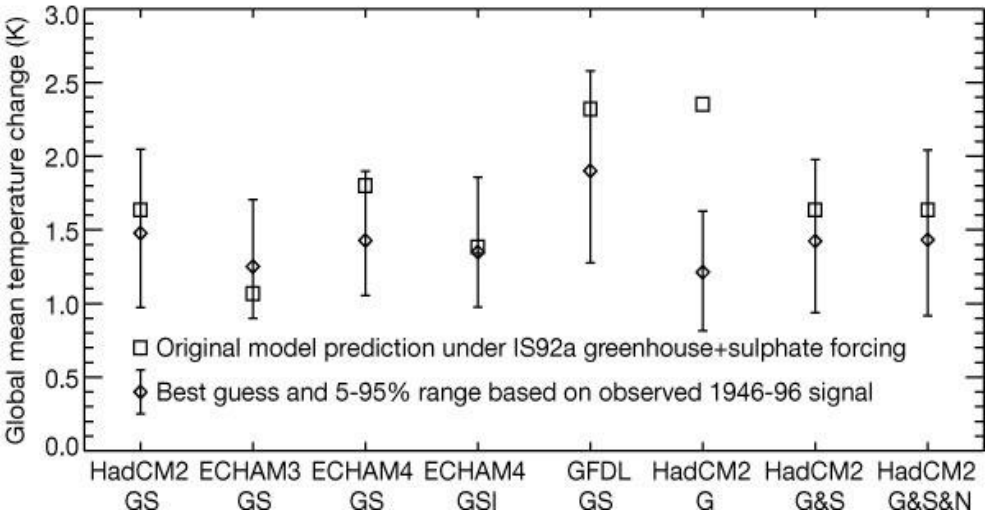

Figure 2.4.*Global mean temperature change comparison between projections obtained by general circulation models for the* year*2040 under IS92a scenario (Allen et al., 2000).*

Several authors reported that AOGCM models tend to overestimate the number of rainy days and underestimate the amounts of rainfall, called drizzle (Challinor *et al.,* 2009; Baigorria *et al.,* 2008). To solve this problem, daily-bias correction is used (Baigorria *et al.*, 2007; Ines and Hansen, 2006). Another strategy is to work with the difference between simulated present-day and future climates (Räisänen, 2007). In addition, the validation for using AOGCM for projecting climate change has some unsolved issues. There are temperature variations on the ocean stream flow due to differences in salinity concentration, the so-called thermohaline circulation (Toggweiler and Key, 2003; Clark *et al*., 2002; Vellinga and Wood, 2002). They can drastically affect the climate system. Furthermore, the water vapor feedback (Cess, 2005; Held and Soden, 2000), the potential increase of greenhouse gases originated by the tundra melting soils permafrost (Wille *et al*., 2008; Osterkamp and Burn, 2003), and the future changes on the land cover (Räisänen, 2007) are factors that may cause unexpected results.

Some phenomena affect the climate, but they are not used in climate models. For instance, volcanic eruptions produce important effect of climate system. Although it is impossible to forecast volcano eruption emissions of sulphurous and aerosols, we use stochastic models to simulate them (Collins *et al*., 2007). Other climate disturbance phenomena are not explicitly modeled in long-term climate projections, such as ENSO and OAA cycle (Räisänen, 2007).

Finally, it is important to emphasize that AOGCM scenarios are used to enable policy makers for developing new environmental strategies and mitigation control measurements (IPCC, 2001; 2007). In this way, IPCC developed improved projections indicated in the fifth report (AR5), which considers better feedback (mainly improved land use projection and mitigation countermeasures).These projections includes the effect of the phenomena causing climate disturbances such as ENSO and Monsoon at an improved scale (Stocker *et al*., 2010).

2.4. Scale Issue

To model the impact of climate conditions, we need to understand two facts: (i) climate is continuous on the space, but it shows an important spatial variability, and (ii) this variability is related with the level of generalization to understand the phenomenon. For example, if we want to represent the air temperature, we can consider it homogeneous inside a small field, but there are important differences in different sections of each field. To understand the climate effect on the crop system, we need work under a scale concept.

2.4.1 What is Scale?

Scale is a critical concept in physical and natural sciences (Turner et al., 2001). Scale is defined as the spatial or temporal dimension of an object of process (Turner et al., 2001) providing a link between the phenomenon and its representation (Atkinson and Tate, 2000). Since our work is focused on the spatial issue, we refer only to spatial dimension, but the same ideas could be generalized for temporal dimension.

Duncan et al (2002) recognized three components of scale: (i) ecological, i.e. the real scale at which a phenomenon happens, (ii) analytical, i.e. the minimum area considered as homogeneous when we analyze a phenomenon, and (iii) sampling i.e. the scale defined by the sampled data used for describing the phenomenon. Thus, in a climate grid, analytical scale is determined by the grid cell size, the sampled scale is determined with the density of meteorological stations or the final climate model resolution, and the ecological scale is intrinsic of the phenomenon to represent. Although the ecological component is the true scale of the phenomenon, we can only determine it based on the sampling and analytical component (García, 2006). Several techniques were developed to identify the ecological scale. The most used techniques are: high resolution transects (O'Neill et al., 1991), up-scaling (Angulo et al, 2013), correlograms (Pearson, 1995), and semivariograms (Rahman et al., 2003).

Geographical Information Systems (GIS) provide methods for changing the data scale and they integrate different phenomenon on a unique spatial framework (Atkinson and Tate, 2000). In fact, several phenomena cross many scales. For quantifying their spatial pattern, we need to understand how these pattern changes with the scale (Levin, 1992). Is there a right scale? A right scale should represent the phenomenon, but it does not complicate the data manages and the phenomenon understanding. In fact, the optimal scale is not necessary the highest scale. When the resolution is high, the details hide the general patterns. On the other hand, higher scales require more computational resources.

Scale changes affect the spatial pattern of the phenomenon producing the well known modifiable areal unit problem (MAUP; Angulo et al., 2013; Openshaw, 1984; Openshaw and Taylor, 1981). MAUP is originated in different ways once the work domain is divided into homogeneous areal units (e.g. pixels). It implies that a geographical data shows different values depending of the selected way that the work domain is divided. This areal unit does not have an intrinsic geographical meaning and it does not have any validity independent of the units which are being studied. MAUP encompasses two components

called (i) scale problem and (ii) aggregation problem. The former represents the variation in the results that can be obtained when we used progressively larger scales. The latter represent the differences produces when the grid is move in different directions.

2.4.2 Scale and climate models for crop modeling

American Meteorological Society's Glossary of Meteorology (2013) defined three types of scales for clime: Synoptic (>2,000 km), Mesoscale (2 to 2000 km of grid size) and microscale (<2 km of grid cell size). Moreover, mesoscale is divided in meso-α (2000-200 km of grid cell size), meso-β (200-20 km), and meso-γ scales (2–20 km of grid cell size). However, it is necessary to fit this definition when we work with climate models. AOGCM work with meso-α scale usually referred as "global scale" and "mesoscale models" corresponding to scales from 20 km to 50 km (Räisanën, 2007; Giorgi y Mearns, 1999). Also, Plants are affected by the site-specific (*in-situ*) environmental conditions and it is very difficult to obtain the climate variables for representing these conditions. When we model a crop system based on a climate grid, we are representing the crop spatial variability derived from the climate grid. Thus, climate model output scale is an important issue for understanding the crop model uncertainties and its applications in climate change research.

AOGCM are based on grid cells which are homogeneous representing the zonal values. However, grid cells cover areas, and the climate variables are referred at specific points which change inside a grid cells. In 1991, Grotch and MacCracken compared AOGCM outputs and observed that the spread in the zonal average records for the same zones increases when is considered small areas. Later, Zorita and Von Storch (1997) re-interpreted this work, claim that at finer scale climate models reduce their skill. Both works hint that there is a minimum scale where the model effectively represents the phenomenon, and higher resolution show important errors explained by the scale differences. This scale was defined as skillful scale, and it is about eight times the grid size, although this may be modified by (i) the choice between atmospheric spectral models or grid-point models; (ii) the numerical integration schemes and discretization; and (iii) the surface process parameterization schemes (Benestad et al, 2007). Therefore, AOGCM outputs database are not used in crops simulation models, because crop models are designed to work with point simulations (Baron *et al*., 2005; De Witt *et al*., 2005; Hansen *et al*., 2006). In fact, most of the current simulations linking crop models with climate models work with mesoscale model, improving the quality of the output database simulations (Baron *et al*., 2005; Mearns *et al*., 2003). Challinor and Wheeler (2009) give another alternative developing a crop model adapted for AOGCM as climate input. The model is named GLAM (General Large-Area Model), and it has been used to develop global crop projection (Challinor *et al*., 2009; Challinor and Wheeler, 2008).

Scale problem would be extrapolated to temporal resolution as AOGCM outputs reliable for monthly values. In addition, AOGCM works with simplified years (*i.e.* years of 360 days), hence, we cannot overlap the AOGCM outputs with yearly meteorological records. This is more important on the Southern Hemisphere, where crop seasons include the days between consecutive years. Temporal fitting is solved by stochastic weather simulation models, *i.e.* simple algorithms that generate a random variable with the same

probabilistic distribution functions for monthly meteorological data (Wilk and Wilby, 1999). In addition, this technique adds the effect of climate variability on crop simulations (Mearns *et al*., 1996; Semenov and Porter, 1995).

Stochastic weather simulations have uncertainties. This technique assumes that local weather parameters are homogeneous across each grid cell, which is not always the case at large scale. In addition, the stochastic simulations of estimated weather variables are independent from neighbor pixels in contrast to meteorological variables (Wilks and Wilby, 1999). This was explained by the regionalized geostatistical theory (Isaaks and Mohan, 1989). Another disadvantage is simulating interannual variability and anomalies in the climate cycle (Wilks and Wilby, 1999). However, stochastic weather simulators have been improved by generating spatially consistent weather time series (Quian *et al.*, 2002). The most used stochastic weather simulators are WGEN (Richarson, 1981) and LARS-WG (Semenov, 2007), both were used for developing several high resolution climate projection database such as: ELPIS (Semenov *et al.*, 2010) for Europe, and ELPIS-JP (Iizumi *et al*., 2012) for Japan. Spatial fitting is more difficult than temporal fitting. Several authors use data interpolations for spatial fitting of AOGCM output to crop models. Data interpolations are unsuitable for improving the spatial resolution, because they do not recognize spatial perturbations that occur as a result of topography and land-cover. However, they are used in some studies (Jones and Thornton, 2003; Prudhome *et al*., 2002).

We conclude that downscaling is the best method for fitting the scale. Downscaling transforms dataset from a global to local scale (Hewitson and Crame, 1996; Kim *et al*., 1984; Wilby *et al*., 2004). Notice that only a few papers on local scale crop simulations have been published. In the Web of Knowledge, there are only 62 researches related to climate change and crop using "downscaling", and most of them on mesoscale approximation (*i.e.* 20-50 km of grid cell size), which is lower than optimal for crop system. We found only two papers using grid size less than 10 km (Semenov 2007, Zang *et al.*, 2005). Downscaling will be explained in the next section.

2.5. Downscaling

Crops are affected by site-specific condition which do not are represented AOGCM (Hansen and Indeje, 2004; Zhang, 2005). Therefore, we require method for change the scale from the AOGCM scale (about 300 km) to a scale with represent the site-specific spatial variability. These methods are called downscaling. Downscaling is a mathematical method for transforming a dataset from a global to local scale (Hewitson and Crame, 1996; Kim *et al*., 1984; Wilby *et al*., 2004). Downscaling is classified into two groups: statistical (or empirical) and dynamical. We discuss them as follows,

2.5.1 Statistical downscaling

It consists in obtaining a statistical relationship between the data at the global-scale with the data at a local-scale (Hanssen-Bauer *et al*., 2005; Solman and Nuñes, 1999; Wilby and Wigley, 1997). Thus, we fit an algorithm (transfer function) that links known variables (predictors) with the output (predictands).

The predictor must meet several conditions: (i) highly correlation with predictands, (ii) easy to obtain or estimated with high quality, (iii) sensitive to predictor changes (correlation must not be spurious), (iv) the relationship between predictors and predictands should not be modified under the simulated condition (stationary), and (v) ideally, their selection should be based on physical laws (Benestad *et al*., 2007; Wilby and Wigley, 2000). Some predictors used in downscaling for climate change scenarios are relative humidity on specific geopotential height (measure in terms of barometric pressure), wind speed profile, and index related to either NAO (North Atlantic Oscillation) in Europe or ENSO in South America (Linderson 2004, Zagar *et al.*, 2004; Wilby, 2001, Wilby *et al*., 2002, Fischer *et al.,* 2004)., These models are called large scale process driver models (LSPDM), because the main predictors are based on climate forces and they are available like software applications such as SDSM (Wilby, *et al.,* 2002) and CLIM.PACT (Benestad *et al.,* 2008).

As LSPDM translate grid-dataset into dot-dataset (one prediction for each meteorological station), they require a density meteorological station network with large time series records for making reliable high resolution grids and require interpolation algorithms for mapping. This could restrict the use of these models, especially in places, where there are few meteorological records. On the other hand, when we model one meteorological station, it is impossible to validate the final output using a different dataset from the one they used for calibrating the model, unless we use a fragment of the dataset for calibrating it. For solving these problems, spatial statistical models were developed. One of the most common ways for this downscaling is the random cascade approximation (Grupta and Waimire 1993). This approximation subdivides the rainfall in a specific zone (*e.g.* pixels or watershed) at a fine scale iteratively until the required resolution is achieved. Thus, a probabilistic model is fitted with the *in-situ* records located inside each subdivision (Gropelly *et al*., 2011). The most common models are: Bartlett-Lewis pulses, the Neyman-Scott pulses, Markov Chain, and other derivations based on them (Kaczmarska, 2013). They are also called multifractal (Rupp *et al.,* 2012). The topographical models are another alternative method for downscaling. They consider precipitations inside a low resolution grid cell and they distribute them among the high resolution pixels by empirical functions based only on topographical predictors. These models compute a deterministic function, which is used directly, or for fitting a random cascade function. The most prominent of them is PCASOA (Guan *et al.,* 2009).

Statistical downscaling can be addressed by two ways: (i) there is a unique transfer function for all situations (*perfect-prog*, also called linear methods), and (ii) there are many transfer functions fitted to different situations (*non linear methods*) (Benestad *et al*., 2007). For (ii), clustering algorithms are used to obtain homogeneous areas. These are: the Model Output Statistics (MOS) (Allen and Erickson, 2001), the artificial neuronal networks (*i.e.* computational algorithms that can learn and recognize selected patterns in its operation) (Yuval and Hsieh, 2003), and the method of analogues (Timbal and McAvaney, 2001).

Before fitting statistical models for downscaling, several authors used "empirical orthogonal functions" (EOF) to remove temporal trends and minimizing computations (Benestad *et al*., 2007, Wilby and Wigley, 1997). The most used method is Principal Component Analysis.

The main advantage of statistical downscaling compared to dynamical downscaling is simplicity. Therefore, statistical downscaling requires less amount of computing time than dynamical downscaling, which reduces implementation costs (Zorita and Von Storch, 1999) with low numerical diffusion errors. On the other hand, these techniques mitigate errors inherited from global models by incorporating meteorological records (Benestad *et al.*, 2008). Unfortunately, these techniques assume that future conditions are inside the range of data used for fitting, which can be criticized from climate change scenario points of view (Easterling, 1999; Wilby and Wigley, 1997).

It is observed that AOGCM underestimates the variance of the predictand (Burger, 1996; Von Storch, 1999). For solving this problem, the authors introduced a factor for adjusting variances. This is called expanded downscaling. Although this method was used in several works, Von Storch (1999) showed that this technique induces bias.

Among the statistical downscaling methods, the most frequently used are: (i) the regression fittings (Hessami *et al*., 2008; Foody, 2008; Hewitson and Crane, 1996), (ii) mathematical algorithms based on multivariate statistics, such as canonical correspondence analysis (*e.g.* Temebl, 2005; Benestad, 2007), (iii) approximation by climate profiles (Yarnal *et al*., 2001), and iv) stochastic climate generation (Bannayan and Hoogenboom, 2008; Semenov and Barrow, 1997). In addition, algorithms based on artificial neural networks have also been used (Cannon, 2007; Dibike and Coulibaly, 2006).

2.5.2 Dynamic downscaling

Dynamic downscaling is based on atmospheric models nested to AOGCM (Prudhomme *et al*., 2002) using the output of AOGCM as boundary conditions. They are called regional climate models (RCM) (Giorgi y Mearns, 1999) or limited-area models (LAM), because they simulate a bounded area (domain). In this thesis we named this model as RCM. The main RCM are shown in Table 2.5.

Table 2.5. *Most used RCM[1] in climate change research.*

RCM	Research group	Reference
DARLAM	CSIRO (Australia)	Koe *et al. (*2003)
NCEP-RCM	NCEP (USA)	Juang *et al. (*1997)
SweCLIM	Swedish Meteorological and Hydrological Institute (SMHI), Stockholm University and Göteborg University (Swedish)	Rummukainen *et al.*,(2004)
RegCM2	NCAR-Universidad de Pennsylvania (USA)	Giorgi *et al.*,(1993 a,b)
Scripps RSM	National Meteorological Centre (NMC) USA	Juang and Kanamitsu, (1994)
ClimRAMS	Colorado State University (USA)	Pielke *et al.*,(1992)
CRCM	Université du Québec à Montréal and the CCCma global climate modeling team in Victoria (Canada)	Caya y Laprice *et al.*,(1999)
HIRHAM	DMI (Damich)	Christensen *et al.*,(1997)

PROMES	Complutense de Madrid (Spain)	Gaertner *et al.*,(2001)
PRECIS/HadRM	Hadley Centre (U.K.)	Momber and Jones,(2004)
MM5	Pennsylvania State University and NCAR (USA)	CHEN and DUDHIA, (1999)
WRF	National Centre for Atmospheric Research (NCAR), National Centers for Environmental Prediction (NCEP), Forecast Systems Laboratory (FSL), Air Force Weather Agency (AFWA), Naval Research Laboratory, University of Oklahoma, and Federal Aviation Administration (FAA) (U.S.A.)	Skamarock, (1999)
REMO	MPI (Germany)	Jacob and Podzum, (1997)
CLM	GKSS Forschungszentrum (Germany)	Steppeler *et al*. (2003)
RCAO	SMHI Rossby Centre	Döscher *et al.*,(2002)
ARPEGE	ECMWF (E.C.)	Déqué *et al.*,(1998)
CHRM	ETH Zurich. Swedish	Lüthi D *et al.*,(1996)
RACMO	KNMI (Netherlands)	Lenderink *et al.*,(2003)

[1]Regional climate models

Several nested simulation with boundary conditions uses “one way” strategies, *i.e.* no feedback is allowed (Denis *et al*., 2002), but nowadays it is corrected. Current RCM do not consider only boundary conditions, but also forcing interior grid cell using terms in the spectral domain. This method is called spectral nudging (Radu *et al*., 2008; Von Storch *et al*., 2000).

According to Giorgi and Mearns (1999), there are nine key issues to develop dynamic downscaling: (i) mathematical formulation of nesting, (ii) spatial resolution of input and output grid, (iii) spin-out of AOGCM and RCM, (iv) update frequency of lateral boundary condition, (v) physical parameterization consistence between global and nesting model, (vi) horizontal and vertical interpolation (vii) domain size, (viii) quality of AOGCM, and (ix) climate drift and systematic error.

The main disadvantage of dynamical downscaling is the computational cost for its implementation (Hewitson and Crane, 1996; Pinto *et al*., 2014). Another disadvantage is the difficulty for testing the regional model. These models generate grid data, although available climate datasets consider only point data. Therefore, for indirectly validating the algorithms and the parameterization methods, several techniques have been created, which are summarized in Table 2.6.

Table 2.6. *Main climate model validation methods*

Method	Description	References
Big brother experiment	It is based on a comparison between "big brother" grid and "little brother" grid. The "big brother" grid is the original RCM projection, whereas the "little brother" is a RCM performance, which uses as boundary condition a low resolution grid obtained by filtering the "little brother".	Dennis *et al.*,(2002)
Cross validation method	Consists of systematically deleting one or more cases in a dataset and predict the deleted data with a model calibrated using the remaining data. Finally, the predicted values are compared with the deleted original	Michelsen, (1987)
Non dimensional index	Is based on the computing of indexes to quantify the climate model accuracy with respect to current and/or past observations (hindcast)	Watterson (1996)
Ensembles	Is based on the comparison among several climate models, using them as individual observations.	Christensen *et al.*,(2007)

Although the RCM is used for forecasting meteorological conditions and projecting climate change condition, both issues are different. The long term simulation models (*i.e.* referred to several years) need specific parameterizations and simplifications. In fact, a long term simulation considers dynamic subroutines (*e.g.* carbon cycle and ice cover). In this way, an important issue is the effect of the land cover, which is more important on high resolution grids (Betts, 2005).

In Europe, mesoscale resolution (20-50 km) climate projection has been developed on Prudence Project (Déqué *et al.,* 2004). In these works, United Kingdom was a pioneer with UKCIP project (Semenov, 2007). There are also many researches based on statistical downscaling (Bergström *et al*., 2001; Hanssen-Bauer *et al*., 2005). However, only regional approximation (*i.e.* grids size about 50 km) has been used on crop simulation (Challinor and Wheeler, 2008; Olesen *et al.,* 2007). This pattern is observed in others countries where recently it has been developed regional crop simulations: China (Xiong *et al*., 2009), U.S.A. (Doherti *et al*., 2003; Tsvetsinskaya, 2003) and Argentina (Magrin *et al*., 2009).

There are few projects for AOGCM downscaling for South America. The main are: CREAS (Regional Climate Change Scenarios for South America) in Argentina, Uruguay, and Brazil (Marengo and Ambrizzi, 2006), and Climate Variability on Chile for XXI Century (Fuenzalida, 2006). Both projects were developed in association with Hadley Centre and they used the PRECIS model and HadCM3 output as boundary condition.

2.6. Concluding remarks and future prospects

AOGCM coupled with crop models do not only project future scenarios, but also allow us to guide future policy making. If we can project climate change conditions and crop yields, we can evaluate and guide agronomic countermeasures such as: changing sowing dates, selecting the best crop (or cultivar) for the new conditions, moving crops to areas where conditions are suitable, building dams, improving irrigating systems, developing new varieties, fitting agricultural supply productions, among others. However, there are several issues to be solved.

First, we should use ensemble climate scenarios for supporting decisions based on crop modellig. Scenarios are defined without probabilities, and there are differences among AOGCM which produce uncertainties which improve when several scenarios and AOGCM are used. Current efforts on this matter are significant. For example, European project ENSEMBLES demonstrates the awareness and concern about climate change issue. In this way, new developments of the involved processes need: water vapor feedback, sulphured aerosols, and subroutines of these gas cycles. Moreover, it is important to build scenarios, which include thermohaline circulation effects, melting of permafrost soils, and volcano eruptions. This is a great challenge to improve climate projections. It is important to remark that several uncertainties on climate model outputs have been mitigated by computer technological advances, which reduce numerical diffusion.

Second, we need to improve crop models. Crop simulation modeling needs to be tuned and widely validated by local-scale scenarios for both global circulation models and local crop simulation together. In addition, crop models need to consider the non-stationary relationship between temperature and phenology (Zhang et al, 2008).

Third, a non-explored strategy for improving the linking crop model with climate model output is to define the optimal cells grid size, which allows represent the spatial crop variability using the minimum computing. This strategy could be based on topography, which is the main driver to determine the spatial climate variation.

Finally, downscaling allows the conversion of global scale to local scale. These techniques are able to simulate scenarios at agricultural management-scale, although few attempts have been performed. Besides, downscaling will extrapolate from CCM to microclimate conditions, which has not been applied for agricultural projections.

2.7. Acknowledgements

We acknowledge grant funding from grant by FONDEF DO6I 1100 “Sistema de Soporte de Decisiones Para Cultivos Tradicionales Basados en Integración SIG y Estaciones Meteorológicas”. Besides, R. Orrego was funded by a national grant (CONICYT Ph.D doctorate scholarship), and this study is also funded by Ph.D program of Ciencias de los Recursos Naturales (Universidad de La Frontera).

Chapter 3

Validation and correction of dynamically-downscaled projections of 21st century rainfall scenarios for the Araucanía Region

R. Orrego[1], R. Abarca del Río[2], A. Ávila[1,3] and L. Morales[4]

Paper submitted to Atmósfera

[1] Scientific and Technological Bioresource Nucleus, Universidad de La Frontera, Chile

2 Departamento de Geofísica, Universidad de Concepción, Concepción, Chile

[3]Centro de Modelación y Computación Científica, Universidad de La Frontera, Chile

[4] Departamento de Ciencias Ambientales y Recursos Naturales, Universidad de Chile, Santiago, Chile

3. Validation and correction of dynamically-downscaled projections of 21st century rainfall scenarios for the Araucanía Region

Abstract

In Chile, a mesoscale (25 km) database was generated by the Departamento de Geofísica, Universidad de Chile using HadCM3 and PRECIS model along all Chilean continental territory, hereafter DGF-PRECIS database. We compare the baseline DGF-PRECIS rainfall projection with *in-situ* rainfall records (56 meteorological stations) located in Araucanía region (37° to 40° S and 71° to 74° W), in order to validate and correct the climate projection (A2 and B2 scenarios of IPCC) at 25 km grid in our study zone. Araucanía region is important area because it concentrates about 35.4% of national cereal agricultural surface. Since one of the main climate driver in Chile is ENSO (not considered in DGF-PRECIS database), we also asses these effects comparing DGF-PRECIS database with the time span where the phenomenon occurs in order to test whether DGF-PRECIS database simulate the ENSO patterns on the region. Based on these comparisons we describe the main rainfall pattern on Araucanía region, and corrected the simulated climate dataset by computing a monthly ratio between *in-situ* and the modeled data. The result indicated that ENSO impact the PRECIS model output (DGF-PRECIS), which tended to underestimate the precipitation when La Niña and El Niño dominate. Only the neutral phase was well modeled with an error <30%. This do not affect the reliability of the climate projection, but could affect the futue climate variability estiamation. However the database presented a dryer summer and rainier winter. Consequently we corrected DGF-PRECIS using empirical coefficients values in Araucanía Region. Nonetheless, the previous results pose the questions why the DGF-PRECIS database does not perform well for La Niña and El Niño, and the extreme response differences of rainfall. To search for these errors we compared the DGF-PRECIS database with whole continental Chilean territory rainfall. However, there is an important lack of historical records baseline (1961 and 1991) to perform a proper validation at whole country territory. For increasing the rainfall density data a global mesoescale grid rainfall database from Global Precipitation Climate Centre (GPCC) was obtained. GPCC database was compared with *in-situ* meteorological records spread all over the whole continental Chilean territory (12240 records from 34 meteorological stations). As the difference between GPCC and in situ data was < 10 %, we conclude that the GPCC database can be used (including ENSO phases) to validate and correct DGF-PRECIS database. Our result indicated that DGF-PRECIS reproduced well the rainfall pattern from central to southern Regions (>30º S) under neutral conditions of ENSO influence. However, in the northern regions (< 30º S), DGF-PRECIS database showed unacceptable error (> 30 %). This was explained based on climatic pattern influenced by stationary Pacific Anticyclone in Northern Chile.

Key words: Mesoescale models, validation, climate change projection

3.1 Introduction

Due to ongoing and predicted future climate change (IPCC, 2007), studies investigating how these changes affect the agriculture and other socio-economic fields represents one of the main areas of worldwide interest field research (Mearns, 2001; Caldeira & Rau, 2000; IPCC, 2007). Atmosphere Ocean Global Climate Models (AOGCM) scenarios are used to enable policy makers to develop new environmental strategies and mitigation methods (IPCC, 2007). Several different prospective scenarios (see SRES 2000 for a review) have been projected, computing the potential economic and social impact of climate change with particular focus on population growth, environmental policies, technological growth, social inequality and globalization. Two scenarios have been investigated representing high CO_2 emissions (A2) and moderate CO_2 emissions (B2) (IPCC, 2007). In fact, they are used for assessing model by several researches (Krugër *et al*., 2012; Conde *et al*., 2011; Rupa Kumar *et al*., 2006; Räisänen *et al*., 2004).

Although physical laws which drive the atmospheric-oceanic circulation are well-identified, and the global-scale boundary conditions for modeling are well established with high precision (Collins, 2007; Räisänen, 2007), climate models have different error sources. Several authors have reported that AOGCM tend to overestimate the number of rainy days and underestimate the amount of rain falling as drizzle (Baigorria *et al*., 2008; Challinor *et al*., 2009). In addition, the validity of using AOGCM for projecting climate change is questioned by a number of unsolved remaining issues such as the impact on thermohaline circulation and its effect on climate (Clark *et al*., 2002), water vapor feedback (Cess, 2005), the potential increase in Methane caused by melting of tundra permafrost (Wille *et al*., 2008), and future changes in land cover (Räisänen, 2007). Furthermore, AOGCM were developed for global conditions (Zorita, 2000) and they produced low scale resolution climate projections (about 200 to 300 km). Downscaling techniques (Wilby *et al*., 2004), either statistical or dynamic (Zorita, 2000), are used to improve this information at a higher resolution. Although these techniques are commonly used worldwide (Karmalkar *et al*., 2013; Déqué *et al*., 2005; Bergström *et al*., 2001; Hanssen-Bauer *et al*., 2005), there are few projects carried out in South America, among them CREAS (Regional Climate Change Scenarios for South America) in Argentina, Uruguay and Brazil (Marengo & Ambrizzi, 2006) and Variabilidad Climática para el Siglo XXI performed recently for Chile (Fuenzalida *et al*., 2006). Adaptation strategies are evaluated and designed for local scales; hence, downscaling output validation is a very important challenge.

For use the AOGCM outputs as support for design adaptation strategies to climate change, we require that they are validated. This validation must be based on the phenomena which drive the climate pattern in a specific work domain. Several databases are developed combining models and historical dataset for validating forecasts and researching atmospheric behaviors. One of the main database is the Global Precipitation Climatology Centre (GPCC), which is a rainfall monthly term grid (Huffman *et al*., 1997). In the last version, this database has a 0.5° grid size and it contains historical rainfall records from 1900 up to 2013.AOGCM are developed for global conditions (Zorita, 2000) at low scale resolution (about 200 to 300 km). To minimize the impact of these errors, downscaling techniques are applied at higher resolution (see Wilby *et al.*, 2004 for a review).

Downscaling techniques are classified into statistical and dynamic (Zorita, 2000). Statistical downscaling consists of fitting a probability distribution (transfer function) based on the relationship between the data from the global-scale (predictors) and the data at a local-scale (predictands) (Hanssen-Bauer *et al*., 2005; Solman and Nuñes, 1999; Wilby and Wigley, 1997).

Other issues affecting the climate projection reliability is El Niño Southern Oscillation (ENSO) phenomenon. In South America, ENSO is one of the main drivers of the climate variability (Montecinos and Aceituno, 2003). It involves two phenomena: El Niño current, and the southern oscillation. Both phenomena affect the Pacific Anticyclone, the main barrier to the fronts which produce rain in southern and central Chile (Montecinos and Aceituno, 2003). El Niño is a warm current which move from the North Australia to central Chile when the Alisios winds (global winds which almost always run from central-southern Chile to North of Australia) are weakened. Southern oscillation is a temporal pattern in the difference between the pressure measured in two places Darwin (Australia, 12º 27' S, 130º 50ºW) and Papetee (Tahiti, 17º 32' S, 140º 34'W). In normal conditions Papetee shows higher pressures than Darwin, but when the El Niño current affect Chile, this relationship is shifted (Kiladis and Val Loon, 1988; Guevara-Díaz, 2008). Moreover, sometimes the pressure difference between Papetee and Darwin is increased which match with a cooling in the sea temperature in the coastal Chile (Kiladis and Val Loon, 1988). This phenomenon is called "la Niña". Thus three phases of ENSO are defined: La Niña, Neutral, and El Niño (Montecinos and Aceituno, 2003). There are several criteria to define the ENSO phases, which are based on: i) sea surface temperature anomaly on specific zone, and ii) pressure difference anomaly between Papetee and Darwin. For the last criterion the most used is the called Southern Oscillation Index or SOI (Kiladis and Val Loon, 1988; Guevara-Díaz, 2008).

Althoght ENSO is not explicitly included in long-term projections from AOGCM (Räisänen, 2007) both, La Niña and El Niño synoptic condition are obseved in the simulated long term time series. Assessing the rainfall pattern under non-neutral ENSO phases allow to understand the climate varability under extreme condition. However, since La Niña and El Niño conditions are not the typical pattern, it is required to check if climate models represent the climate variability under these phases, which are not performed for Araucania region.

The first Chilean projection was performed by Departamento de Geofísica from Universidad de Chile (DGF) with a dynamic downscaling of Hadley Centre Coupled Model (HADCM3) output through the PRECIS model (Fuenzalida *et al*., 2006) and involved projecting baseline data (between 1961 and 1991) together with A2 and B2 scenarios (between 2070 and 2100) at 0.25º resolution in Chile. The result showed a temperature increases along the country with a decrease in rainfall in northern (18º-30º S) and central regions (30º-40º S). This database (hereafter DGF-PRECIS) project a rainfall decreases produced an increased in the evapotranspiration, and lower summer snow reserves.

Climate projection is especially important for the Araucanía Region, which is located between 35° 35' S and 39°37' W and between Argentina and the Pacific Ocean, because agronomic economy is largely composed of rainfall-dependent agriculture (INE, 2010). Its climate is characterized by a dry season between December and March with

minimum rainfall varying from 50 to 70 mm *per* month, and a wet season from May to September with maximum rainfall of about 250 mm *per* month. Annual precipitation ranges between 800 and 1200 mm *per* year (about 45% is received between May and August; Rouanet, 1983). Within the seasonal/annual temperature cycles, the warmest months are from December to February, which show a temperature mean about 15 °C (with a maximum of 25-27 °C and minimum of 10 °C). Mean winter (June to August) temperatures are about 8 °C (with a registered maximum and minimum of 12 °C and 4 °C, respectively) (Rouanet, 1983). This zone is affected by ENSO cycles (Montecinos and Aceituno, 2002).

The aim of this research is to build a complete precipitation database with the seasonal rainfall influence under El Niño, La Niña conditions to evaluate the impact of ENSO condition on rainfall. We also include the neutral effect without ENSO influence. The second goal of this study is to compare the baseline between 1961 and 1991 of HadCM3downscaled by PRECIS dynamic downscaling projections, particularly for the different ENSO conditions, and based on this comparison, to generate a corrected projection for the A2 and B2 climate change scenarios. The expected result will give a reference framework for measuring the impact of the high resolution model performances.

3.2 Data and Methodology

3.2.1 Dataset

We selected 56 meteorological stations located in the Region (Figure 3.1) with a complete rainfall records from 1961 to 1991 (see below), whereas a few stations (5) presented other climate records such as photosynthetically active radiation (PAR) and temperature. Using the rule of decade continuous years or 15 years of non-continuous precipitation records between 1961 and 1991, The 10 selected stations were used for calibrating the mesoscale DGF-PRECIS database, whereas the 46 remain were used to validate the model. These criteria were defined to include the records within one Pacific Decadal Oscillation, which is the main source of climatic variability in the Region (Newman *et al.*, 2003). To complete the data gaps, the extended discrete Fourier transformation (Zhang *et al*., 2008) was used. To check the data quality, we used the 'double mass curves' method (Searcy and Hardison, 1960). This method is based in a regression models between the cumulated rainfalls in two close meteorological stations. This approach has been used successfully in several studies, including validation of Galician rainfall records (Mirás-Ávalos *et al*., 2009) and the development of ecologically relevant hydrological indexes by the United State Geological Service (USGS; Esralew and Baker, 2008).The remain meteorological station was used for validating the results

3.2.2 ENSO classification

For assess the impact of ENSO on rainfall pattern and climate projection, we require defining the ENSO phases for both: observed and simulated condition. When the ENSO is in positive phase (*i.e.* Niño) there is a high temperature in the Pacific Ocean, whereas when

ENSO is in negative phase (La Niña) there is less temperature in the Pacific Ocean. This can be assessed in many places defining the ENSO index which are differences (anomaly) between the normalized sea surface temperatures respect to the averages of a reference period (1971-2000), defined in an specific zone. The most common is the ENSO 3.4 which is defined between 120W-170W and 5N-5S.We started classifying the *in-situ* data into ENSO and Neutral years according to IRI criteria (see Guevara-Diaz (2008) for a review) based on ENSO3.4 index (http://iridl.ldeo.columbia.edu/) to classify months as representing 'La Niña', 'El Niño' or 'Neutral' conditions. The sea surface temperatures were downloaded (available at http://www.ipcc-data.org/) from 1961-1989 and the relative ENSO3.4 index values were computed using IRI methodology.

The same methodology was applied on the HadCM3 output. Sea surface temperatures were downloaded from the HadCM3 baseline (1961-1991) scenario (available at http://www.ipcc-data.org/) to construct analogue IRI criteria ENSO3.4 index and classify the output according to ENSO cycles.

To assess the ENSO impact on climate rainfall condition, we compare the monthly climate average of each ENSO phases over this baseline time span (1961-1991). These differences were also mapped for identifying the spatial pattern of the ENSO effect. Mapping was performed by interpolation by ordinary kriging (Isaaks and Srivastava, 1989). Both: Monthly rainfall and map are summarized at seasonal level. Finally, we compute rainfall histograms to assess the frequency of the rain and dry month. These histograms were computed using the module *Data Analysis* of Microsoft EXCEL considering intervals of 50 mm.

We also evaluate the statistical significance of the impact of ENSO events of rainfall database HadCM3 downscaled by PRECIS to evaluate its three phases: El Niño, La Niña and Neutral years. , We used a one-way ANOVA test with a 95% significance level performed in the module *Analisis de Datos* of Microsoft EXCEL. ANOVA is a test which assess if there are significant differences among three or more clusters, evaluating the significance of the variable used for defining the clusters. Thus, the sum of the square of the differences among the mean of each group (variance between clusters, in our case the ENSO phases) should be higher than the sum of the square of the differences between each observation. The rate between both values follows a Fisher distribution (F), which allows evaluate the significance of the relationship. When this rate is higher than the critical F value there are significant differences among ENSO conditions (Wilks, 2006).

To performe a most robust test, we used Montecarlo analysis. Montecarlo analysis consists in fit a stochastic model based on the observed data for producing a syntactical data series, which follow the same probabilistic distribution than the observed data. 10.000 rainfall data was generated based on Weibull distribution, which was fitted for each ENSO-condition using the *In-situ* database. Thus the ANOVA was performed using the syntactical instead to the observed data.

3.2.3 Comparison of meteorological records and DGF-PRECIS Outputs.

To assess the DGF-PRECIS outputs, we download the downscaled from the web site of "Variabilidad Climática en Chile" (http://www.dgf.uchile.cl/~maisa/modelacion_climatica/)

performed by Departamento de Geofísica de la Universidad de Chile funded by Comisión Nacional del Medio Ambiente. Since databases was obtained in Net-CDF format, we use a routine programmed in the software MATLAB for pick-up the values corresponding to each meteorological station.

For validating, we compared the downscaled projection over the corresponding baseline for HadCM3 (1961-1991) with its corresponding *in-situ* measurement through regression analysis. Thus, confidence intervals of slope, intercept and standard error were computed. General output trends were also evaluated by global statistics and histogram analysis, because climate models produce results in the form of projections rather than forecasts. Residual and spatial analyses were also performed by mapping *in-situ* and projected annual cumulative precipitation using ordinary Kriging techniques (Isaaks and Srivastava, 1989). Both evaluations were initially carried out using the whole database, and separating ENSO (El Niño, La Niña) and non ENSO (Neutral) conditions defined in 2.2. For all analyses, we considered the whole database in the region

3.2.4 Projected dataset correction

The final step involved the calibration of HadCM3downscaled by PRECIS precipitation data with the *in-situ* time series records to correct the projected rainfall database. Here, we propose a calibration coefficients based on differences between simulated and measured monthly records of precipitation (3.1).

$$fr_m = \frac{rm_m}{re_m} fe_m \qquad (3.1)$$

where fr_m is the corrected projection, rm_m is the monthly average of measured data, re_m is the monthly average of estimated data and fe_m is the HadCM3 downscaled by PRECIS projected data. This coefficient was computing using all the *in-situ* data, obtaining a globally coefficient for each month. Thus the final product is the same DGF-PRECIS dataset (the same grid) but without bias.

3.2.5 Extend climate model validation and ENSO effect over the whole continental territory.

Finally we analyzed the general trend of model performance in the whole continental territory for understanding the error models. This work repeats the same methodology used for Araucanía region. However, is observed a lack of *in-situ* data for validating the model in the whole country considering explicitly the spatial pattern of the rainfall. For solving it we validated the model using the Global Precipitation Climatology Project (GPCC) database. This database is based on a merged analysis incorporating precipitation estimated from low-orbit-satellite microwave data, geosynchronous-orbit-satellite infrared data, and rain gauge observations (Huffman et al., 1997). This database originally provides monthly mean

precipitation grids on a global resolution of 2.5° × 2.5° for the period 1986–2000. However, the 3rd version is a monthly rainfall on a global 0.5° x 0.5º grid (about 50 km of grid cell size) from 1901 to 2007. This database is available in the World Wide Web on the site http://climexp.knmi.nl/selectfield_obs.cgi. We spatially interpolated the database using a bilinear method from the original 0.5° to an overlapping 0.25° to PRECIS database for generating a monthly rainfall grid dataset from 1961 to 1991

For whole country validation, the first step was validated the GPCC database. We selected 34 *in-situ* rainfall complete records which are spread over all the Chilean territory. Since Coastal and Andean Cordillera are not regarded, we select *in-situ* records located over the latitude between 17ºS and 56ºS S. Based on these criteria, only 34 meteorological stations were chosen for this research (Figure 4.1). Moreover, we select eight meteorological stations to observe the typical climate patterns in different climate zones. Six of them are located on the typical climate types defined on the genetic classification (Peña y Romero, 1977). These station are: Iquique (20°12'S, 70°11'W) and Copiapó (27°21'S, 70°24'W) for northern zones, San Felipe (32°45'S, 71°15'S) for central zone, Temuco (38°45'S, 72°38'W) for central-southern zone, and Punta Arenas (53°10'S, 70°54'W) for southern zones. The remains two are located near of the boundary of these zones. These are: Concepción (36°50'S, 73°3'W) the limit between the central and the southern zone, Puerto Montt (41°28'S, 72°56'W) the rainiest forest zone, and Chile Chico (46°36'S, 71°41'W) for Patagonia zone (Figure 3.1)

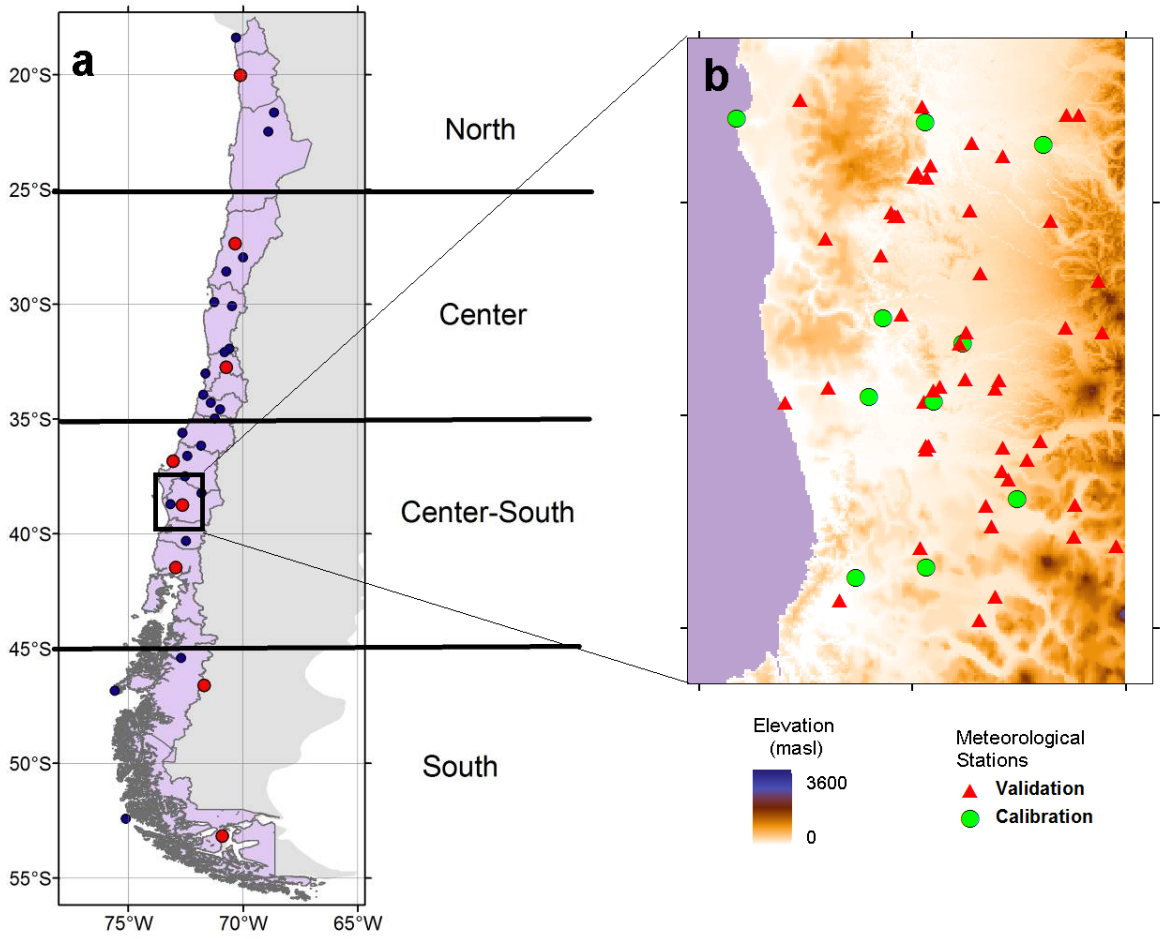

Figure 3.1.*Meteorological station network used in this work. a) show the stations used on whole country validation. Here in red are showed the station used as reference for different climate zones. Sorted from North to South they are: Iquique, Copiapó, San Felipe, Concepción, Temuco, Puerto Montt, Chile Chico, and Punta Arenas. In b are showed the station used in Araucanía región validation overlapped over a digital elevation model. Triangles show the station used for validate the database and cycles show the station used for corrected the model.*

3.3 Results

3.3.1 Regional climatology

Our analyses show that Araucanía Region is characterized by mean annual accumulated precipitation of 1497±59 mm. From a geographic point of view, a positive precipitation gradient from North West to South East is observed. The largest rainfall amount is observed over the South East (39-39.5º S, 72.5-71.5º E) about 1000 to 2500 mm *per* year and the lowest, about 800 mm *per* year over the West coast (37-37.5º S, 73-73.5º E) increasing in a

gradient of 4.78 mm km^{-1}. Higher rainfall levels occur during autumn-winter (May-July, of about 250 mm *per* month) and lower levels during summer-autumn (Jan-Mar, 40-50 mm *per* month) (Figure 3.1a). The left-skewness of the monthly precipitation curve shows that most monthly precipitation is distributed between 5 and 150 mm *per* month, with a median of 90 mm *per* month (with a roughly frequency of 7%) and a peak of 25 mm *per* month(14%) (Figure 3.1b). Months without rainfall occur with a frequency of about 4.18% (Figure 3.1 b). During the research period from January 1961 to December 1991, we observed 17 months under La Niña and 39 months under El Niño influence. The precipitation was distributed in three events for La Niña and four events for El Niño.

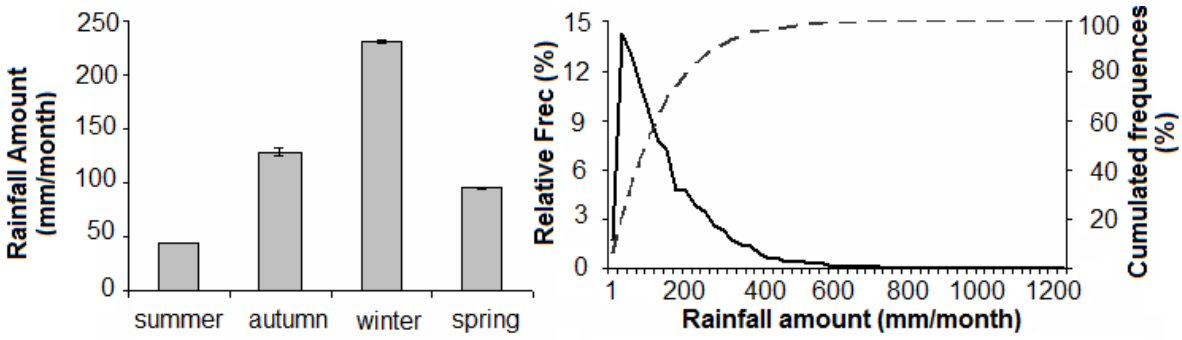

Figure 3.1 *(a) Seasonal precipitation cycle (bars represent standard error) and (b) relative (solid line) and cumulative (dashed line) frequencies of* monthly *precipitation.*

3.3.2 ENSO Effect

Since ENSO is one of the main Chilean climate drivers, we focused our description on its variability. During the research period Jan-1961 to Dec-1991, we observed 17 Niña months and 39 Niño months corresponding to three Niña events and four Niño events. General rainfall spatial distribution patterns were similar under all ENSO conditions. However, there are significant differences among ENSO conditions, which change depending on zone and season. This is a different pattern respect to other Chilean regions classified in the same Mediterraneal clime, where El Niño condition implies rainny years and La niña condition implies dry years (Montecinos and Aceituno, 2002).

During El Niño events, the mean accumulated precipitation is 1600 mm *per year*, to an increase in annually received precipitation of 103 mm *per year*. On the contrary, under La Niña conditions, the mean accumulated precipitation is 1200 mm *per year*, a reduction of about 297 mm *per year*. The winter and spring months of El Niño years are rainier (about 9%, *i.e.* +14 mm *per month*) than those in neutral years, whereas the summer and early autumn months of El Niño are less rainy (50%, *i.e.* 21 mm *per month*) than in neutral years (Figure 3.2 a). In contrast, La Niña winters are rainier in June and July but lesser rainfall in August producing that winter rainfall is less than Neutral rainfall (about 8%, *i.e.* 3.92 mm *per month*). In addition, there is also less rainfall during the rest of the year, except for May (Figure 3.2a). Thus, the rainiest months also change with ENSO conditions. These are July (254 mm) under El Niño, May (303 mm) under La Niña, whereas June (277 mm) is generally under neutral conditions.

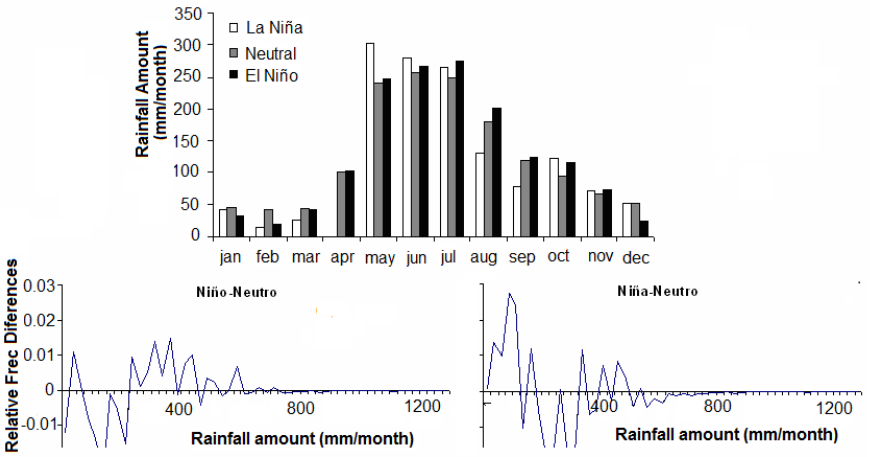

Figure 3.2. *(a) Annual rainfall cycles of ENSO scenarios and differences in* monthly *rainfall amount frequencies between (b) El Niño - Neutral and (c) La Niña - Neutral conditions.*

Rainfall spatial distribution patterns are similar under all ENSO conditions, although a small decrease in the latitudinal precipitation gradient occurs during El Niño and a small increase under La Niña. During winter period, La Niña events are generally characterized by greater precipitation levels in the northern western zone (37º S, 73º W) and reduced levels in the southern-eastern zone (39º S, 72º W), which is generally the region where it rains most. This pattern is reversed under El Niño conditions (*i.e.* during El Niño winters, greater precipitation levels are observed in the South East and lesser in the North West. In terms of the differences in monthly rainfall amounts in ENSO respect to Neutral years, an increase in the number of months of high rainfall (200 mm *per month*) was observed under El Niño conditions (Figure 3.2 b), whereas the inverse pattern occurs under La Niña conditions (Figure 3.2 c). These trends confirm ANOVA test of the Montecarlo analysis outputs, which showed that the rate between the sum square averages between cluster (variance explained by each ENSO condition) and inside cluster variance (total variance) is higher than the Critical *F* values. Therefore, there are significant differences among ENSO conditions.

3.3.3 Evaluating model output

Regression models are developed to assess the lineal correlation between two variables, hence fitting a linear model ($y=ax+b$) between a predictor variable (x) and a predictand variable (y) (Wilks, 2006). Regression model also assesses the explained variance for the model by a R^2 coefficient. Although regression analysis tends to mask biases (see Wilks, 2006) and it has been criticized by several authors as a method for validating models (Mitchell, 1997), it was used here only to investigate general trends.

Regression analyses performed on both models show that the intercept confidence intervals do not span zero, which means that some biases in estimation may arise. The same

situation occurs regarding slope, in which the intercept confidence intervals are significantly lower than one (Table 3.2), meaning that models also overestimate rainfall.

Table 3.2. *Results of in-situ/simulated regression analysis. Intercept and slope are the parameters obtained out of the fitting of regression between measured (in-situ) and modeled data. Adjusted R^2 is the Pearson coefficient adjusted by degrees of freedom, and P value is the probability the slope will be equal to zero (in our case all P-values are close to zero, thus correlations are significant).*

		HADCM3 (1961-1991)			
		All	La Niña	Neutral	El Niño
Intercept	Min.	33.498	3.4537	34.844	16.1486
	Mean.	39.2837	25.6956	41.2837	32.2852
	Max.	45.0695	47.9375	47.7235	48.4218
Slope	Min.	0.7242	0.5487	0.7261	0.6516
	Mean.	0.7573	0.6969	0.763	0.7375
	Max.	0.7903	0.8451	0.7999	0.8234
Adjusted R^2		34.75%	29.52%	34.45%	38.56%
P Value		0	0	0	0
N		3782	204	3125	453
Standard error		113.471	113.471	128.7451	119.327

HadCM3 outputs are fitted to ENSO pattern. In fact, La Niña years are drier than Neutral Years in both models, whereas El Niño years are wetter than Neutral years, which is consistent with the observed rainfall pattern in the region (Figure 3.3).

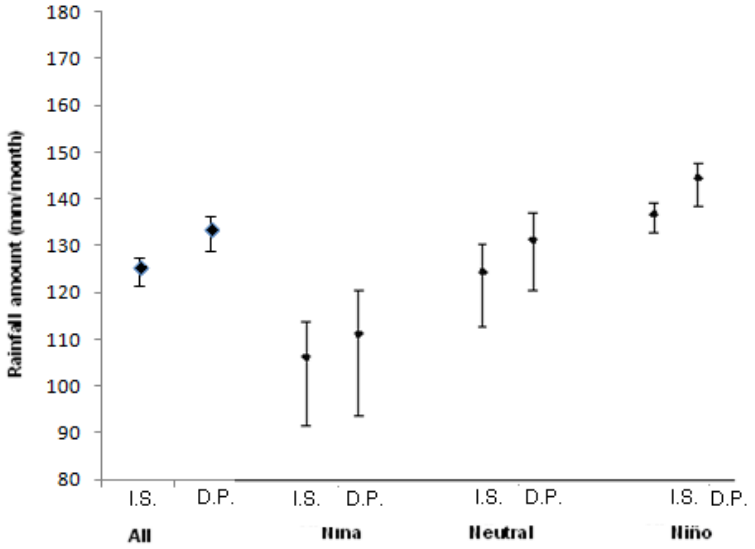

Figure 3.3. *Mean precipitation for In-situ (I.S.) and projected by DGF-PRECIS (D.P.) values under all and ENSO conditions and for global simulation (All). Error bars represent standard error (over) and 95% significance values (under).*

Simulated mean monthly rainfalls (134 mm for HadCM3 in 1961-1991) are higher than the *in-situ* measured values (125 mm for 1961-1991), which confirm the overestimation observed in the previous analyses. This pattern is observed under all ENSO conditions (Figure 3.3). Model error bars overlap (Figure 3.3), which means that there is no significant difference between the *in-situ* measurements and simulated data (Figure 3.3). This fact agrees with the statistical significance testing carried out on the residual (*in-situ* measured vs. modeled) analysis with a T-test (95% significance level; Kleijnen, 1995). In this analysis, we obtained no significant differences between measured (*In-situ*) and HadCM3downscaled by PRECIS rainfall (-8.9 mm representing only less than 7% of the amount of measured annual rainfall).

In relation to monthly rainfall distribution, both models (although we only present HadCM3) present greater seasonal variability than the observed cycle (Figure 3.4a). In fact, simulated summer months are drier (38.3%, *i.e.* -16.8 mm *per month*) whereas simulated winter months are wetter (15%, *i.e.* +34.6 mm *per month*) than those measured (Figure 3.4a). Under El Niño conditions (Figure 3.4d), seasonal distributions of monthly rainfall are overestimated, except during the summer months. In contrast, La Niña conditions are well-estimated for February, March, June, August and October, although there are important differences over the rest of the year (Figure 3.4b).

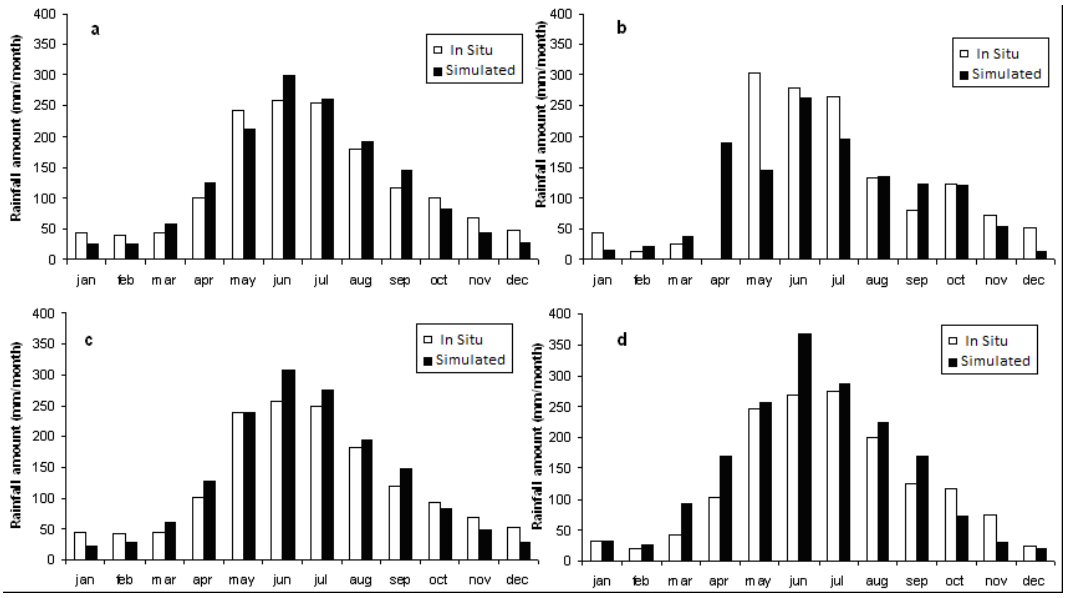

Figure 3.4.*In-situ and simulated (HadCM3 downscaled by PRECIS downscaled)* monthly *rainfall for All-data (a), La Niña condition (b), neutral condition (c) and El Niño condition (d).*

Geographically speaking (Figure 3.5), HadCM3 downscaled by PRECIS underestimates rainfall levels in the North (by about 10%, *i.e.* -10 mm *per month*), and it overestimates them in the South (by about 30%, *i.e.* +50 mm *per month*) under Neutral

conditions. A similar pattern occurs under El Niño and La Niña years, where the model underestimates northern and overestimates southern rainfall rates by about the same values (Figures 3.5b, 3.5c and 3.5d).

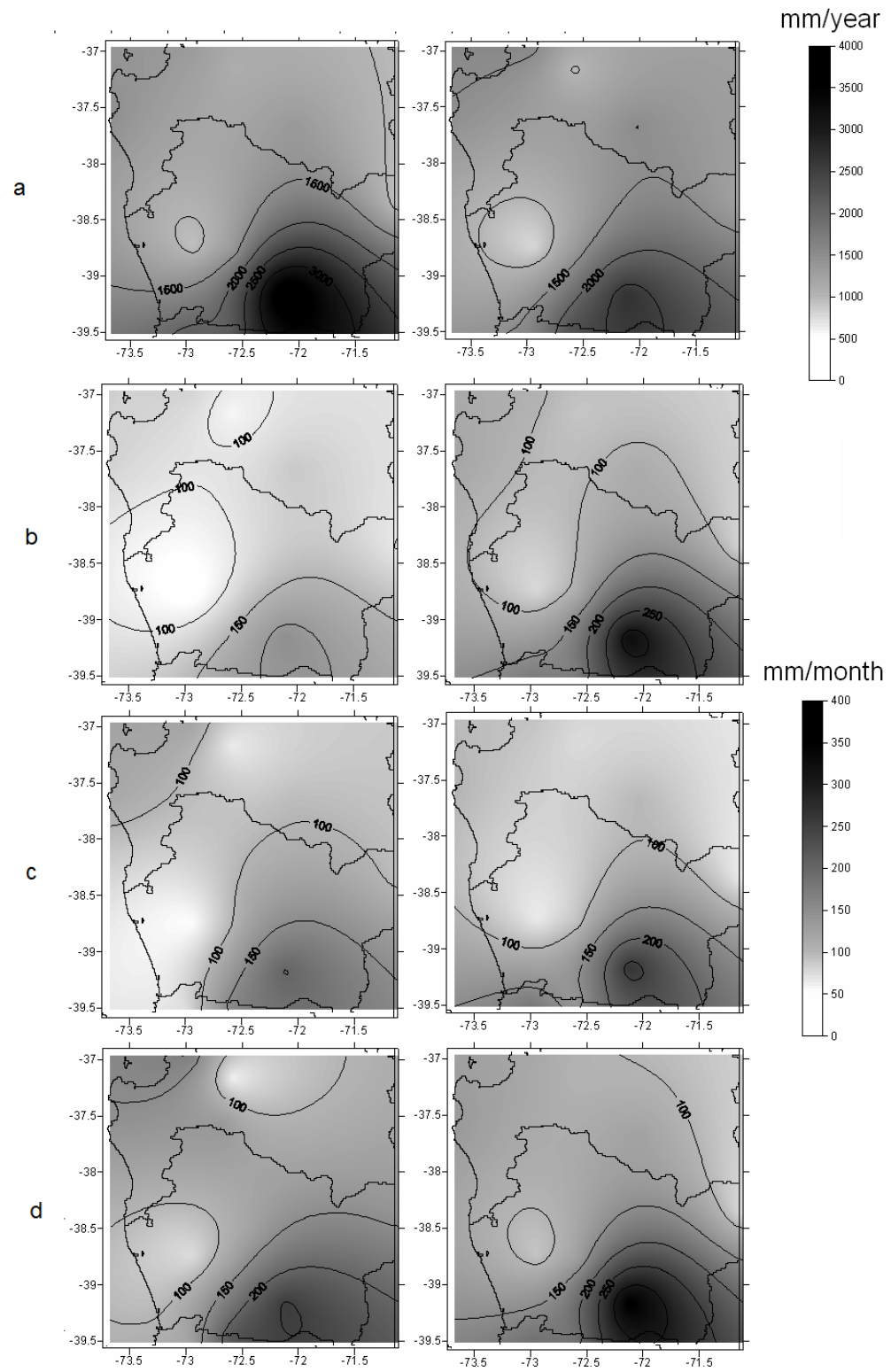

Figure 3.5. *Spatial patterns of measured (in-situ) (left) and HadCM3 downscaled by PRECIS projection over the base line period (1962-1991) (right), considering (a) annual precipitation, (b) averaged 'La Niña' condition, (c) average Neutral condition and (d) averaged 'El Niño' condition.*

Rainfall histograms show a significant overestimation of small rainfall events, with the peak at 50 mm more prominent in the simulated curve than the *in-situ* measurements. This pattern is a good representation of the drizzle effect discussed earlier, which is inherent in all AOGCM (Baigorria *et al*., 2008). Indeed, the HadCM3 downscaled by PRECIS output does not include any months without precipitation, in deep contradiction with the *in-situ* data.

3.3.4 Projected climatology

It is necessary to correct these errors to accurately investigate the projected variability for the last decades of the 21st century (1961-1991) because the model has biases and it also overestimates some values. Therefore, empirical coefficients were obtained based on equation 3.1 to correct the dataset (Table 3.3).

Table 3.3.*Coefficient and change observed under both climate change scenarios. Original refers to the original HadCM3downscaled by PRECIS projection output.*

Month	***In-situ*** **Mean**	**Coefficient**	**Original A2**	**Corrected A2**	**Original B2**	**Corrected B2**
Jan	43.20	0.61	16.04	26.16	10.62	18.68
Feb	39.76	0.78	24.46	31.21	23.22	31.51
Mar	43.40	1.63	45.62	28	53.93	34.03
Apr	100.30	1.40	101.66	72.42	118.06	84.51
May	242.12	1.01	196.65	194.97	228.62	230.13
Jun	259.01	1.23	228.88	185.49	267.34	215.19
Jul	254.25	1.09	209.72	192.62	247.76	229.08
Aug	180.56	1.09	158.58	145.6	220.12	197.86
Sep	117.31	1.28	77.26	60.54	119.61	93.72
Oct	99.87	0.83	39.74	47.67	57.25	68.87
Nov	68.70	0.63	20.2	32.01	24.27	39.11
Dec	48.52	0.56	14.28	25.46	12.72	22.65
Sum	**1497.01**		**1133.09**	**1042.15**	**1383.52**	**1265.34**

Corrected scenarios show a decrease in annual precipitation, which is greater under A2 (a decrease of 30.38%, *i.e.* 458 ±42.4 mm *per year*) than under B2 scenario (15.48%, and 235±87 mm). In both cases, the corrected scenarios represent a greater reduction in precipitation than the original projection simulation (24.3% and 7.6%, *i.e.* 363.92 and 113.6 mm *per year* for A2 and B2 respectively); see Fuenzalida *et al*., 2006 (Figure 3.6).

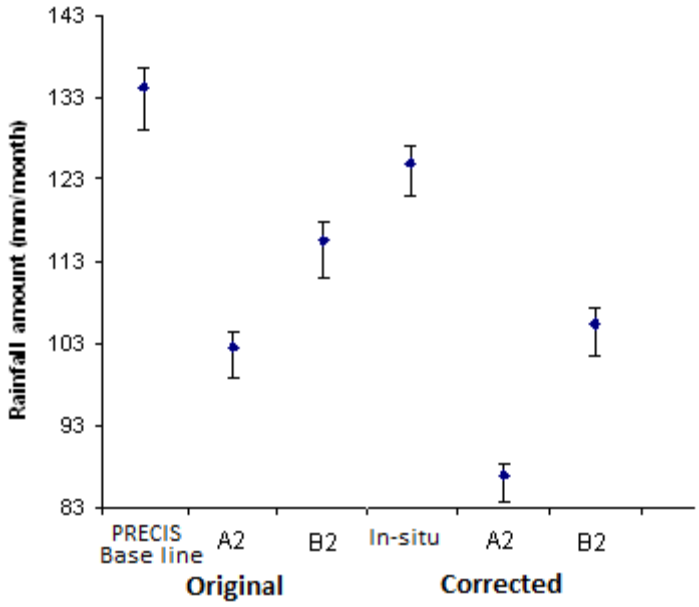

Figure 3.6.*Original and Corrected* monthly *mean rainfall values for all baseline (1962-1981), A2 and B2 scenarios. Error bars represent standard error (over) and 95% of the value based on a T-distribution probability (under).*

Under both scenarios the reduction in precipitation is higher for Summer (37%, *i.e.* 16.2 mm *per month* for A2; 45%, *i.e.* 19.6 mm for B2) and Spring (51%, *i.e.* 48.6 mm for A2; 29%, *i.e.* 28.1 mm *per month* for B2) than for Winter (25%, *i.e.* 56.7 mm *per month* under A2; 7%, *i.e.* 17.2 mm *per month* for B2) and Autumn (23%, *i.e.* 30.1 mm *per month* for A2, and 10%, *i.e.* 12.4 mm for B2). Besides, in both scenarios the reductions are less for Autumn and Winter than the original projection (11%, *i.e.* 14.5 mm *per month* and 14%, *i.e.* 34.13 mm *per month* for A2 Autumn and Winter, respectively, and 4%, *i.e.* 5 mm *per month* and 6%, *i.e.* 14 mm *per month* for B2 Autumn and Winter, respectively) and higher for Summer and Spring (52%, *i.e.* 34.9 mm *per month*, and 58%, *i.e.* 9.5 mm *per month* for A2 Summer and Spring, respectively, and 30%, *i.e.* 19.9 and 65%, *i.e.* 10 mm *per month* for B2 Summer and Spring, respectively) (Figure 3.7).

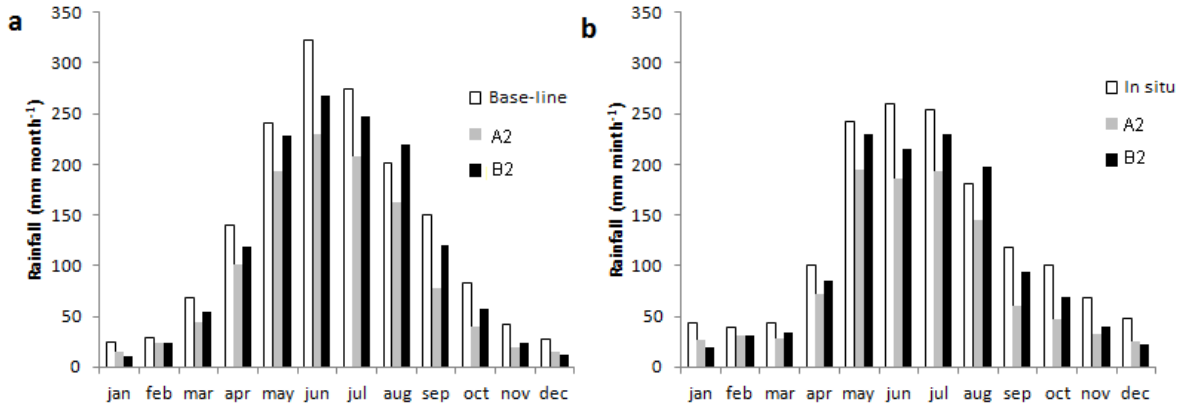

Figure 3.7 *Simulated* monthly *rainfall for all scenarios considering (a) original HadCM3downscaled by PRECIS values and (b) corrected values (current conditions is the in-situ values).*

Although the corrected projections suggest less rainfall during winter and autumn which may explain the lower annual accumulated values, the main differences are observed in summer. The correct summer projection predicts more rain (24 mm) than the original simulation of summer (15 mm). On the other hand, both projections increase the rate of months with lower rainfall (less than 100 mm *per month*) from 57.17% to 68.52% and 64.12% for A2 and B2, respectively. In contrast, there is a small difference of the high rainfall months (more than 450 mm *per month*) from 2.87% to 1.15 and 3.29% for A2 and B2 respectively.

It is interesting to notice that the spatial pattern of precipitation predicted by the climate change scenarios shows that mountain precipitations will increase (by about 120 mm *per year* under scenario A2 and 300 mm *per year* under B2) whereas coastal precipitation will decrease (by about 700 mm *per year* under A2 and 400 mm *per year* under B2). In addition, an increase in precipitation in the north east of the study area, of about 700 mm *per year* under B2 and 70 mm *per year* under A2 is observed (Figure 4.8). In contrast, there is an important decrease in the South of about 800 mm *per year* under A2 and 100 mm *per year* under B2. This is of particular significance, because this area usually experiences the highest levels of precipitation and, as a result, it has become the location of important agricultural centers.

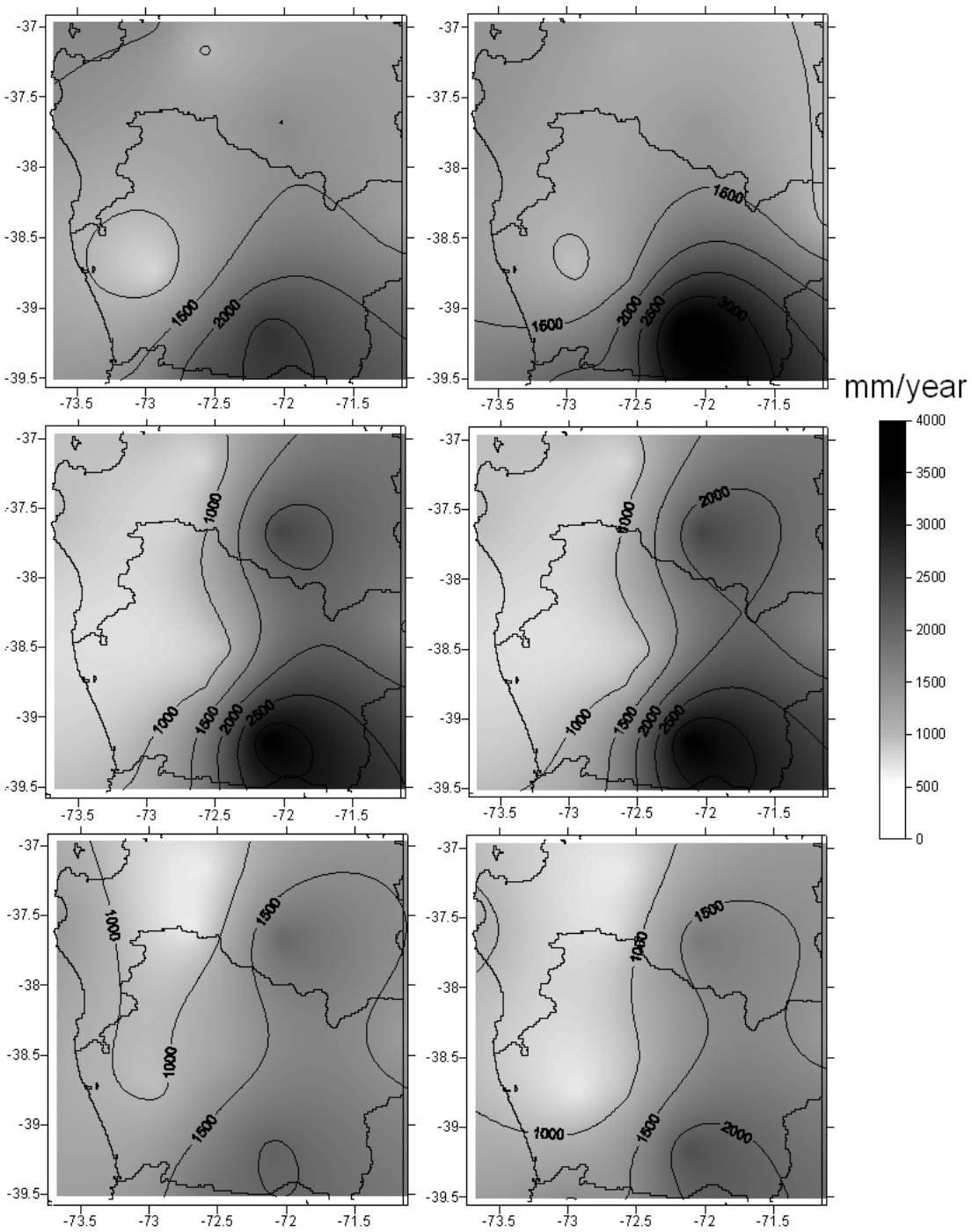

Figure 3.8 *Spatial patterns of precipitation for original (left) and corrected (right) values under (a) Current (baseline epoch, 1961-1991), (b) A2 (2070-2100) and (c) B2 (2070-2100) scenarios.*

3.3.5 Whole country results

3.5.1 Evaluating GCPC database through *in-situ* meteorological data

GCPC annual accumulated amounts data follow the meteorological record pattern (Figure 3.9 a). In fact, regression analyses show that the intercepting confidence intervals do not span zero, which means that some biases in estimation appeared. The same situation occurs with slope, where the confidence intervals do not include 1. However, there are two stations (Embalse Lautaro 27° 58'S 72°W and Puerto Aysen 45° 24'S 72° 42'W) showing overestimation between GCPC and *in-situ* annual cumulate data (R^2 of 0.43 and 0.88 respectively). The same pattern was observed when we considered the long -term average scale (Figure 3.9 b), where both stations show very high correlation (R^2 of 0.99 and 0.92 respectively), but they are far from the bisector. We suggest that records have uncertainties since both stations are independent and they are located on remote zones with problems for collecting data.

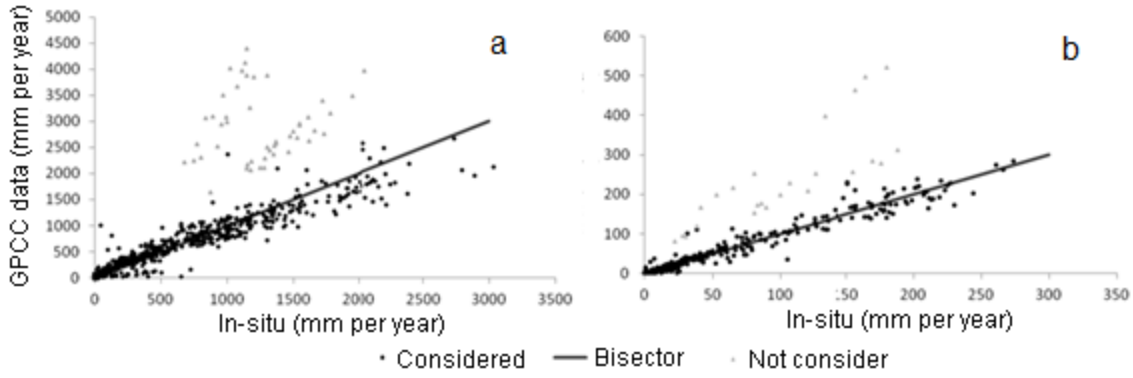

Figure 3.9. *Scattered plot among in-situ records and their corresponding GCPC data. In the figure all the cumulate* year *amount (a) and* month*ly the climatic average are showed (b). Gray dots show Embalse Lautaro and Puerto Aysen outlier stations.*

Since a high correlation is observed between GPCC and *in-situ* dataset at both levels (annual amount and long term averages), we used the GPCC database fitted to the DGF-PRECIS climate pattern. Therefore, we use it for describing Chilean climate patterns, and for correcting the PRECIS dataset.

3.3.5.2 ENSO Effects

In the northern Region (from the northern boundary to 25°S), a permanent dry condition takes place (Figure 3.10). However, Altiplano rainfall increase takes place (about 100%, 500 mm) in La Niña months, but a very small increase (about 4%, 20 mm) in the Altiplano rainfall under El Niño. Both issues could affect the neighboring zones. On the remaining months, there were no observed important differences among ENSO conditions.

In the central Region (from 25°S to 35.5°S), there was about 20% rainfall increase under El Niño and a decrease under La Niña from 3 mm onto 40 mm on the southern boundary (Figure 3.10). This pattern has been reported by several authors and it is a

characteristic of this zone (Montecinos and Aceituno, 2003; Di Castry and Hayek, 1976). In summer, it is observed that zone without rainfall is larger under La Niña than under Neutral and El Niño conditions (Figure 3.10b). In fact, the northern boundaries of these zones are at 31° 30’ S under Neutral and El Niño conditions, but 29° 00' S under La Niña condition. Notice that there are no changes at the southern boundaries.

In the southern-central Region (from 35.5°S boundary to 42°S), the increase is less than in the north (Figure 3.10). In fact, this trend is reverted with respect to the Neutral condition at 40°S. On the other hand, during El Niño events on this zone, the observed rainfall increase is about 1%. This zone is commonly included in the central zone, but some authors identify ENSO difference pattern. In fact, Montecinos and Aceituno (2003) reported differences in wet years and dry years when comparing rainfall among 30°S-35°S, 35°S-38°S and from 38°S to 42°S.

In the southern zone (from 42° to southern boundary), ENSO effect is changing through seasons (Figure 3.10). In summer, there is a rainfall decrease under La Niña (about 30%, i.e about 33 mm) and no clear effect under El Niño (Figure 3.10b). In autumn, a small rainfall decrease under El Niño condition is observed and no clear effect under La Niña 30% (Figure 3.10d). In winter, there were no effects on rainfall due to ENSO (Figure 3.10c). In spring, there is a rainfall increase under La Niña (20%), and no clear effect under El Niño (Figure 3.10a).

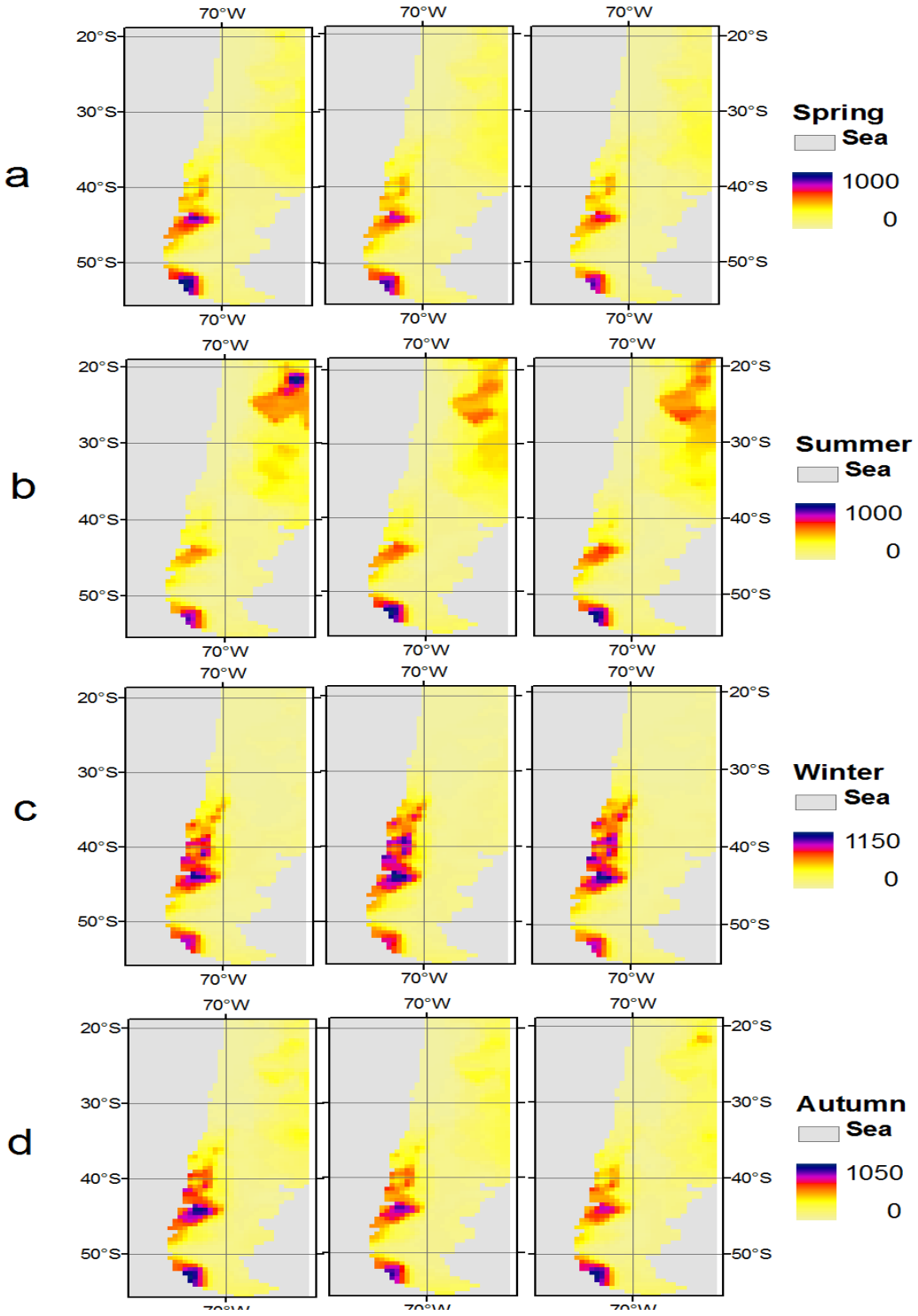

Figure 3.10.*Seasonal map for each ENSO condition. a) Spring, b) summer, c) winter, and d) autumn. Left images show La Niña, central images show Neutral condition, and the right ones show El Niño conditions*

In the North (Iquique), most records correspond to no rainfall and ENSO does not show any clear effect on this zone. In the northern-central transition zone (Copiapó), we observed the typical pattern in the Southern Pacific Anticyclone influence zone, *i.e.* a rainfall increase during El Niño and a rainfall decrease during La Niña. However, we observed an area increase without rainfall under El Niño.

In the central zone (San Felipe), Montecarlo simulation shows the expected pattern, *i.e.* a rainfall increase during El Niño and a rainfall decrease during La Niña. In fact, we observed a14% increase in months with rain over 4 mm during El Niño, but there are practically no events under La Niña condition. This effect is noticed in the dry months, which increase in 100% under La Niña, and decrease in 50% under El Niño (Figure 3.11).

In southern-central transitional zone (Temuco, Concepción), there is over 150 mm increase in rainy months and a 75 mm decrease in rainy months amounts, but under El Niño event there is an increase in the no-rain months (Figure 3.11d).

In the limit of the southern-central zone (Puerto Montt), we observed a rainfall decrease about 20% under El Niño and 60% under La Niña (Figure 3.11e). South (Chile Chico and Punta Arenas) is out of the influence of ENSO zone (Figure 3.11f).

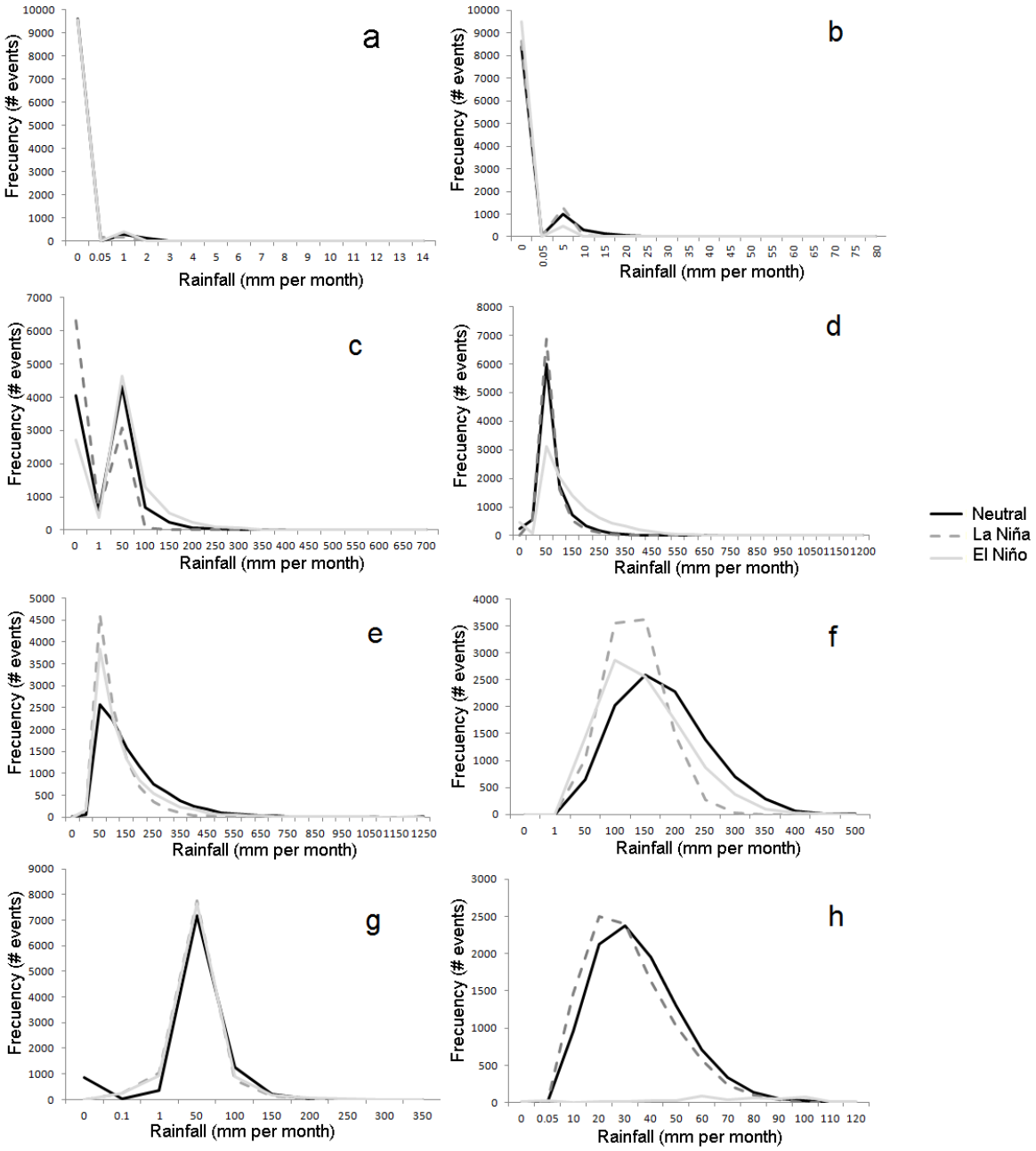

Figure 3.11. *Histograms of rainfall in each selected in-situ meteorological station considering each ENSO phases. a) Iquique, b) Copiapó, c) San Felipe, d) Concepción, e) Temuco, f) Puerto Montt, g) Chile Chico, and h) Punta Arenas*

3.3.5.3 DGF-PRECIS Validation

When we compared the monthly climatic averages, we observed that differences depend on location. In the North, the model has large errors and a general pattern is not observed. For example, in Copiapó (Figure 3.8b), PRECIS model underestimates about

45% (2.44 mm *per year*) during July, but it overestimates in about 85% the annual amount (9.3 mm *per year*). On the other hand, in Iquique (Figure 3.8a), the DGF-PRECIS tends to overestimate about 43316% (37 mm *per year*) the whole year. Notice that this zone is very dry. In fact, there are some months with rainfall mean is zero and we cannot compute relative errors.

DGF-PRECIS performance improves when it is evaluated in southern stations. In central stations (Figure 3.12c), this model tends to reproduce the annual cycle, but it estimates the maximal rainfall peak in June instead of July, which is the month when we observed this peak. This issue is improved in the station located in southern-center (Figure 3.12d), but the peak estimation fails again at the southern boundary of the southern-central zone (Figure 3.12e). Less rainfall during the summer is explained by the southern location of the anticyclone (Saavedra *et al*., 2003), which blocks the fronts.

Therefore, when the anticyclone is in the most northern place (July), we expect highest rainfall zones. Since the front moves to South, we expect rainfall peak in June for places located in the South of the anticyclone. Thus, DGF-PRECIS fixed the rainfall pick at June, suggesting that the model did not simulate the North-South anticyclone change. In fact, Fuenzalida *et al* (2006) and Seth and Rojas (2003) compared NCEP-NCAR reanalysis with this model and they observed a fitted pressure field pattern in summer, and a different pattern in winter. Comparing the new and the DGF-PRECIS database, we conclude that the pressure is not well represented in time.

In the South, the model tends to overestimate systematically the rainfall in about 44% (156 mm *per year*) on Punta Arenas (Figure 3.12f). Therefore, we observed that in all zones estimated rainfall peak was in June, whereas in the observed rainfall peak was in July in zones located between North and central zones, June in the southern-central transitional zone, and May in the South (Figure 3.12f). Overestimation in southern stations is consistent with the report by Fuenzalida *et al*., 2006, which proposes that HadCM3 should model a deeper Antarctic Circumpolar Current (ACC) than the observed data. In fact, a deeper ACCT implies higher rainfall.

In the north, the model has important differences compared with measurement. In fact, the whole area is located in the North of Vallenar (28.5° S, 71.25° W) and the DGF-PRECIS is overestimated in 100%. These differences could be explained by the altitude gradient of this zone (Altiplane). In fact, the main errors are in the mountain zones (Figure 3.12). This error is inherited from the global model which showed an important underestimation compared with NCEP-NCAR Reanalysis (Fuenzalida *et al*., 2006). Although Fuenzalida *et al* (2006) proposed that this error was an artefact explained by the sea level correction, this difference shows an important effect on the northern rainfall patterns. On the other hand, errors showed a temporal pattern Thus, in summer the relative errors are lower than in other seasons and and higher in spring months. In fact, in summer the largest area showed errors over 100% (Figure 3.12). In summer, Altiplane also showed errors less than 100% (Figure 3.12).

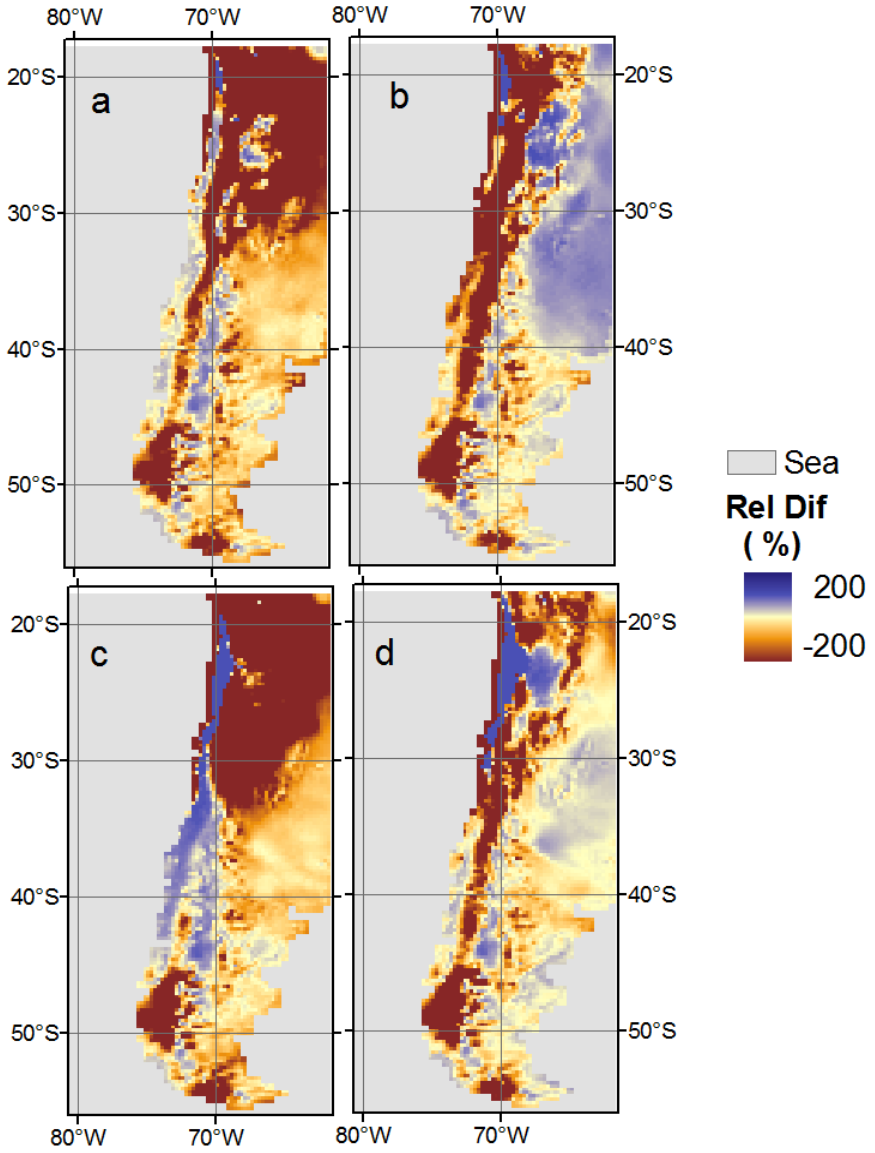

Figure 3.9.*Spatial pattern relative errors (real-estimate)/real for each climatology season. a) Winter b) autumn, c) spring, and d) summer. The zone without rainfall was masked before computing the relative errors (their values are maximum, i.e. 200)*

3.4 Discussion and concluding remarks

In the first section of this paper we discussed the annual and seasonal variability of precipitation in the Araucanía Region in Chile under Neutral (not ENSO years), annual rainfall 1497 ± 59 mm *per year* with a positive gradient from North-West to South-East of about 4.78 mm km^{-1}. Higher rainfall occurs during a period which covers the last portion of autumn and winter (May-July, of about 250 mm *per month*) and lower levels during summer and the beginning of autumn (Jan-Mar, 40-50 mm *per month*). In winter, the greatest amount of precipitation is received over the South East of the region (39.25º S, 72º

W), whereas in summer the lowest levels of precipitation take place over the North West (37.25º S, 72.5º W). Depending on the phase of ENSO year, the amount of annual accumulated precipitation either increases (during El Niño years, by about plus 103 mm *per year*) or decreases greater or lower levels of precipitation in winter (+14 mm *per month* during El Niño), and in summer (-3.92 mm *per year* during La Niña, respectively) when compared with Neutral years. Geographically speaking, a La Niña year is characterized by lesser precipitation levels in winter in the South East (39º S, 72º W), where it rains the most, and there are greater levels of precipitation in the northern western area of the region (37º S, 73º W). This pattern is reversed during an El Niño year.

This research aims at investigating how these patterns could change during the remainder of this century. The predicted changes in precipitation could have a dramatic impact on several socio-economic fields, especially agronomy. For example, the combination of changes in soil-plant systems (Clark and Lynch, 2009) and an increased probability of flooding (Rosenzweig *et al.*, 2002) may cause additional crop damage. Besides, accelerated population growth will put increasing pressure on supplies of freshwater. Therefore, improved projections are vital if the impact of climate change is to be mitigated. Correction of dynamically downscaled projections is a need, especially since it is well known that it contains a level of bias (Baigorria *et al*., 2008). HadCM3 model tend to overestimate precipitation variability. Thus, the standard deviation of precipitation over 1961-1991 period for the HadCM3 simulation is 157 mm, whereas it is 122 for the real *in-situ* data. It should be noted that although very little research has been carried out in our geographical area, there is a comparison of the quality of the different simulations performed by Doherty and Mearns (1999), who evaluated the validity of HadCM3 data using an equivalent area located at about the same latitude on the Pacific coast of the U.S.A.

Although closer to the *in-situ* data, we observed an overestimation of winter rainfall of the HadCM3 downscaled by PRECIS dynamical downscaling on the southern-eastern zone. This pattern could be explained due to an error inherited from HadCM3 model. When we analyzed the whole Chile projection we observed that mesoescale resolution tends to produce a smoothed topography condition, which implies that projections estimate less rainfall than original projection except on mountain zones. An extreme case can be observed in the Altiplane. Here important elevation differences are observed. Moreover, in this zone, these differences affect downscaling performance. Both differences imply that DGF-PRECIS are not reliable in places near the Altiplano. In fact, we omit the zones located in the North of Vallenar (28.5° S, 71.25° W) in our dataset.

Temporal and spatial distribution of the error suggests that the model projects a different anticyclone dynamics from the observed, and an underestimation of ENSO effects. Therefore, our results suggest that HadCM3 models project less variability on Southern Pacific Anticyclone than the observed in climate records, which are most evident under non neutral ENSO conditions. On the other hand, our research is focused on ENSO, but there are other phenomena, which affect the climate condition in the work domain such as Antarctic Oscillation, which should be included to improve climate change projections.

Our work Non-neutral ENSO effects on rainfall are understiated, but it not invalidated the climate change projections because the typical condition is well-estimated.

However, PRECIS climate projections do not reproduce adequately the climate pattern under ENSO synoptic condition which could be affect the projected climate variability. Although there is an important discussion about the behavior of the ENSO under climate change, we do not know if La Niña or El Niño will be more frecuent under climate change condition (Rosenlof, 2013; Collins, 2005). Independent of this discussion, it is important to include the effect of ENSO on the climate pattern in climate simulation for represent all the climate variability. This could be performed using scenarios which model specifically the ENSO condition.

As a consequence, it is probable that projections also overestimate precipitation level for the end of the 21st century (1970-2100). Thus, taking into account the rated overestimation of precipitation carried out during 1961-1991, both A2 and B2 scenarios were corrected. After those corrections, the less critical scenario – in this case B2 - predicts a reduction in annual precipitation of about 15.48%, equivalent to 235±87 mm mm *per year* less rainfall than a present Neutral year. Contrarily for the corrected A2 scenario, a decrease in annual precipitation of about -458±42.4, that is 30.38% less than a present-day Neutral year, was predicted. Seasonally, this decrease is greater during winter (mean of -56.7 mm *per month* and -17.2 mm *per month* for A2 and B2, respectively) and it is predicted to affect particularly the South East of the region (39º S, 73º W). Interestingly enough, in both scenarios the final amount of precipitation theoretically reaching the region is less than the one received on average during La Niña years from 1961-1991, which is a significant decrease.

The generated database identifies the main uncertainties and improves the current provided information for making policies and climate change adaptation strategies. Thus, we expect that this work will be an important step to support decision making system and design suitable countermeasures to help the Araucanía Region adapt for future climate conditions.

3.5. Acknowledgements

Original projected database (HadCM3-PRECIS) were obtained from Estudio de Variabilidad Climática en Chile para el Siglo XXI project (PBCT ACT-19, http://www.dgf.uchile.cl/PRECIS/), performed by Departamento de Geofísica (DGF) from Universidad de Chile and funded by Comisión Nacional de Medio Ambiente (CONAMA), Chile. We are highly indebted with Direction General de Aguas (DGA, Chile) and Armada de Chile for the *in-situ* meteorological data. Advisory by Engineer F. Echeverria (DGEO), who tabulated part of the original data from different supports, as well as constructed and checked such data in order to achieve their homogeneity are deeply acknowledged.

Mr. R. Orrego was funded by a national grant (CONICYT Ph.D doctorate scholarship, 23110112) and by FONDEF DO6I 1100 “Sistema de Soporte de Decisiones Para Cultivos Tradicionales Basados en Integración SIG y Estaciones Meteorológicas” R. Orrego is funded by a national grant (CONICYT Ph.D doctorate scholarship), and this study is also funded by Ph.D program of Ciencias de los Recursos Naturales (Universidad de La Frontera).

Chapter 4

Downscaling climate projection

High resolution rainfall projection based on topographical downscaling modeling Araucania region, Chile

Orrego, R[1]., , Abarca-del-Río, R[2] and Ávila A.[1,3]Guan, H.[4]

Draft paper

1.- Scientific and Technological Bioresource Nucleus, Universidad de La Frontera, Chile

2. Departamento de Geofísica. Universidad de Concepción, Concepción, Chile

3. Centro de Modelación y Computación Científica, Universidad de La Frontera, Chile

4. School of Environmental, Flinders University. Adelaide, Australia

4. High resolution rainfall projection based on topographical downscaling model in Araucania region, Chile.

Abstract

Atmospheric models have been used for assessing the impact of climate change on rainfall in water supply, human health, and other issues. These models are performed at mesoscale resolution (25 km), which is larger than the optimal to achieve the information requirement to face the climate change impacts. To solve the scale problems, statistical downscaling techniques were developed. Topographic based model, *i.e.* statistical models which used topographic variables as predictors, are the best alternative in places where there is a lack of historical dataset and complex topography, as occur in our study area. One of the most prominent models is Precipitation Characterization with Auto-Searched Orographic and Atmospheric (PCASOA). The aim of this work is to generate and validate a high resolution rainfall projection (1 km of grid size) using PCASOA model. This projection was performed in Araucanía region (37°S to 40°S and from 71°W to 74°W), of Chile one of the most important cereal crop production area. Our database improved the current climate projection in about 20%, mainly in summer, when the downscaled grid bias was <10%. We project a decrease in rainfall about 30% mainly in summer and spring. In addition, downscaling improved the observation of the orographic rainfall (rainfall differences between opposite mountain sides in Nahuelbuta Mountain), detecting a marked differences under climate change condition in the western part of the region.

4.1. Introduction

Understanding the changes on rainfall distribution is one of the main concerns for mitigating the climate change impact (Hawkins and Sutton, 2012; Piao *et al.*, 2010; Hewitson and Crane, 1996). Nowadays, temperature increases affect the evaporation and snow reserves (IPCC, 2013; Vicuña, *et al.*, 2011), agricultural areas and food security (Schmidhuber and Tubiello, 2007; Patz *et al.*, 2005), among other issues. To estimate the long-term impact of climate change, several Atmospheric and Oceanic Global Circulation Models (AOGCM) project the future rainfall amounts and distribution. However, AOGCM outputs models are produced at low resolution grids (about 300 km of grid cell size), whereas police makers and support cropping decisions requires information at local scale (<5 km of grid cell size). Downscaling techniques have been developed for solve the spatial resolution problem (Wilby and Wigley 1998; Wilby *et al.*, 2004). They are divided into two different classes: dynamical and statistical (Wilby and Wigley 1998, Zorita, 2000).

Dynamic downscaling consists of solving a system of partial differential equations, where an AOGCM is used for computing boundary and initial conditions. These techniques perform a climate model on a specific work domain area to obtain higher resolution fields (Räisänen, 2007). The main disadvantage of dynamic downscaling is the high

computational cost for its implementation (Schoof, 2012). Some examples are: Purves and Hulton, 2000 in England based on UKCIP project; Déqué *et al.,* 2005 in Europe, based on several models framed on the PRUDENCE project; Almazroui, 2013 on Arabian Peninsula, based on ERA40 database and PRECIS (Providing Regional Climates for Impact Studies) model, CREAS (Regional Climate Change Scenarios for South America) for Argentina, Uruguay and Brazil (Marengo and Ambrizzi, 2006), and Climate Variability for 21st century performed for Chile (Fuenzalida *et al.,* 2006). These projections downscaled climate input from global (about 300 km) to mesoscale resolutions (between 50 and 25 km cell grid size). Chilean projection produce the DFG-PRECIS database, which involved projection on the baseline data between 1961 and 1991 together with A2 (850 ppm of CO2 eq and 3°C for the year 2100) and B2 (621 ppm of CO_2 eq ppm and 1°C for the year 2100) scenarios for 2070 and 2100 at 0.25º resolution (about 25 km).This database was obtained by downscaling the output of Atmospheric and Oceanic Global Climate Model (HadCM3) using a regional climate model PRECIS.

Although these mesoscale climate projections help to understand the changes on rainfall pattern, the phenomena which impact the human activities require higher resolutions scale. For example, the effect of climate change on the microclimate is a very important issue for human health (e.g. Paaijmans and Thomas, 2011); crops system (*e.g.* Sutherst *et al.*, 2011) and species distribution (*e.g.* Gillingham *et al*., 2012). Improving resolution has been performed using statistical downscaling. It consists of obtaining a statistical model between the global-scale data and the local-scale data by fitting a mathematical transfer functions (Hanssen-Bauer *et al*., 2005; Solman and Nuñes, 1999; Wilby and Wigley, 1997). Thus, it links known variables (predictors) with output variables (predictands) that are normally meteorological records. For performing a statistical downscaling, the most common strategy is the perfect prognosis (PP; Rummukainen, 1997). This strategy includes tree steps: calibration, validation and projection of output dataset from the transfer function in order to generate a projected rainfall for each meteorological station. PP models are available such as SDSM (Wilby, *et al.,* 2002), or CLIMPACT (Benestad *et al.,* 2008) among others. Although this strategy is very much used (Linderson 2004; Zagar *et al.,* 2004; Wilby and Wigley, 2000), PP models requires dense meteorological station network with long time series records for building a reliable high resolution grid. In addition, since climate projections are the same meteorological records, there is no independent sample for the validation step.

To avoid the lack of meteorological data records and independent sample requirement for validation, other statistical downscaling models have been developed based on topographical variables as predictor. One strategy for perform this kind of downscaling is distribute the precipitations simulated for a low resolution cells among all the high resolution cells inside. This distribution is based on to fit a regression using topographical variables as predictors. The most important topographical downscaling model is Precipitation Characterization with Auto-Searched Orographic and Atmospheric effects (PCASOA) (Guan *et al.,* 2009) that includes variables obtained from a digital elevation model (DEM), where elevation, slope and aspects are regarded to improve spatial representation of rainfall

In this paper, we downscaled a high resolution rainfall projection (1 km of cell grid size) over central-southern Chile (37 - 40 °S and 71 -73 °W) from a mesoscale resolution rainfall grid (25 km of grid cell size) using PCASOA model (Guan *et al.*, 2009). Thus we generate a high resolution rainfall dataset (1km) for baseline conditions which was validated using *in-situ* meteorological records. Based on this validation, we generated a high resolution rainfall dataset for the A2 scenario.

We first present a general description of the work domain including main climate characteristics (section 2.1). Next, we give details about the PCASOA model (section 2.2). In the section 2.3 we give details about the topographical data set and the length and localization of the *in-situ* meteorological data set used here. In section 2.4 we describe the downscaling methodology. In the section 2.5 we describe the validation methodology and in section (section 2.6) the climate change scenarios downscaling methodology. Results are shown in section 3, following the same scheme of section 2 that is climatology downscaling (section 3.1), validation (section 3.2) and high resolution climate change projections (section 3.3). Finally, we discuss our results (section 4) and concluding about them in section 5.

4.2. Study area description, data set and methodology

4.2.1. Study Area

The study area is located from 37° to 40° southern latitude and from 71° to 74° Western longitude. From a topographical point of view, this area is longitudinally crossed by two mountains ranges: Cordillera de los Andes (AM) and Cordillera de Nahuelbuta (NM). In between, we observed the costal zones (CZ) and Central valley (CV) (Figure 4.1) (Börgel, 1985)

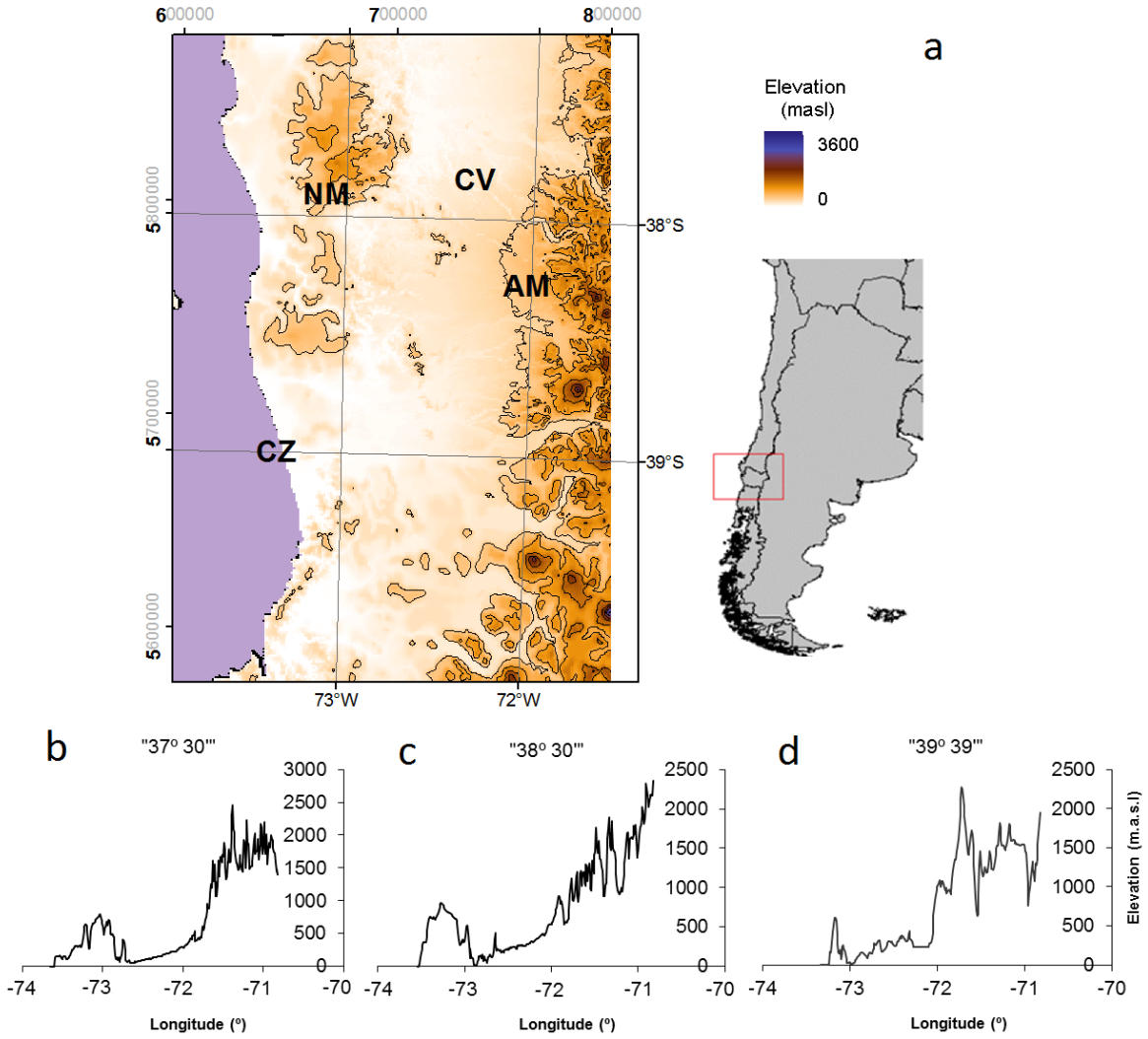

Figure 4.1.*Study area digital elevation model (37°S to 40°S and 71°W to 74°W). In the figure are also showed the main topographical zone: Cordillera de los Andes (AM), Cordillera de la Costa (NM).the costal zones (CZ) and Central valley (CV). Elevation in three selected longitudinal profiles are showed in b, c and, d.*

Climate of study area is characterized by a dry season between December and March with minimum rainfall varying from 50 to 70 mm *per month* and a wet season from May to September with maximum rainfall of about 250 mm *per month*. Annual precipitation varies between 800 and 1500 mm *per year* on CV (about 45% received between May and August; Rouanet, 1983). Within the seasonal annual temperature cycle, the warmest months are from December to February with mean about 15 °C (maximum of 25-27 °C and minimum about 10 °C). Winter mean (June to August) temperatures are around 8 °C (with a registered maximum and minimum of 12 °C and 4 °C, respectively) (Rouanet, 1983). Note that dry season matches with the warmest months showing a Mediterranean climate (Rouanet, 1983).The highest rainfall levels occurs in the South East (about 4,000 mm *per year*) and the lowest one in the West coast (about 800 mm *per year*). In addition, this region is affected by El Niño Southern Oscillation (ENSO; Montecinos and Aceituno, 2003). In fact, ENSO is one of the main sources of climate variability on the region. This

phenomenon generates changes up to -99 mm *per month* during La Niña phase and +34.3 mm *per month* during El Niño, being one of the main regional climate variability sources (Montecinos and Aceituno, 2003).

4.2.2 PCASOA model description

PCASOA is based on a multivariate regression using topographic variables as predictor. The multivariate regression searches some regional and local climatic settings (*i.e.* the spatial gradient in atmospheric moisture distribution and the effective moisture flux direction) that are related with some predictors (*i.e.* topography), which are used for precipitation mapping. The regression is designed to auto-search selected climate and orographic processes on an empirical relationship between topographic and meteorological variables. Thus, the program fits a statistical model among monthly rainfall and topographic variables: northern coordinates (related with latitude), eastern coordinates (related with longitude), altitude, slope and aspect (see equation 4.1; Guan *et al*., 2009).

.

$$Y = b_0 + b_1 Xf_1 + b_2 Xf_2 + b_3 Xf_3 + (b_4 Xf_4 + b_5 Xf_5) Xf_6 \quad \text{(Eq. 4.1)}$$

where Y is the rainfall, $Xf_1$and $Xf_2$are the Easting and Northing coordinates respectively (in UTM projection corrected by a scale factor), $Xf_3$is the altitude (in km), $Xf_4$is the Sine of the aspect (degree respect to the North), Xf_5 is the Cosine of the aspect (degree respect to the North), $Xf_6$is the slope, and b_0-b_5 are the related coefficients.

Aspect, slope, altitude, eastern, and northern coordinates are derived from a Digital Elevation Model (DEM) of the study area. A DEM is a grid which each cells represent the Elevation of a specific site. Thus PCASOA uses only a mesoscale precipitation grid and a DEM.

4.2.3 Climate dataset and Digital Elevation Model (DEM)

In our work domain there are 86 meteorological stations, 25 belonging to Dirección general de Aguas, and 61 to Dirección Meteorólogica de Chile. However, many of them present important gaps in the timespan from 1961 to 1991, affecting their representativeness. For solving it, we selected 56 *in-situ* meteorological stations located in the Region (Figure 4.2), using the rule of decade continuous years, or 15 years of non-continuous precipitation records. Also, the 10 selected stations used for calibrating the mesoscale DGF-PRECIS database where not used in the validation for ensure the independence of the validation sample. These criteria were defined to include the records within one Pacific Decadal Oscillation, which show an important correlation with the ENSO variability (Newman *et al.,* 2003). The remaining 46 stations were used to validate the PCASOA output.

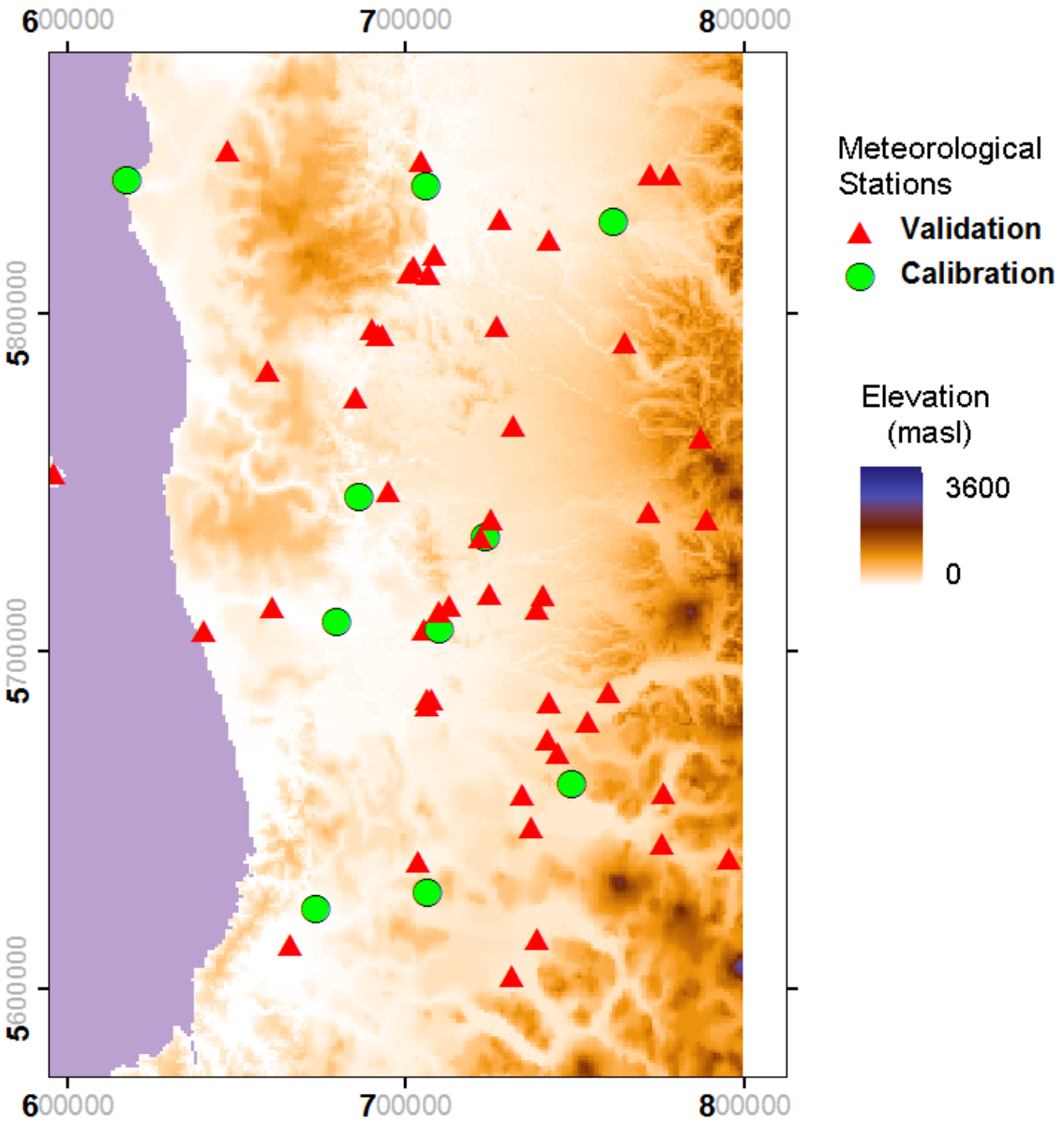

Figure 4.2.*Meteorological stations location overlapped over a DEM. Gray area show the Pacific Ocean*

We select a Digital Elevation Model (DEM) from the Global Topography at 30 arc-second (GTOPO30) project (Harding *et al.*, 1999) downloaded from the United States Geological Service (USGS) web site in: http://eros.usgs.gov/#/Find_Data/Products_and_Data_Available/gtopo30_info. This DEM is a horizontal grid spacing 30 arc-seconds (approximately 1 kilometer) which is projected in latitude-longitude. Since PCASOA needs this information in regular grids, it was changed to UTM (Zone 18 South).

4.2.4 PCASOA implementation

The first step for implementation the PCASOA model was to obtain the mesoscale rainfall grids for downscaling. These grids were obtained from PRECIS model applied to the continental Chilean territory between 1961 and 1991 (Fuenzalida *et al.,* 2006). DGF-PRECIS dataset considered 42 climate variables including photosintetically active radiation (PAR), temperature, and rainfall. We consider 108 pixels of 25 km from DGF-PRECIS database. The simulated rainfall was validated by comparing the mean of each month with *in-situ* climatology records (1960-1991) for each of the ten selected meteorological stations. The DGF-PRECIS database underestimated the rainfall in winter and autumn, but overestimated this variable in summer and spring. Thus, the database was corrected by computing a monthly ratio between the *in-situ* and the modeled data. The ratio was multiplied by each monthly value of DGF-PRECIS. Therefore, a corrected mesoscale monthly rainfall was produced.

The second step is to identify the significant predictors which model the rainfall. PCASOA is based on the relationship between the topography and the synoptic condition. The main climate driver of the synoptic condition is the Pacific Anticyclone (PA) which location presents a characteristic and periodic interannual pattern. The PA is the main climate driver of the continental entrance of frontal systems in the Pacific (Montecinos and Aceituno, 2002) affecting the frequency, direction and the intensity of weather frontal system. Therefore, topographic effects change based on the P.A variability, which implies that we should compute a different set of coefficients of equation 4.1 for each monthly grid. Moreover, as PA location follows a periodic pattern, it is expected that some variables considered in equation4.1 show a significant effect by the influence of PA, and these variables change through the years, but not among years. Since equation 4.1 coefficients change throughout the season, we should identify which variables are significant to explain the climate variability, which can be selected to simulate the monthly records. Thus, downscaling model should be fitted for each climate grid using only the significant variables selected for its corresponding climate month. The variable selection was performed using a T-test with 95% of significant level applied to the meteorological station climatology. This analysis is including in the same routine of the PCASOA, and test if there are significant differences between zero and each coefficient in a regression. T-Test was performed for the monthly climate average using the calibrating station as input. The results are reported in Table 4.1.

Table 4.1.*Significance of each variable (* >0.1 ; ** > 0.05, *** > 0.01) used in the final model (equation 5.1). Xf1 and Xf2 are the Easter and Northern coordinates respectively (UTM corrected by a scale factor), Xf3 is the altitude (km), Xf4 is the Sine of the aspect, Xf5 is the Cosine of the aspect*

Month	Intersep	*Xf1 East*[1] *(m)*	*Xf2 North*[2] *(m)*	*Xf3 Elevation (km)*	*Xf4 Sin(aspect)*	*Xf5 Cos(aspect)*
Dec	*		***		***	***
Jan	***		***	**		***
Feb	***		***	***		**
Mar	***	***	***		**	
Apr	*	***	***		***	
May	***	***	***		**	
Jun	***	*	**	**	**	**
Jul	***		***	***	**	
Aug	***		***	***	**	
Sep	***		***	**	**	**
Oct	***	***	***	*	**	
Nov	***		***	***		**

[1]*X UTM coordinate corrected by a scale factor*
[2]*Y UTM coordinate corrected by a scale factor*

Finally, based on table 4.1, PCASOA fit a model for each climate grid considered in our corrected mesoscale rainfall database, using the corresponding for its month high resolution (1 km) topographic variable as predictors. Thus, the output PCASOA model is a monthly rainfall database for all periods (1961-1991), which is in grid format and downscaled at 1 km.

4.2.5 Downscaling validation

Validation was performed by comparing the *in-situ* record and the grid containing in PCASOA output, and also in DGF-PRECIS for to quantify how much downscaling enhances quality. These comparisons were performed using four statistical methods: (i) Roots Mean Square Error (RMSE), (ii) Pearson correlation index (R^2), (iii) bias (*i.e.* the averages of the difference between the downscaled data and its corresponding *in-situ* data),

and (iv) bias absolute values. Finally, the relative differences of climatologies were spatially interpolated through ordinary kriging (Isaaks and Srivastava, 1989) to identify spatial pattern of the downscaling error.

4.2.6 Model Projection

The last step of this research was to build a high resolution projected database based on PCASOA. Following the methodology presented in Section 2.4, we downscaled the corrected DGF-PRECIS database for A2 scenarios for the 21st century, and use it for obtaining a high resolution (1 km) projected rainfall for this climate change scenario. Thus we constructed a climatology which was analyzed.

4.3. Results

4.3.1 Downscaling validation with climatology

The PCASOA and DGF-PRECIS at 25 km reproduce the main regional climate patterns (Figure 4.3). In fact, in Figure 4.3 we recognized the Northern-Southern gradient which increased the rainfall to the South, and the typical regional seasonal behavior characterized by lower rainfall in summer and higher rainfall in winter. For autumn-winter, PCASOA downscaling indeed improved the precision of DGF-PRECIS. Thus, we observed the positive relationship between rainfall and altitude, and the effect of valley on rainfall. It is interesting to note that PCASOA improved the representation of the characteristic rain-shadow zone located in the Northern region (about the 5.800.00 S, 700.000 W, UTM 18s; 37.8°S and 72.7 W) described by Luebke (2008). This gives us some hints about the spatial patterns at high resolution shown in Figure 4.3. Due to the high rainfall differences among seasons, it was not possible to keep the same color range along the year.

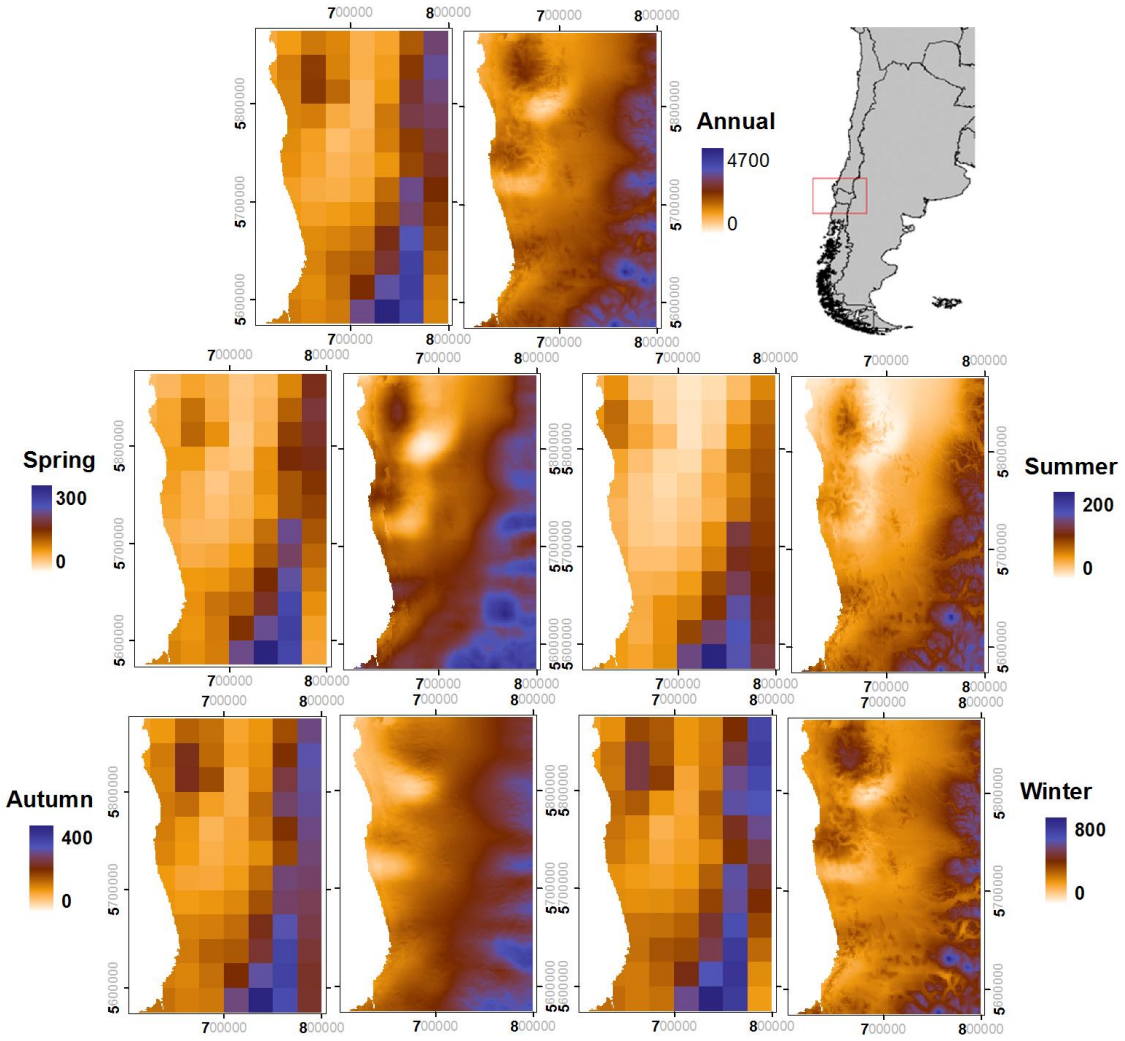

Figure 4.3.*Comparison between PRECIS (left) and PCASOA (right) outputs at climatic seasonal average levels (mm).*

In relation to the results of the validation processes, we compared the monthly climatologies, *i.e.* the 48 *in-situ* meteorological station compared with the PCASOA output and with DGF-PRECIS. For these analyses we computed the average biases and RMSE for each month considering each comparison as observation. These results are presented in Figure 4.4a and 4.4b respectively. Figure 4.4a shows also the standard error computed between both models and it corresponds to *in-situ* data in each month. We noticed in the bias (Figure 4.4a) and in the root square of the mean square error (RMSE) (Figure 4.4b) that PCASOA reduces the climate errors over nine months, except for February, May and July. Comparing DGF-PRECIS with PCASOA scatter plots (Figure 4.4c and 4.4d respectively) although R^2 is somehow lesser in the second case (8% difference), the slope is closer to one (0.59 and 0.8 for DGF-PRECIS and PCASOA respectively) and it intercepts closer to zero (39 and 11 for DGF-PRECIS and PCASOA respectively). These results suggest that PCASOA improved the climate projection but generated some out-layers (see Figure 4.4d) affecting the global performance of the correlation.

Except during summer, it is possible to observe a positive bias along the year, especially in the higher resolution grid. In addition, PCASOA model improves a lot the quality of the data. It still tends to overestimate the rainfall means (by more than 20 mm *per month*), but this occurs in autumn (April and May mainly) and only over a month in winter (June). For the remaining months, PCASOA improves the rainfall estimation. Also, but this overestimation are also observed in DGF-PRECIS database. In fact, PCASOA show a not significant improvement in these months. The remaining months, PCASOA significantly enhance in the rainfall estimation. Although winter and autumn are the rainiest season, rains fall during spring and summer are critical for several productive activities (*e.g.* agriculture, forest, and human water supply).

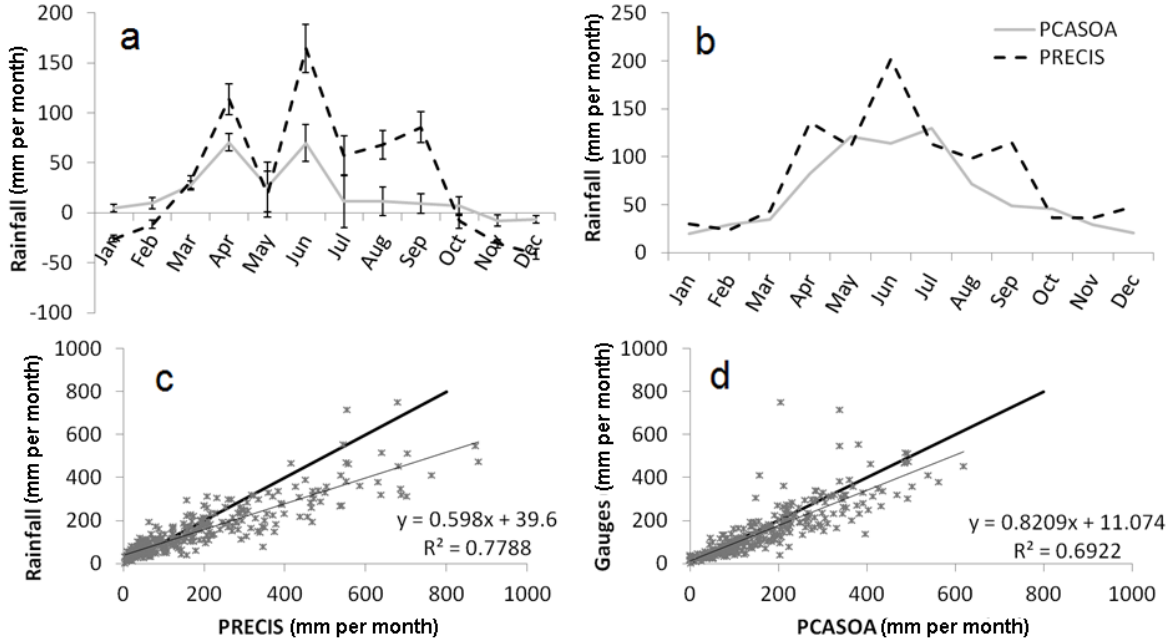

Figure 4.4. C*omputed* monthl*y station averages based on climate averages. In the figure a) Bias, b) RMSE, c)Scatter plot of PRECIS and measures data and d) Scatter plot of PCASOA and measures data and modeled data. In a) Error bars show the standard error, in c) and d) solid line shows the bisector (X =Y).*

Concerning spatial patterns (see Figure 4.5), PCASOA results show larger errors over high altitude zones, but it is inherited from PRECIS model (Fuenzalida, 2006). Also, we note that in all cases, the errors are reduced by big amounts (about 200 mm) when they are compared with errors found with the low resolution climate field (DGF-PRECIS). For PCASOA, these differences are about 15%, (*i.e.* 300 mm) in wet zones located in the Southern-Eastern region (about 38° 60' S, and 72° 00' W, *i.e.* about 700,000 W, 5,800,000 S, UTM18s, here it rains about 3,000 mm *per year*), and about 30 %, (*i.e.* 250) mm on dry locations in the Northern-Western region (about 37° 30' S, and 73° 00' W, *i.e.* about 800,000 W, 5,600,000 S, UTM18s, here it rains about 750 mm) zones. The same spatial pattern is observed for DGF-PRECIS, but these errors are higher than PCASOA (20% on wet zones and 40% on dry zones), and the zone located in the rain-shadow zone (about 680.000 W, 5.800.000 N UTM 18s; about 37.8 S, 73.0 W) where DGF-PRECIS

underestimates the rainfall (about 40%) whereas PCASOA overestimated (about 10%) (Figure 4.5a), whereas DGF-PRECIS underestimate about 20%.

The spatial pattern of the error is correlated with the DGF-PRECIS errors. This proves that downscaling improves the precision, but not changes the patterns. These patterns change along the season. In winter (the rainiest month) HR rainfall was underestimated by about 40 mm season^{-1} (about 20%) the dry zone, and the wet zone was overestimated by about 100 mm season^{-1} (about 14 %) (Figure 4.5e). The same pattern is observed in DGF-PRECIS, but the differences are higher than the downscaled grid. The DGF-PRECIS underestimates about 60 mm season^{-1} (about 30%) the dry zone, and overestimates about 200 mm season^{-1} (25%) the wet zone (Figure 4.5c).

During summer, (DJF, driest season) we observed different spatial rainfall pattern in HR respect to DGF-PRECIS. In PCASOA driest zones rainfall were slightly overestimated (differences about 10 mm, 20% of the monthly accumulated precipitation), and the wet zone rainfall was underestimated by only 5 mm (0.6% of the monthly accumulated precipitation). On the other hand, in DGF-PRECIS dry zone rainfall was underestimated in about 10 mm season^{-1} (about 20%), and the wet zone rainfall in about 400 mm (58%) (Figure 4.5c).

During spring an overestimation is observed (about 10 mm which correspond to 10%) in the PCASOA rainfall on the centre zone, and overestimation on the rest of the zone (about 50 mm which correspond to 30%, Figure 4.5 b), whereas a not clear spatial pattern in the DGF-PRECIS is seen. Finally, during autumn an overestimation is observed (about 200 mm, 100%) on all regions which are higher on the eastern-northern zone for both models (Figure 4.5d).

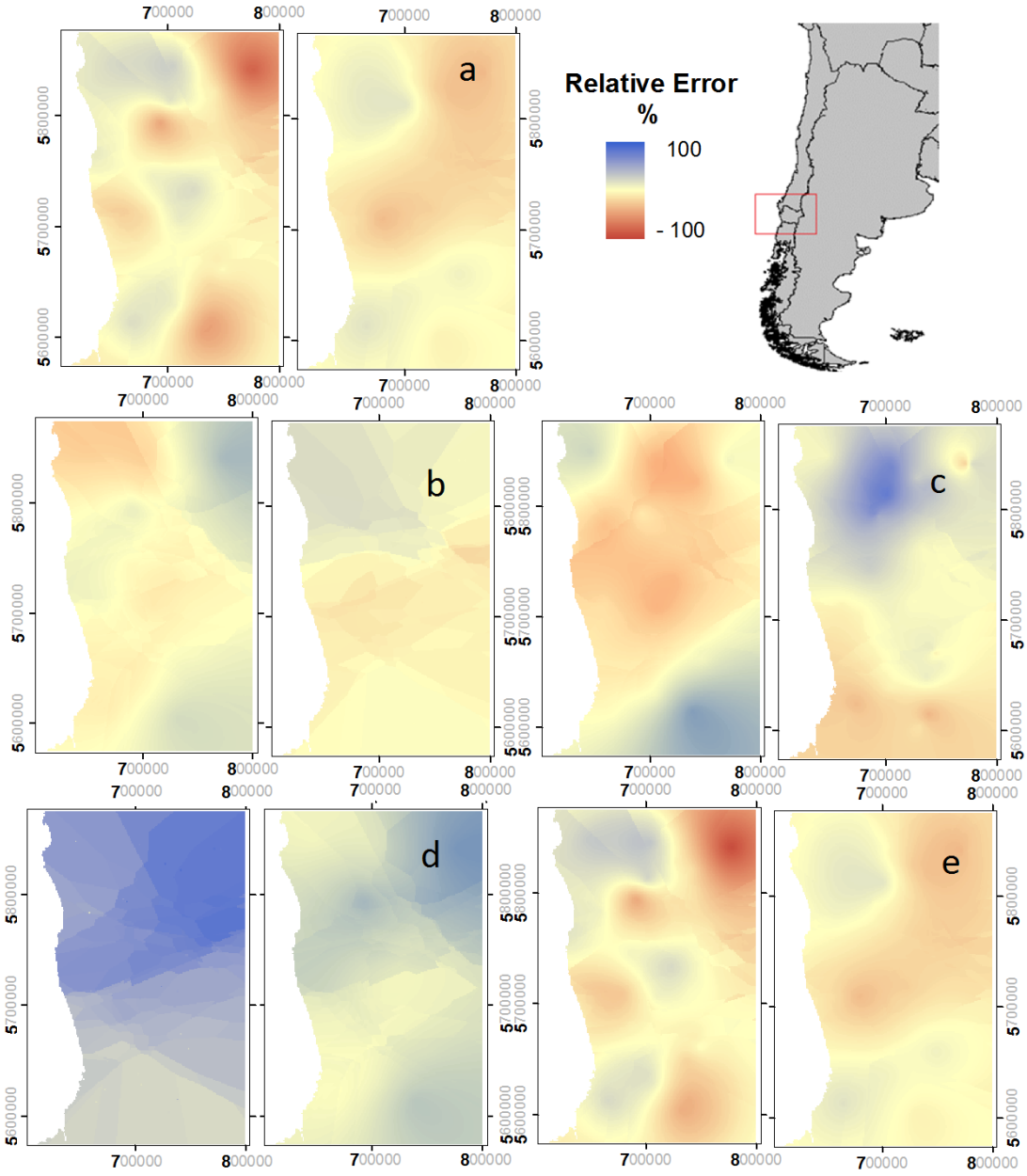

Figure 4.5. *Spatial pattern of PRECIS (left) and PCASOA (right) relative errors ((in-situ-modeled)/in-situ).a) Annual, b) spring, c) Summer, d) autumn, e) winter*

We observed a homogeneous rainfall change pattern on flat zones (between -800 and -500 mm *per year* on Valle Central and from -100 and 50 on the Coastal zones) and high variability of changes on mountain zones (between -500 to 1,000 mm *per year* in Nahuelbuta range and between -400 to 1200 in Andes range). We suppose that topography is related to the downscaling effect. Except for some zones located near the sea, on flat zones we observed higher rainfall in PCASOA output than in DGF-PRECIS outputs. On Mountain zones, we observed both negative and positive values. Negative values are related to valleys located in the East and North-East sides of mountains and hills. Positive values are related to high zones and West or South-West sides of mountains.

These rainfall patterns are explained by the existence of mountains changing the rainfall pattern by the front interaction. For example, Nahuelbuta range produces low rainfall in the opposite sea side, and high rainfall on the sea side and on the higher zones. This phenomenon is reported by authors and is called orographic rainfall (Luebke, 2008). Now, high resolution rainfall is based on a high resolution DEM, which is smoother than the low resolution. Therefore, higher rainfall is expected on high resolution than on low resolution on valleys. This increase in the rainfall implies that rainfall is more overestimated by DGF-PRECIS than PCASOA on higher zones, and that there is a similar bias on flat places.

4.3.2 Climate change projection

Under climate change condition a decrease is observed on the region rainfall (30%), which is higher than reported by other authors (Fuenzalida, 2006; Seth and Rojas, 2003). The low resolution model also projects an increase on the rainfall (6%), but a decrease on the central zone. Seasonally, we observed a decrease in rainfalls in spring (about 30%, *i.e.* from 356 mm to 250 mm, Figure 4.6e) and summer (about 70%, *i.e.* from 80 mm to 24 mm, Figure 4.6b), whereas an increase in the rainfall in winter (about 20% from 870 to 1050, Figure 4.6d) and autumn (about 20%, from 592 to 700, Figure 4.6c).

Our results show important spatial variability. In autumn, a decrease is observed in the rainfall (about 40%) on the West side of the Nahuelbuta range, and an increase on the East side (about 80%), whereas it is observed an increase in winter, and a decrease in summer and spring in all Nahuelbuta range zone.

The central zone shows a small decrease in the winter rainfall (about 20%), an increase in the autumn rainfall (about 50%) and an important rainfall reduction in summer and spring (60% and 70 % respectively). These patterns are translated into a reduction on the annual cumulative rainfall (about 30%). In our work domain, the Andes range (about 760.000 W UTM 18s; about 18s, 71º 20'w) shows an increase in the rainfall except for summer, which is directly correlated with altitude. Moreover, in the rain-shadow zone a decrease is observed in the rainfall (about 10%, from 603 mm to 543 mm) and in the Nahuelbuta range the maximum increase is observed on the rainfall in about 48%, *i.e.* from 600 to 880.

In our work domain, the rainfall pattern is explained by the location of the mean of MPL (maximum pressure latitude, Saavedra *et al*. 2002), which is a proxy of Pacific Anticyclone (P.A) location. Thus, when MPL is located in the northern region, PA covers completely the region reducing the rainfall, as it occurs in summer and spring. On the other hand, when MPL is located in the South of the region, PA uncovers completely our work domain as it occurs in winter. In autumn MPL is located at 38.7ºS, just over the South of Nahuelbuta range. The observed climate changes suggest that climate change strengthens PA and increases the front frequency. Therefore, in autumn the stronger Pacific anticyclone reduces the rainfall on the west side of Nahuelbuta range, but also the most frequent fronts

affect the east side of the mountain. The same phenomenon explains the small increase in the rainfall on the central zone, when PA does not cover our work domain (winter), and the decrease when it does (spring and summer).

The increase in the rainfall on Andes range and the increase on the difference between the Nahuelbuta range and the shadow rainfall zone could be explained as an increase in the Föhen effect (Barry and Chorley, 1992), which is product of the expected increase in temperature, producing an increase of the evaporation. In fact, the highest increase occurs on Nahuelbuta range, which is the highest place located close to the Pacific Ocean.

During summer an increase (about 800 km^2) is observed in the area without rainfall (Figure 4.6b). Moreover, this season starts in November under climate change condition, whereas it starts in December under base-line condition. In addition, the season without rainfall ends in March under climate change condition instead of ending in April under base-line condition.

Although general patterns are fitted with the *in-situ*-observation, there are some out-layers which could be observed mainly on Nahuelbuta range (about 680.000 W, 5.800.000 N UTM 18s; about 37.8 S, 73.0 W) and around the shadow-rainfall zone in spring and summer. In Figure4.6, we present the differences between climate change and current condition.

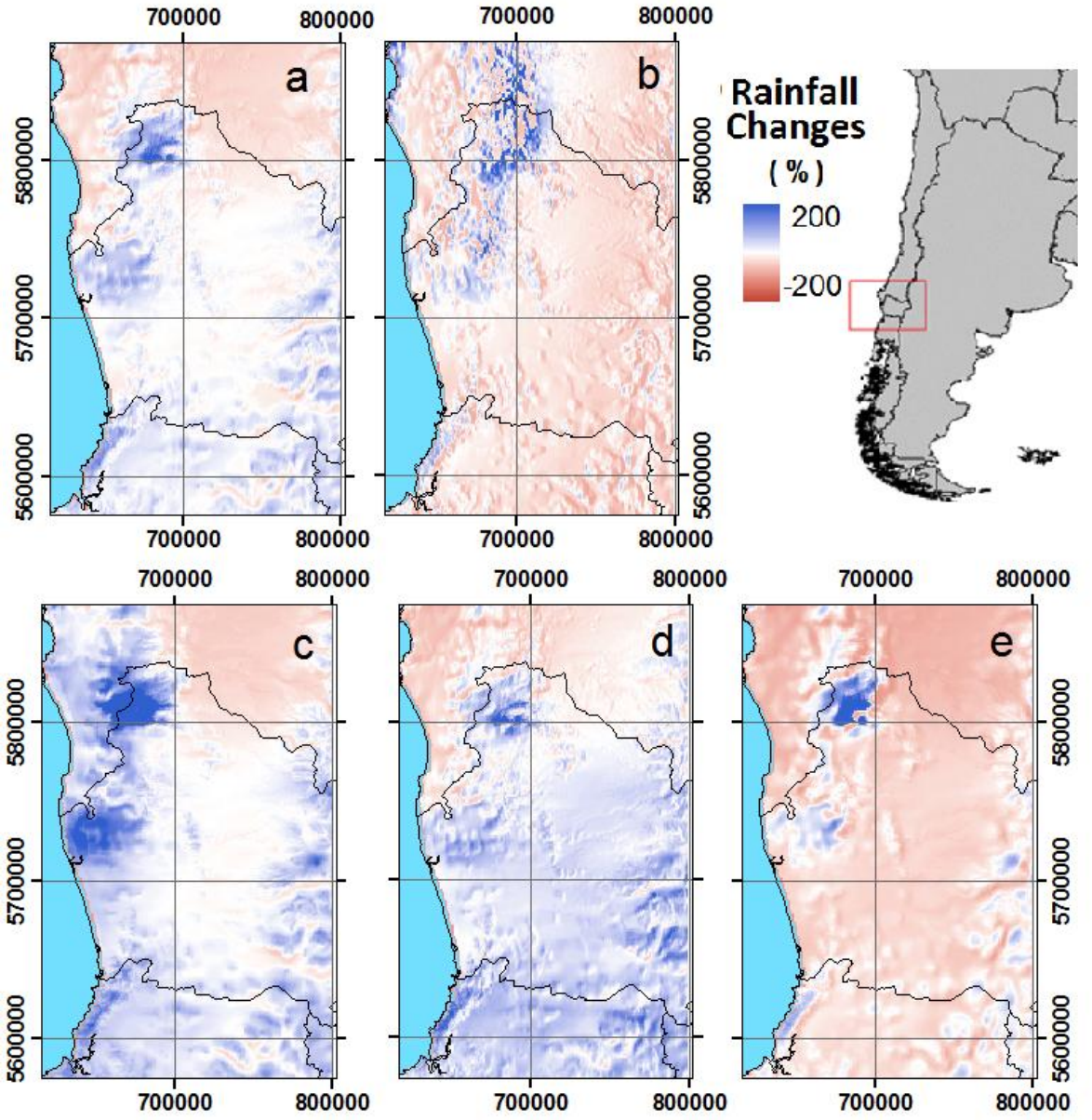

Figure4.6. *High resolution relative differences ((projected-base line)/base line, %) between climate change projection and current condition a) annual amount, b) Summer, c)autumn, d) winter and e) spring*

4.4. Conclusion and remarks

We developed a 1 km high resolution climate dataset for current and projected rainfalls. This dataset was developed using a topographical model based on topographical variables. This downscaling does not only enhance the projection in about 20%, but it also increases the model precision (from 25 km to 1 km) when there are insufficient climate dataset and/or less computational power than it is used for long term high resolution climate model. In

fact, we proved that this technique is successful even in places with few meteorological stations.

PCASOA shows a better performance than the original PRECIS outputs in practically every month. The highest improvements are observed in spring, and in June (the highest rainfall month). In summer high resolution model tends to reduce the bias in 17%, but RMS is similar. We observed important changes when comparing low resolution with high resolution outputs. These differences are larger in complex topography zone, mainly on the zones affected by orographic rainfall, and on the Andes ranges. In fact, we observed a change of 10% on rainfall shadow zone, whereas this zone is not observed in DGF-PRECIS. It is important to remark that downscaled grid represents the same general pattern than DGF-PRECIS, but the increase of the resolution accentuates the differences allowing a better observation of the patterns.

Under climate change condition, we expected a general decrease on rainfall, but there is an important spatial variability. Our result suggests an increase in the front frequency due to increase in the evaporation as consequence of climate change, and the increase of blocking due to strength of Pacific Anticyclone. Besides, we expected an increase on the rainfall on the zone with the driest summer. Resolution increasing shows details that we are not able to observe at mesoscale resolution. As example, we observed a change of 10% on rainfall shadow zone, whereas this zone is not observed on mesoscale resolution model.

We found only two climate change projections with similar output resolution which were developed by Gropelly *et al* (2012) and Hijsman *et al.*, 2005. The first dataset is at 2 km of resolution and was developed using a random-cascade approximation on Oglio river watershed. These authors obtained a good reproduction of spatial and temporal pattern with errors of about 4%. The other works another work with project climate condition is the World-Clim database (Hijsman *et al.*, 2005). This database projects several AOGCM outputs from their original resolution to 30 seconds (about 1 km) for the entire world. This database shows only the climatic averages and there are a few references about their performance. Both are performed using topographic approximation proving that this method is a promising strategy for improving the climate projection, mainly in complex topography zones.

These climate datasets are an important improvement, which could be used for several issues related to climate change impact assessment, such as agronomy, habitat suitability, water supply and human health in places with low dense meteorology record on the region. In fact, the characteristic rain-shadow on the Northern region, the gradient of less rainfall-high rainfall observed from north-west to South-East, and the valley effect on rainfall are observed. This zone is an important place for Chile from an agricultural view point. Another issue which we can investigate based on high resolution projection is microclimate indeed assessing the impact of climate change of them. Since they are very valuable zones for agriculture, forest activity, and human health, microclimate research is an important challenge. One of the main applications for this database is assessing and mitigation of climate injuries on agricultural systems. In fact, the best performance of PCASOA model was during spring and summer which matched with the crop-season. In

fact crop research requires a dense network of meteorological stations (Mitchel and Jones, 2005), or high resolution climate in order to produce optimum simulation data (Baron *et al.*, 2005; Mearns, 2003; Tsvetsinskaya, 2003), and there are a few papers referring to the of use high resolution grid for assessing the impact of climate change on crop systems.

4.5. Acknowledgements

The original dataset was obtained from Estudio de Variabilidad Climática en Chile para el Siglo XXI project (PBCT ACT-19, http://www.dgf.uchile.cl/PRECIS/), performed by Departamento de Geofísica (DGF) de la Universidad de Chile, and funded by Comisión Nacional de Medio Ambiente (CONAMA). We are highly indebted with Direction General de Aguas (DGA, Chile) and Armada de Chile for the *in-situ* meteorological data. We acknowledge help by Ing. F. Echeverria (DGEO), who tabulated part of the original data from different supports, who constructed and checked the homogeneity of the meteorological data. We are also highly indebted with the Groundwater group of Flinders University by the help in the PCASOA implementation.
Mr. R. Orrego is funded by a national grant (CONICYT Ph.D doctorate scholarship), and this study is funded by Ph.D program of Ciencias de los Recursos Naturales (Universidad de La Frontera) and End of Thesis Scholarship given by Graduate School of Universidad de La Frontera.

Chapter 5

PROJECTION A2 CLIMATE CHANGE SCENARIO USING HIGH RESOLUTION GRID CELL ON CROP YIELD OF WINTER WHEAT IN ARAUCANIA REGION

Raúl Orrego[1], Andrés Avila[1,2]., Francisco Matus[1,3]

Draf for paper

[1] Scientific and Technological Bioresource Nucleus, Universidad de La Frontera, Chile

[2] Centro de Modelación y Computación Científica, Universidad de La Frontera, Chile

[3] Departamento de Ciencias Químicas, Universidad de La Frontera, Chile

5. Projection A2 climate change scenario using high resolution grid cell on crop yield of winter wheat in Araucanía region.

Abstract

Several authors have projected a reduction in the food security due to climate change, which has been evaluated using climate msoscales (e.g. 25 km grid) models coupled with crop models (CCM). However, crop models have been designed for evaluating environmental condition at local scale, whereas climate models output are at low resolution. For solving this problem downscaling techniques are proposed. We project a crop yield under climate change (A2 scenario, the most extreme, *i.e.* 850 ppm of CO_2 eq and 3°C for the year 2100) based on downscaled high resolution projection (1 km). Climate projection was obtained from the regional climate model (25 km) DGF-PRECIS, which was corrected using *in-situ* records and downscaled using a topographic approximation (Precipitation Characterization with Auto-Searched Orographic and Atmospheric, PCASOA). We projected the winter wheat (*Triticum aestivum, cv. Winter-Europe*) yield growing in the Araucanía Region (37-40 S and 71-73 W) leaving the soil characteristics constants. The yield was increased 52.5% compared with the base line (1961-1991). Yield changes are explained and discussed on CO_2 base. A high spatial and temporal variability is observed which increases under climate change scenarios. We propose earlier seeding date in dry zones and later seeding date in wet zones together with adaptation strategies of winter wheat as climate risk countermeasurements. .

Key words: Climate Change Impact, Downscaling, Crop Modeling.

5.1. Introduction

Nowadays, global warming is an important issue affecting crop yields as envisaged by the International Panel of Climate Change (IPCC, 2007; 2007). One of the main concerns is the climate impact on food security and worldwide crop production (Seo and Mendelsohn, 2008; Slingo *et al*., 2005). To understand the vulnerability of crop production under climate change scenarios considering both climate changes and CO_2 increase, the most used technique is the crop-climate modeling approach (Meza *et al*., 2009; Challinor *et al.*, 2009; Thomson *et al*., 2005), *i.e.* to perform a crop model using projection based on a climate change input dataset. A good yield projection may guide research line for the choice of new cultivars, to identify required inputs, and to evaluate agronomic counterparts to allow crop adaptation to the new environmental conditions (Challinor *et al*., 2009).

Crop simulation models allow a systemic evaluation of weather, soil data and management variables on crop responses. These models are important tools to assess the climate change impact on local weather conditions along with other environmental interactions. Dijkstra *et al*., (2010) used a crop simulation model for estimating the

combined effect of elevated CO_2 and global warming in semiarid grassland in a *mesic Aridic Argiustoll* soil. They found that soil inorganic nitrogen (N) pool decreased significantly under elevated CO_2 by increasing microbial N immobilization, whereas soil inorganic N and plant N pool increased significantly with the increasing temperature. Steduto *et al*., (2009) quantified the water impact on the crop yield based on the Aquacrop model and assessed the main phenological processes which were affected. Rosenzweig *et al*., (2002) evaluated the impact of flood on crop (Maize) using CERES model and they estimated the losses by crop damage in US$3 billion *per year* in USA.

On the other hand, climate models are used to estimate the effect of greenhouse gases (GHG) on climate systems and projection on changing conditions.They simulate the global atmospheric state based on air flows generated by the warming differential of solar radiation on the earth surface (Zorita, 2000). These models simulate the state of the atmosphere on the entire world linking ocean dynamics, atmosphere activity, ice covering land, and biology-soil carbon cycle. Since they simulate the whole atmospheric and oceanic systems, they are called Atmosphere and Oceanic Global Circulation Models (AOGCM) (IPCC, 2001; 2007). For simulating the future climate conditions, AOGCM require the future greenhouse gas concentration. The IPCC defined GHG emission scenarios based on expected social and policy behaviors (IPCC 2001; 2007), projecting the future concentration of GHG and its climate consequences. The scenarios are classified into two groups: high and moderate emissions, namely A and B scenarios, respectively. Among these scenarios, A2 is the most used for assessing the climate change impact representing the high level of carbon emission (850 ppm of CO_2 eq and 3°C for the year 2100) and B2, representing moderate level of carbon emission (621 ppm of CO_2 eq and 1°C for the year 2100) (IPCC, 2007). These scenarios are commonly used for assessing the climate change projected for the model output in crop modeling (Soussana, 2010). In addition, IPCC (2007) defined a base-line condition for giving a reference to make comparisons. Thus, baseline is defined with the atmospheric condition observed between 1961 and 1991, which are driven by a CO_2 concentration of 330 ppm.

One of the main problems for crop projection response is the scale resolution of the climate data generated by AOGCM models. There are important differences between low resolution climate model output (grid cell size of 200-300 km) and local climate estimation (pixel size of 0.5-1 km), which generate uncertainties on crop projections (Challinor *et al*., 2009; Baron *et al*., 2005; Tsvetsinskaya, 2003). Mearns *et al*. (2003) reported changes in about 25% in spring rains when AOGCM outputs (pixels about 400 km) are compared with mesoscale climate models (50 km grid cell size), which imply higher differences in the crop such as downscaling techniques projections (up to 20% differences on crop yield). However, optimized protocols have been developed, which translate low resolution climate grid to the higher local data (Hanssen-Bauer *et al*., 2005; Wilby and Wigley, 1999).Two kinds of downscaling techniques are the most used: statistical and dynamic (Zorita, 2000). The statistical downscaling consists of a model (transfer function) fitted to a data from global- to local-scale climatic variables (Hanssen-Bauer *et al*., 2005; Solman and Nuñes, 1999; Wilby and Wigley, 1997). Consequently, dynamic downscaling is based on atmospheric models nested into AOGCM (Prudhomme *et al*., 2002). The AOGCM output is used as boundary conditions for regional models normally scaled from 200-300 km to mesoscale (50-20 km of grid cell size; Räinsänen, 2007). For instance, PRUDENCE is

projected over Europe (Déqué *et al*., 2005) and CREAS model is projected over South America (Marengo and Ambrizzi, 2006).

In Chile, a dynamic downscaling was carried out over the complete territory (Fuenzalida *et al*., 2006) based on Hadley Centre Coupled Model (HadCM3) which was downscaled using a model called Providing Regional Climate for Impact Studies (PRECIS). The national database called DGF-PRECIS involved the projected baseline climatic data (25 x 25 km) of A2 and B2 scenarios for 2070 and 2100 for air temperature (2 m), rainfall rate (mm s^{-1}), solar radiation (PAR, Watt m^{-2}), among other atmospheric variables. Moreover, DGF-PRECIS involved simulations for the base-line condition (from 1961 to 1991), which can be used for representative current conditions. These projections expecte temperature would increase all over Chile, and rainfall decrease from northern regions (between 18º - 30º S) to central-southern regions (between 30º - 40º S). Such reduction in rainfall would increase the potential evapotranspiration of crops and lower snow reserves in the costal and Andean range representing a significant decrease in water supply in the country.. Although DGF-PRECIS database is an important progress for understanding the climate change effects on Chile, its spatial resolution is not appropriate for local assessments scale (1 x 1 km) as requires agricultural crops.

In the present study we assessed the impact of Chilean climate change crop yield at local scale in winter wheat (*Triticum aestivum L*). We use nested statistical downscaling based on topographic approximation technique (Rupp *et al*., 2012) and random cascade algorithm (Grupta and Waymire, 1993). This allows us to obtain the projected climate for the time spam 2070-2100 under climate change scenario (IPCC, 2007) using topographical variables as predictors (Guan, 2009a). The work domain was Araucanía Region (35º35' - 39º37' S, and 71º to 73º W). We selected a winter wheat crop because it represented 33.7% of the total wheat production in Chile in just 35.2 % of the total agricultural land in this Region (about 1.7 millions) (INE, 2007). Winter wheat is widely cropped by farmers and it is commonly sown in volcanic soils close to the Andes range. The volcanic soils in Southern Chile represent 5.1 million ha and most agricultural soils from Araucanía are *Andisols Alfisols* and *Ultisols* (Matus *et al*., 2006). To our knowledge, there is no paper in Chile that evaluates a crop projection yield response to 2070-2100 for A2 and B2 scenarios respectively (IPCC, 2007) at high resolution sacle (1 km). Since it represents the most extreme condition, and allows appreciate more clearly the differences, our work is based on A2 scenario.

The specific goals of the present paper were: (i) to downscale climate conditions generated by DGF-PRECIS database from 25 km to 1 km considering the topographic downscaling technique and topographical variables (Guan *et al*., 2009b). This model includes the effect of topography and elevation and, (ii) to project the winter wheat crop yield in the Araucanía Region (1 km) under A2 and baseline scenarios from IPCC using CERES crop simulation model(Decision Support System for Agrotechnology Transfer Package, DSSAT).

5.2 Methodology

5.2.1 Climate dataset

The first step of our research was to select *in-situ* meteorological station in order to calibrate the mesoscale database (DGF-PRECIS) and validate the high resolution climate database (Precipitation Characterization with Auto-Searched Orographic and Atmospheric, hereafter PCASOA). For instance, we required rainfall, photosynthetically active radiation (PAR), and temperature. We selected 56 meteorological stations located in the Region which showed a complete rainfall records from 1961 to 1991 (see below), whereas a few stations (5) presented other climate records such as PAR and temperature. Mesoscale database and PCASOA model were calibrated using ten selected stations, based on 10 continuous years or 15 years of non-continuous precipitation records within the periods 1961 and 1991. These criteria were defined in order to include the records within one Pacific Decadal Oscillation, which is the main source of climatic variability in the Region (Newman *et al*., 2003).

Mesoscale database was obtained from DGF-PRECIS database. This database was created in 2006 to simulate the impact of climate changes from dynamic downscaling at 25 km grid from HadCM3 model (300 km) (Fuenzalida *et al*., 2006). The DGF-PRECIS database considered 42 climate variables including PAR, temperature and rainfall. The simulated rainfall was validated by comparing the mean of each month with *in-situ* climatology records (1960-1991) for each of the ten selected meteorological station. DGF-PRECIS database underestimated the rainfall in winter and autumn, but overestimated this variable in summer and spring. Thus, the database was corrected by computing a monthly ratio between the *in-situ* and modeled data. The ratio was multiplied by each monthly value of DGF-PRECIS. Therefore, a corrected monthly rainfall was used. Since the temperature and solar radiation could not be validated, these variables were used directly from the original database.

The corrected DGF-PRECIS was downscaled from 25 km to 1 km using PCASOAmodel (Guan *et al*., 2009). This is a statistical model based on regression rainfall mapping at 1 km grid cell (Guan *et al*., 2009) using topographic significant variables (coordinates, elevation, slope and aspect). To run the PCASOA model we need (i) the corrected DGF-PRECIS database as ASCII list format at UTM projection coordinates and (ii) a DEM model in ASCII grid format projected in the same geographical area. Detailed knowledge to run the model was also considered as indicated by Guan *et al* (2009). The DEM were obtained from the Global Topography at 30 arc-second (GTOPO30) database (Harding *et al.,* 1999) for the Araucanía Region. This consists of 30 arc-second (about 1 km) altitude maps obtained from radar satellite records. The PCASOA was calibrated by fitting a multiple regression model using topography characteristics as independent variables (x) and the corrected DGF-PRECIS rainfall grids as dependent variable (y). Only the significant topographical variables (< 0.05) were considered for the parameterization of the equations. The output PCASOA model was the rainfall grid downscaled at 1 km impacted by significant topographical variables.

The downscaled rainfall records were validated by comparing the climate average of the remaining 46 meteorological stations records. In general, the validation showed a

positive bias through the year, except for summer season. However, this bias is less than 30 % of recorded rainfall, and less than 15% in the growth season (data not shown). This error should be assessed with respect to the crop modeling impact, but it is comparable with other models validated in similar topography zones (Diaz *et al*., 2010).

Crop model requires a daily step hence we required to project the monthly term projection. For performing it, we fitted the monthly data using the stochastic weather generator climate generator (CLIMGEN, Thimgen *et al*., 2007) which uses simple algorithms to generate a random variable with the same probabilistic distribution functions for the simulated meteorological data (Wilk and Wilby, 1999). The CLIMGEN uses Markovian chains to generate the rainfall, and two sinusoidal functions (one for dry days, and other for wet days) for temperature and solar radiation. Based on CLIMGEN model, we generated a time series of 50 years for each meteorological station. Each of them simulates temperature, rainfall and solar radiation under base line and A2 scenarios. The generated rainfall dataset (commonly called synthetic time series) was validated for avoiding the cumulate error of all processes. Validation was performed based on a test, which compared the observed climatology (*i.e.* the averages of the monthly rainfall during the whole considered period) computed for each *in-situ* meteorological station with the computed synthetic climatology based on the corresponding grid cell at high resolution grid (PCASOA) using CLIMGEN. The comparison test was performed by a Standardized Major Axis analysis developed by Warton *et al*., (2006). This method was used to examine bivariate relationships among climatic properties. This package computes standardized major axis (SMA), which minimizes variance from the line in both dimensions, *x* and *y*. in contrast to least squares (or "model I") regression, (Warton and Weber 2002; Sokal and Rohlf 1995). This is important when primary concerns are the slope and/or interception of a relationship, rather than a significant correlation or predicting one variable from another. Use of least squares regression will give misleading estimation of the slope of such relationships when correlation coefficients are low. For performing the crop simulation we selected the meteorological stations which satisfy three criteria: itsR^2>0.6, its slope is not significantly different to 1 ($p<0.05$), and its intercept is not significantly different from zero ($p<005$). Thus, we obtained 28 *in-situ* meteorological stations, which satisfy these criteria (Table 5.1).

Table 5.1.*Standardized Major Axis analysis results. Gray rows show the selected station.*

Station	R^2	P*	Slo**	Int.***	P Slo	p Int.	Station	R^2	P*	Slo**	Int.***	P Slo	p Int.
Angol (DGA)	0.79	0.00	1.07	-10.56	0.66	0.60	Loncoche aeródromo	0.81	0.00	0.75	23.79	0.06	0.31
Angol (Esc Norm)	0.38	0.03	0.91	-16.68	0.72	0.58	Los Sauces (EAP0 DOS)	0.52	0.01	1.27	-1.71	0.29	0.93
Angol (Los estanques)	0.20	0.14	0.85	-20.20	0.59	0.57	Los Sauces (Sendos)	0.12	0.28	0.98	-10.77	0.94	0.64
Collipulli (DGA)	0.82	0.00	1.64	-4.73	0.00	0.87	Los Sauces Fdo (Ofic)	0.44	0.02	1.14	-12.05	0.59	0.59
Cunco (DGA)	0.88	0.00	1.21	-8.04	0.12	0.76	Manzanar (DGA)	0.91	0.00	1.35	-23.09	0.01	0.44
Curacautin (DGA)	0.96	0.00	1.34	-7.00	0.00	0.66	Mulchen (Riego)	0.60	0.00	1.60	-21.80	0.04	0.62
Curarrehue (DGA)	0.93	0.00	1.43	-30.61	0.00	0.26	Nacimiento	0.79	0.00	1.10	-16.91	0.52	0.54
Cerro Nielol (DGA)	0.98	0.00	1.35	-7.87	0.00	0.29	Nueva Imperial	0.80	0.00	1.87	-16.89	0.00	0.42
Carahue	0.78	0.00	1.06	3.51	0.70	0.79	Pueblo Nuevo (DGA)	0.94	0.00	1.42	-10.02	0.00	0.45
Carillanca Campex	0.61	0.00	1.19	-2.56	0.39	0.94	Puerto Saavedra (DGA)	0.68	0.00	1.48	-21.19	0.05	0.48
Central Pullinque	0.60	0.00	1.03	5.46	0.87	0.91	Padre de las Casas	0.73	0.00	1.31	-16.30	0.13	0.56
Contulmo	0.83	0.00	0.85	3.39	0.27	0.89	Panguipulli	0.73	0.00	0.97	20.74	0.83	0.58
Curaco (balsa)	0.80	0.00	1.02	-11.17	0.90	0.74	Purulon	0.85	0.00	0.95	1.19	0.67	0.96
Curanilahue	0.93	0.00	1.17	-28.81	0.10	0.16	Quecherehua (DGA)	0.92	0.00	1.44	-36.74	0.00	0.16
El Morro (DGA)	0.91	0.00	1.32	-21.16	0.02	0.47	Quillen (DGA)	0.98	0.00	1.73	-24.11	0.00	0.02
El Vergel (DGA)	0.83	0.00	1.27	-10.78	0.10	0.50	San José dela Mariquina	0.82	0.00	0.71	21.21	0.03	0.19
El Tambillo	0.61	0.00	1.27	-18.71	0.25	0.61	San Gerardo	0.72	0.00	1.45	5.93	0.04	0.86
Freire (DGA)	0.86	0.00	1.28	-16.21	0.06	0.49	San Luisa Meluen	0.86	0.00	1.61	-17.69	0.00	0.43
Freire Campex	0.91	0.00	1.12	3.63	0.26	0.83	Santa Adela (fundo)	0.75	0.00	0.87	11.13	0.40	0.75
Freire Sendos	0.98	0.00	1.27	-4.42	0.00	0.59	Santa Barbara	0.70	0.00	1.35	-17.58	0.11	0.65
Flor del Lago	0.73	0.00	0.77	14.97	0.14	0.67	Temuco (Maquehue)	0.71	0.00	1.47	-22.90	0.04	0.45
Galvarino (DGA)	0.97	0.00	1.55	-9.06	0.00	0.29	Vicun (DGA)	0.95	0.00	1.39	-19.46	0.00	0.23
Granja V Hermosa	0.67	0.00	1.42	-22.78	0.08	0.42	Villarrica (DGA)	0.93	0.00	1.00	2.87	0.98	0.87
Lautaro (DGA)	0.95	0.00	1.46	-23.54	0.00	0.10	Victoria (Oficina0 FACH)	0.88	0.00	1.42	-18.23	0.01	0.42
Llafenco (DGA)	0.97	0.00	1.08	-40.35	0.19	0.06	Vilcun	0.72	0.00	1.24	-11.61	0.23	0.75
Los Laureles (DGA)	0.93	0.00	1.14	-9.38	0.14	0.62	Villacura dimilhue	0.76	0.00	1.40	-23.27	0.05	0.54
Lumaco (DGA)	0.96	0.00	1.78	-24.51	0.00	0.06	Villarrica	0.82	0.00	1.01	-11.69	0.93	0.71
Lago Caburga (DGA)	0.95	0.00	0.64	32.00	0.00	0.05	Pichoy	0.84	0.00	0.56	19.55	0.00	0.20
Lautaro (DOS)	0.70	0.00	1.27	-7.88	0.20	0.80							

* *P-value of the regression*
** *Slope of the regression*
*** *Intercept of the regression*

5.2.2 Crop Model

The crop response to change climatic scenario A2 was estimated by using the Decision support system for agro technology transfer package (DSSAT) version 4.0. (Jones *et al*., 2003; Jones and Thornton, 2003). The DSSAT contains several models such as CERES (mainly for cereals) and CROPGRO (for legumes). DSSAT models are the most used software for estimating the climate change impact on crop system (Meza *et al*., 2008; Long *et al*., 2006; Jones *et al*., 2003). This model allows manipulating 23 input parameters such as CO_2 concentration, plant nutrition, irrigation schedule, and plant varieties (Jones *et al*., 2003). Each cultivar is defined by genetic coefficient, *i.e.* coefficients which drive the responses and interactions with environmental and management conditions (Pabico *et al*., 1999). In our case, we used Winter-Europe cultivar, which is defined by seven coefficients: Vernalization days (60 days), Photoperiod effect (75 days), grain filing duration (500 °C degree days base 10 °C), kernel number (30 units kg^{-1}), kernel average weight under

optimum condition (40 mg), stem and spike dry weight at maturity (1.5 g), and phyllochron interval (95 °C degree days base 10 °C).

The CERES crop model also requires some initial parameters which are defined by the farmer practices, such as dates and methods of fertilization (phosphorous and nitrogen), irrigation and planting, deep planting and density, row spacing and stubble incorporation. Since the present study focused on determining the effect of climate grid cell size based on the simulated grain yield, we fixed soil data obtained from the generic soil default in DSSAT (IB00000002). For the simulation, phosphorous and other nutrients in soils were not limited, except for nitrogen, which was not considered (Angulo *et al.*, 2013; Palusso *et al.*, 2011). The CERES model was previously validated by comparing the observed and simulated winter wheat yield in two season years (2008 and 2009) seeded in an experiment carried out at the Experimental Station (38º50 S, 72º41 W) from Universidad de La Frontera. In these experiments we seeded winter wheat (*cv. Kumpa*) under unlimited phosphorous and 5 levels of nitrogen fertilization (urea) including a control without nitrogen. We also considered other experiments (1988-2007) of non-nitrogen fertilizer winter wheat across the region (Campillo *et al.*, 2010; Campillo *et al.*, 2007; Rouanet, 1994). Model showed non-significant differences with the experiment (Figure 5.1).

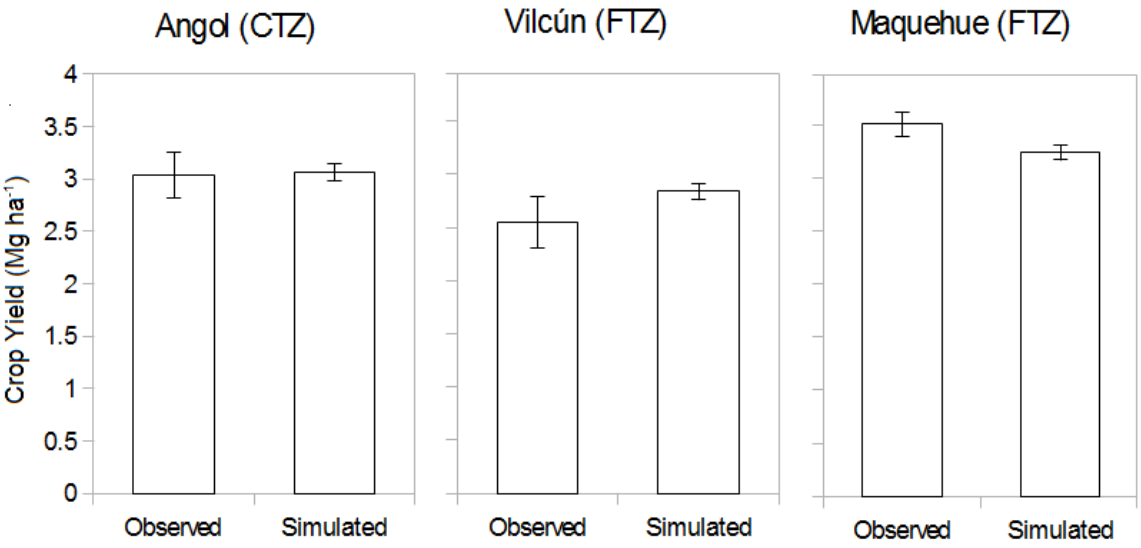

Figure 5.1. *Average of observed (1988-2007) winter wheat yield field experiments from Vilcún (n=6), Maquehue (n=14) and Angol (n= 15) (see Fig 1) representing the flat topography zones (FTZ) and complex topography zones (CTZ) in Araucanía Region of Chile as compared with the simulated (DSSAT) winter wheat yield average (1961-1991)in the same locations. Bars represent standard error of the mean.*

The simulations were performed based on the local climate generated by CLIMGEN. We evaluated three sowing dates: April 1, May 1, and June 1), and irrigation was not considered as long as the common practices are not irrigated in most southern volcanic soils. However, we did not consider nitrogen applications and optimal phosphorous as fertilization. The plating methodology was seeding using 250 plants m^{-2} and 16 cm row spacing.

To estimate the climate change impact on crop response we performed the model for the baseline (BL) condition and for A2 condition, and we compared their yield at physiological maturity. For separating climate and CO_2 effects, two dummies conditions were also included in this analysis: baseline with A2 expected CO_2 concentration (800 CO_2 ppm BL-800), and A2 with baseline CO_2 concentration (330 CO_2 ppm, A2-330). Fifty simulations were performed for each climate condition and we tested significant differences using a t-test (95% of significant level) in all cases.

To assess the impact of climate change on crop systems including the expected variability, we estimated crop yield exceedance density probability function under both, baseline and A2 conditions. Crop yield exceedance density probability function is a curve representing the probability of obtaining yields higher than a giving value (Piechota *et al.*, 2001), and it is estimated by equation 5.1.

$$Pex = \frac{n}{N+1} \quad (5.1)$$

Where *Pex* is the exceedance probability for a yield, *n* the position of the yield in a sorted list from the lowest to the highest and *N* is the total number of data. This analysis was conducted for the yield of winter wheat crop to look at the pattern across the climatic information and find the most impacted area for the dry and wet condition.

5.2.3 Spatial projections of baseline and A2 crop yield

One of the main advantages of performing adownscaling is the possibility of improving the precision of yield estimation. For analyzing the crop yield changes spatial pattern, we mapped the differences on crop yield, rainfall, temperature, and solar radiation modeled for baseline and A2 scenario. These analyses were performed based on the selected station (Table 5.1) and we plotted the yield differences obtained from our simulation using spline interpolation (Bosque, 1992). This interpolation method was applied using Arc-Gis 9.2 (Redland California, U.S.A.).

5.2.4 Yield behavior in temperature-rainfall hot-map

Finally, to investigate the crop yield response under different climate conditions and assess the sensitivity of crop yield to climate changes, we estimated the yield crop response surface plot (temperature - rainfall hot-map). This analysis consists of a surface plot, which represents the crop yield in a color scale with respect of the season average temperature (*x* axis) and the season cumulated rainfall (*y* axis), respectively. Thus, we interpolated all the data output using the inverse square of distance algorithm (Bosque, 1992).

5.3 Results

5.3.1 Crop performance

We observed a yield increase under climate change conditionsA2. This yield increase was observed even when comparing the impact of climate change under the same CO_2 concentration (Figure 5.2). This fact suggests that CO_2 concentration and climate condition under A2 scenario increases crop yield. This effect is observed under all seeding dates, but the yield increase is higher when we consider an earlier seeding date (April 1st) in dry zones (Angol)and later (Jun 1st) seeding date in wet zones (Cunco)

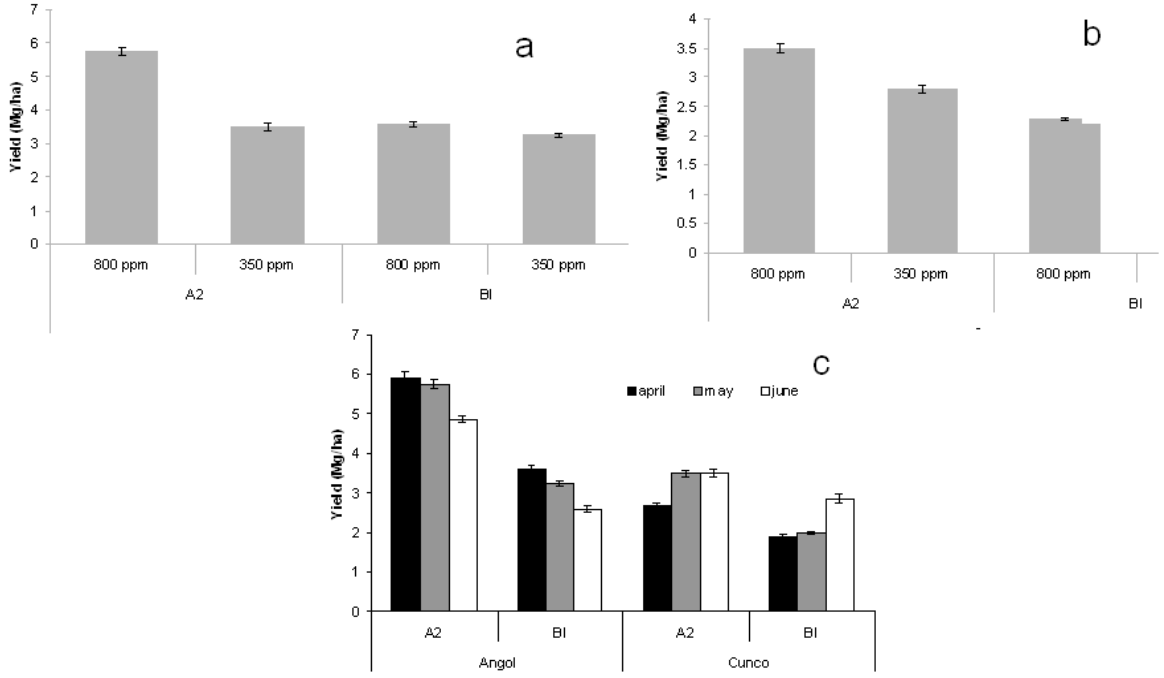

Figure 5.2.*Crop yield (Mg ha^{-1}) under base line (Bl) and climate change conditions (A2) in two model zones: a) Angol and b) Cunco. c) crop yield comparison considering three seeding dates. (a) April 1st, (b) May 1st, and (c) June 1st. Error bars represent the standard error computing based on the 50 synthetic* years *of simulation.*

Although an increase is expected on crop yield, we observed an important increase on the yield variability, which changes among different sites and is larger in dry zones. For example, in Cunco we observed an increase on the variation coefficient from 7.8% to 14.5% whereas in Angol the variation coefficient is from 14.1% to 14.7%. However, there is a significant decrease of the low yield probability under climate change condition (Figure 5.3).

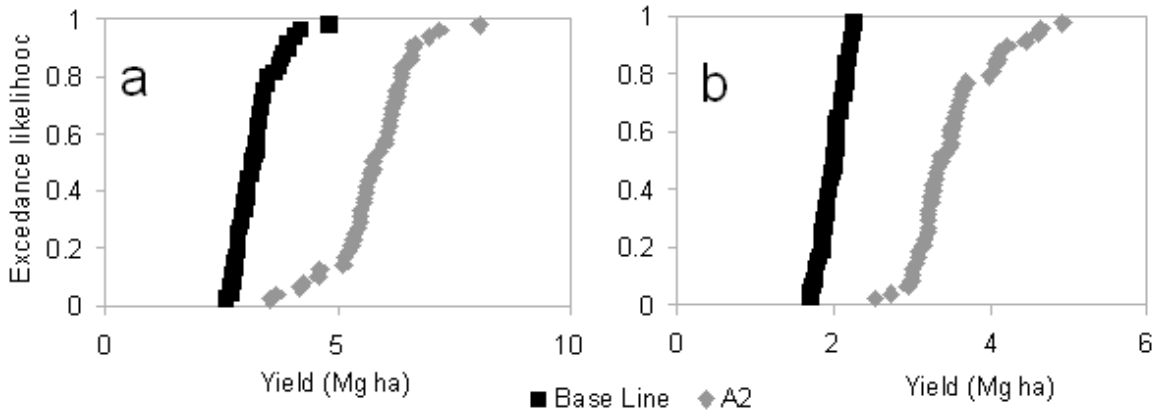

Figure 5.3. *Crop yield exceed likelihood under climate change condition and under baseline condition on two model zones (Cuncoon the leftside and Collipulli on the right side). We considered May 1st as seeding date.*

In the region, crop yield changes range from 92% to -128 %. In the northern and western zones of the region a yield increase is observed on the crop yield, whereas in zones located in the southern zone of the region and an increase is observed close to thesea. Thus, the total yield effect is an increase about 52.5% (Figure 5.4).

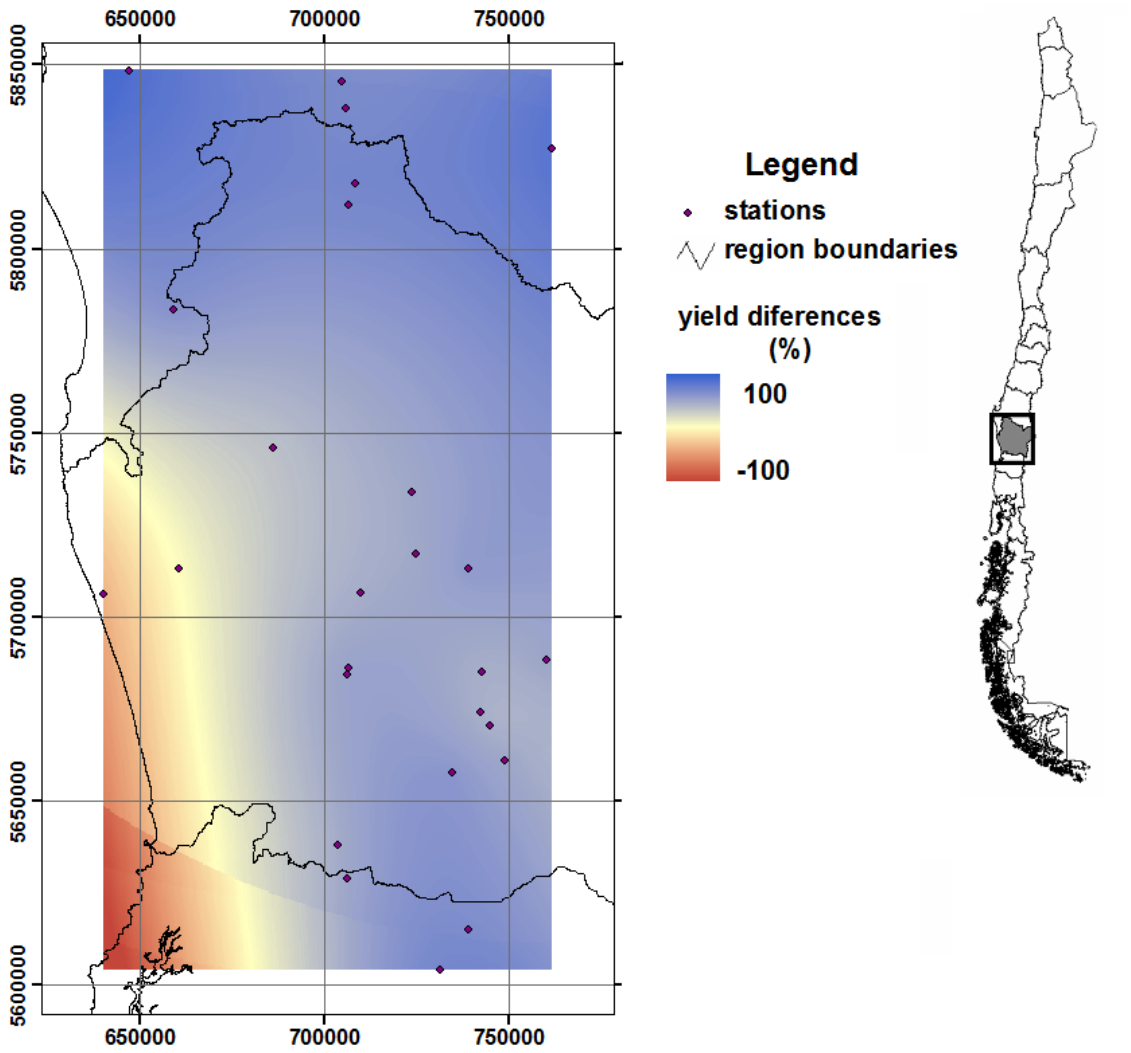

Figure 5.4. *Crop yield differences (%) between current and future ((A2-Bl)/Bl) conditions. We also showed the meteorological station used in the interpolation.*

5.3.2 Yield behavior in temperature-rainfall plane (hot-map)

A hot-map is a plot with represents the yield (color scale) respect two variables: temperature (X-axis) and rainfall (Y-axis). Thus, it allows identifying the yield pattern respect the rainfall and temperature changes. Although it is expected that crop yield is directly related to rainfall, higher yields are observed in the lesser rainfall zone of the hot-map. Thus, climate change causes the simulates crop yield get closer to the "high yield values", which suggest that crop system will be less sensitive under climate change condition (Figure 5.5). CO_2 values affect the yield in the rain-temperature plane. In fact an increase is observed in the "high yield" area.

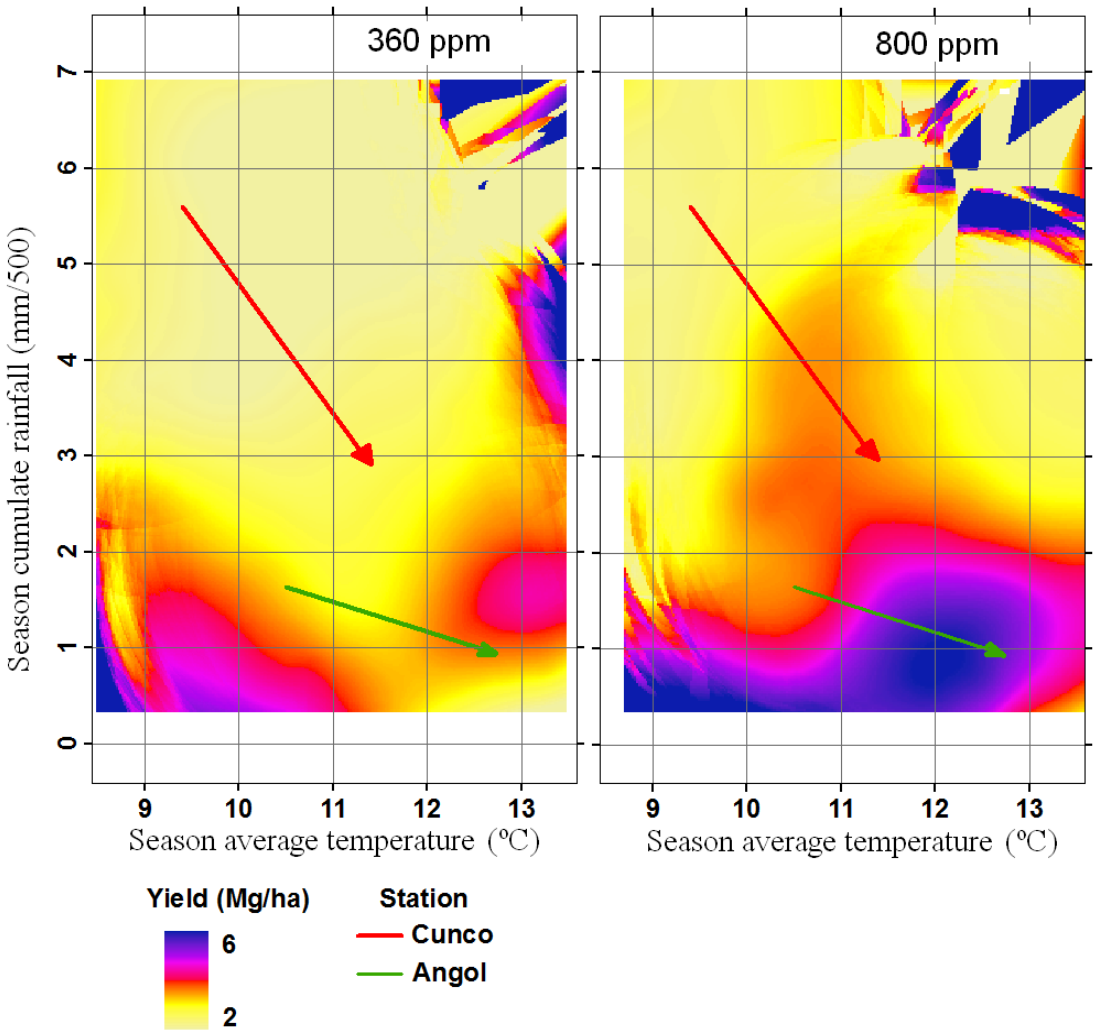

Figure 5.5.*Crop yield (Kg ha^{-1}) in the Rainfall – Temperature hotmap for a) 800 ppm of CO_2 and b) 330 ppm of CO_2. Arrows show the vector which bridges current (foot) and projected (head) rainfall and temperature means. Rainfall values are divided by 500 for scaled the values.*

5.4 Discussion

Our work is a very high resolution projection of crop behavior under climate change condition, which is a less explored way for assessing climate change impact on crop modeling. We found only two papers that use a very high resolution grid, *i.e.* less than 10 km for crop projection in UK (Semenov, 2007). In Chile, where the work was performed, there is no paper on those projections. Semenov (2007) used the United Kingston climate impact projection (UKCIP) database (50 km of grid cell size), which was downscaled by a topoclimate regression and interpolation with irregular triangulation network algorithm.

Zhang *et al* (2005) worked out HadCM3 projection in Oklahoma downscaling climate likelihood curves to site-specific climatic variable records.

Some crop projections at mesoscale (25-50 km) have been developed in Chile. For instance, Meza and Silva (2009) assessed the dynamical adaptation of farmer to climate change condition. Besides, Sauvinet *et al*., (2010) developed a high resolution rainfall climate change projection using Statistical Downscaling Model (SDSM, Wilby *et al.*, 2002), a model based on regressions with modeled meteorological drivers (surface pressure, geopotential high, temperature and humidity at atmospheric high levels) in Chilean arid zone for assessing the changes on watershed.

The results indicated that in Araucanía Region winter wheat yield increased in about 50 % after 100 years of simulation and our results disagree with those presented by Meza and Silva (2009) who indicated a decrease in 20% on winter wheat sowed in August in Temuco. These differences were explained by the selected varieties which present a long cycle (we used a variety with seeding date in May) mitigating the effect of a drier summer. Although under climate change scenario the general trend is to decrease wheat yield, our results are consistent with climate zones, which are similar to our work domain. For example, Mearns *et al*., (2003) reported an increase in 14% of the winter wheat yield on Pacific Coast USA simulated under 540 ppm of CO_2 concentration with consistent climate change condition.

Dummy variable experiments (BL-800 and A2-330) suggest that yield increase is explained mainly by CO_2 increase, but weather effects increase crop yield itself. This fact agrees with the temperature-rainfall hot-map, which shows higher yield values under A2 CO_2 concentration. The positive relationship between CO_2 and yield and its effect of mitigating climate injuries have been also reported by Maerns *et al* (2003) and Meza and Silva, (2009). Moreover, hot-map shows a translation from "low yield dominated area" to "high yield dominated area". Thus, an increase in the yield is expected as general trend. These changes on the yield variability are confirmed by the exceeding probability curves.

We observed an inverse relationship between rainfall and crop yield in the region (see hot-map) increasing crop yield under climate change condition. This result could be explained by nitrogen lixiviation. In fact, in a non- limited nitrogen experiment we observed the opposite pattern, *i.e.* an increase on the crop yield when rainfall is higher. This phenomenon could be mitigated on volcanic soils, as they show higher levels of organic nitrogen (Nanzyo *et al*., 1993). This is not investigated in our work and we did not find research on this issue, the effect of soil properties on climate change impact mitigation is an important future prospect. On the other hand, it is expected that a later seeding date could mitigate the excessive rainfall in wet zones, whereas an earlier seeding date allows collect rainfall in April in dry zones. In fact, the maximum yield was observed in the earlier seeding date in Angol, and in the later seeding date in Cunco.

As it is showed in Figure 6.6, a high spatial variability is observed. In the northern zone it is expected an increase of the crop yield over 92%, whereas on southern-west a decrease is expected (about -128%). Higher changes on crop yield occur on dry zones, where a low effect on temperatures and rainfall is also observed, this could be explained by the climate sensitivity of these zones. Thus, downscaling allow to focus research on valuable specific zones for wheat production. Therefore, we expected an increase on wheat yield in important wheat productive zones (Angol and Cunco) associated to microclimates.

Our research group is assessing the impact of downscaling on crop simulation and our preliminary result suggests that the optimal climate resolution for crop modeling on this work domain is 7 km for complex topography zones, and 25 km for flat topography zones (Orrego *et al*., 2014). These results suggest that under A2 climate change, wheat crop will be an important crop. Therefore we must enhance different choices of varieties and improve public insurance policies to mitigate the expected high variability showed in Figure5.5.

Although crop model assesses climate change impact and a high resolution projection added valuable information for designing adaptation polices, there are issues which should be improved in future works. The first one is plant adaptations to new climate condition, which are not considered when running crop models for scenarios 2070 and 2100. This phenomenon was reported by Zhang *et al*. (2008) observing a non-stationary relationship between temperature and phenology in rice crops. Another issue is soil routines on crop modeling when working on volcanic soils, which are not considered in the initial CERES-DSSAT database. Volcanic soils show some characteristics, affecting crop performance, such as the strong chemical bonds between soil compounds and phosphorous limitation for plants. CERES-DSSAT allows manage both water and phosphorous cycles (Dzotsi, *et al.*, 2010), but there are few works assessing specific volcanic soil chemistry on CERES-DSSAT crop model.

5.5 Conclusion remarks

In this work we project the impact of climate change on wheat yield using a high resolution projection. Based on these results, we measure that the effect of using a high resolution grid improves crop projections.

Although we expected an increase on crop yield under climate change conditions, we also observed an increase on climate sensitivity showed in the temperature-rainfall hot-map. In addition, we expected an increase on climate variability as reported by several authors. Both issues increase crop risk and variability on crop yield. Yield increase is higher when the seeding date is earlier in dry zones and later in wet zones.

Finally, this methodology helps to understand any crop behavior under climate change conditions. Nowadays, there are several mesoscale databases projecting climate change and several models for the main crops. Therefore, our methodology can be extended for several agriculture studies related to climate change adaptation such as planning infrastructure, selecting crop varieties, and changing seeding dates among others.

5.6. Acknowledgements

The original dataset was obtained from Estudio de Variabilidad Climática en Chile para el Siglo XXI project (PBCT ACT-19, http://www.dgf.uchile.cl/PRECIS/), performed by Departamento de Geofísica (DGF) de la Universidad de Chile, and funded by Comisión Nacional de Medio Ambiente (CONAMA). We are highly indebted with Direction General

de Aguas (DGA, Chile) and Armada de Chile for the *in-situ* meteorological data. The crop datasets used for validating and obtaining the initial condition for crop models was obtained based on project FONDEF DO6I 1100 “Sistema de Soporte de Decisiones Para Cultivos Tradicionales Basados en Integración SIG y Estaciones Meteorológicas” R. Orrego is funded by a national grant (CONICYT Ph.D doctorate scholarship), and this study is also funded by Ph.D program of Ciencias de los Recursos Naturales (Universidad de La Frontera).

Chapter 6

Using a crop simulation model to select to select the optimal climate grid cell resolution: a study case of Araucanía region

Raúl Orrego[1], Andrés Ávila[1,2], Francisco Meza[3], Francisco Matus[1,4]

J. Soil Sci. Plant Nutr. vol.14 no.2 Temuco jun. 2014

doi: S0718-95162014005000032

[1] Scientific and Technological Bioresource Nucleus, Universidad de La Frontera, Chile

[2] Centro de Modelación y Computación Científica, Universidad de La Frontera, Chile

[3] Centro Interdisciplinario de Cambio Global. Departamento de Ecosistemas y Medio Ambiente Pontificia Universidad Católica de Chile, Chile

[4] Departamento de Ciencias Químicas, Universidad de La Frontera, Chile

6. Using a crop simulation model to select the optimal climate pixel size

Abstract

Crop simulations are affected by the climatic condition selected by spatial scale. Several crop simulation studies use mesoscale climate database (20-50 km), where topography is neglected. We developed a method to select the optimal climate grid cell size (OCGR) based on winter wheat (*Triticum aestivum* L) yield simulations in complex and flat topographical zones (CTZ and FTZ respectively) in the Araucanía Region (37°35' and 39°37' S - 73º31´ and 71.31´ W). The OCGR was estimated from the simulated crop yield (CERES-DSSAT) using a semivariogram to compute the distance which minimized yield difference in respect to its neighbors. Climate variables were obtained from DGF-PRECIS (25 km) downscaled to a fine resolution (1 km) through Precipitation Characterization with Auto-Searched Orographic and Atmospheric effects (PCASOA) model. They were calibrated and validated from 56 *in-situ* meteorological stations (1961-1991) and field experiments (1988-2007). The crop simulation presented no significant differences (3.02±0.3–3.04±0.1 Mg ha^{-1}) compared with field experiments. The OCGR estimated averaged < 7 km for CTZ, whereas it was > 25 km for FTZ. Our approach can be applied to any zone and crops.any complex topographical zones and crops.

6.1. Introduction

Crop yield estimates using mesoscale (20-50 km) data (*e.g.* CRU; New *et al.,* 1999; GPCC; Huffman *et al.,* 1997; DGF-PRECIS, Fuenzalida *et al.,* 2006) have been used to study local responses from crop simulation models (Hansen *et al.,* 2006). Database from mesoscale models have also been used to feed crop simulation models, evaluate different adaptive management practices (Cooley *et al.,* 2005), selection of irrigation protocols, and assess the future dynamics of pest and diseases (Jara, 2013), as well as overall climate change impacts on agriculture (White *et al.,* 2011; Tan and Shibasaky, 2003).

To improve the representation of spatial heterogeneity, high resolution databases (< 1 km) are needed. However, such databases are obtained only when a dense network of meteorological stations (Mitchel and Jones, 2005), or high resolution climate grids (~1 km) are available (Baron *et al.,* 2005; Mearns*et al.,* 2003; Tsvetsinskaya, 2003). Only few studies have addressed the impact of high resolution climate grid cellon the simulated crop yield (Angulo *et al.,* 2013; Olesen*et al.,* 2000). Most of them are based on meteorological ground records and the spatial density is generated using interpolation techniques, where the unknown values need to be computed. This technique was used on the flat zones (Angulo *et al.,* 2013).

Several downscaling techniques have been performed to improve the characterization of local crop response reducing the grid resolution (Wilby and Wigley,

1997; Guan *et al*, 2009; Daly, 1994). Downscaling produces important differences of climate output, hence, in modeled crop yield response (Baron *et al.,* 2005; Mearns *et al*, 2003; Tsvetsinskaya, 2003). Mearns *et al*. (2003) reported a decrease in 25% in spring rains, downscaling from 400 km to 50 km grid the negatively impacted yield and quality of wheat crop. Similar results were reported by Baron *et al*. (2005) in West Africa and Tsvetsinskaya (2003) in Southern USA. The grid cell resolution change has been computed by dynamical models (*e.g.* WRF, MM5). This is not an easy task because of high number of computations and large numerical errors (Von Hardenberg*et al.,* 2007). To solve this problem, topographic downscaling has been implemented (Rupp *et al.,* 2012; Guan *et al.,* 2009; Daly, 1994) using multi-regression approach. For example, precipitation can be distributed from a low to high cell resolution by empirical functions based on topographical predictors (Grupta and Waimire, 1993). The most important topographical downscaling model is Precipitation Characterisation with Auto-Searched Orographic and Atmospheric effects (PCASOA) (Guan *et al.,* 2009) that includes a digital elevation model (DEM), where elevation, slope and aspects are regarded to improve spatial representation of climatic variables. Since the final scale resolution of topographical downscaling is < 1 km, the question regarding the optimum grid cell resolution to represent the spatial crop yield variability under different topographical conditions became the center of this study. The spatial variability of any continuous variable can be represented using a semivariogram (Hengl, 2007). The semivariogram is a plot where the *x*-axis is the sampling distance from the *y*-axis variable measured from their neighbors. Thus, the *y*-axis is the variance of *y* denoted by [$\gamma(h)$] (Hengl, 2007). The $\gamma(h)$ rises as the distance increases up to a maximum *sill*, a plateau, which is reached at distance *h*, called the range(Hengl, 2007). This technique can be used to estimate *h* (km) in the simulated crop yield for the optimal climate grid cell resolution (OCGR) influenced by topographical effects. Within the range *h*, the crop yield values are autocorrelated, so any unknown yield value can be interpolated from their neighbors at any direction using a selected model. Beyond *h*, the crop yield variance is independent from their neighbors.

Chile has a mesoscale DGF-PRECIS climatic database at 25 km resolution (http://www.dgf.uchile.cl/PRECIS/) for the entire country (Fuelzalida *et al* 2006). In the present study, we developed a methodological tool to predict OCGR, based on a crop yield simulation using high resolution PCASOA model database downscaled from DGF-PRECIS under different topographical conditions (flat topographical zones and hilly side complex topographical zones) in the Araucanía Region of Chile.

The aims of the present study are: (i) to quantify the impact of topographical downscaling (PCASOA, Guan *et al.*, 2009) performed based on DGF-PRECIS database as climate input on a crop simulation model of winter wheat (*Triticum aestivum* L) (CERES-DSSAT, 2008) at 1 km grid, and (ii)to estimate OCGR by using a semivariogram of the simulated crop yield under different topographical zones in Araucanía Region of Chile.

6.2. Methodology

6.2.1 Study area

The region under study corresponds to the Araucanía Region (37°35' and 39°37' S - 73º31´ and 71.31´ W) covering 67,500 km^2. Climate is characterized by a dry season between December and March with rainfall between 50 and 70 mm *per month*, which corresponds to a Mediterranean climate. Wet season is from May to September with maximum rainfall of 220-270 mm *per month*. The mean annual precipitation is 1,200 mm (Rouanet, 1983). The warmest months are from December to February (10°C to 27 °C) and the coldest ones from June to August (3ºC to 8 °C) (Rouanet, 1983). The whole region is influenced by ENSO cycles (Montecinos and Aceituno, 2002), which produce an important interannual variability in precipitation and temperature (La Niña, dry-cold and El Niño, warm-wet phase, Grimm *et al.,* 2000). The Araucanía Region presents important soil variability, mostly influenced by volcanic activity. According to Soil Survey Staff (2008) in the Region, there are Andisols, Alfisols and Ultisols (CIREN-CORFO, 2002). The region presents the typical orographical pattern of central Chile. The Costal range (on average 1,500 m.a.s.l.), called Cordillera de Nahuelbuta in the western side and Cordillera de los Andes in the eastern side (on average 3,500 m.a.s.l.). From North to South, there is an intermediate depression with agriculture valleys of moderate height (Börgel *et al.,* 1979), where most Chilean wheat grain is produced (INE, 2007) (Figure. 6.1).

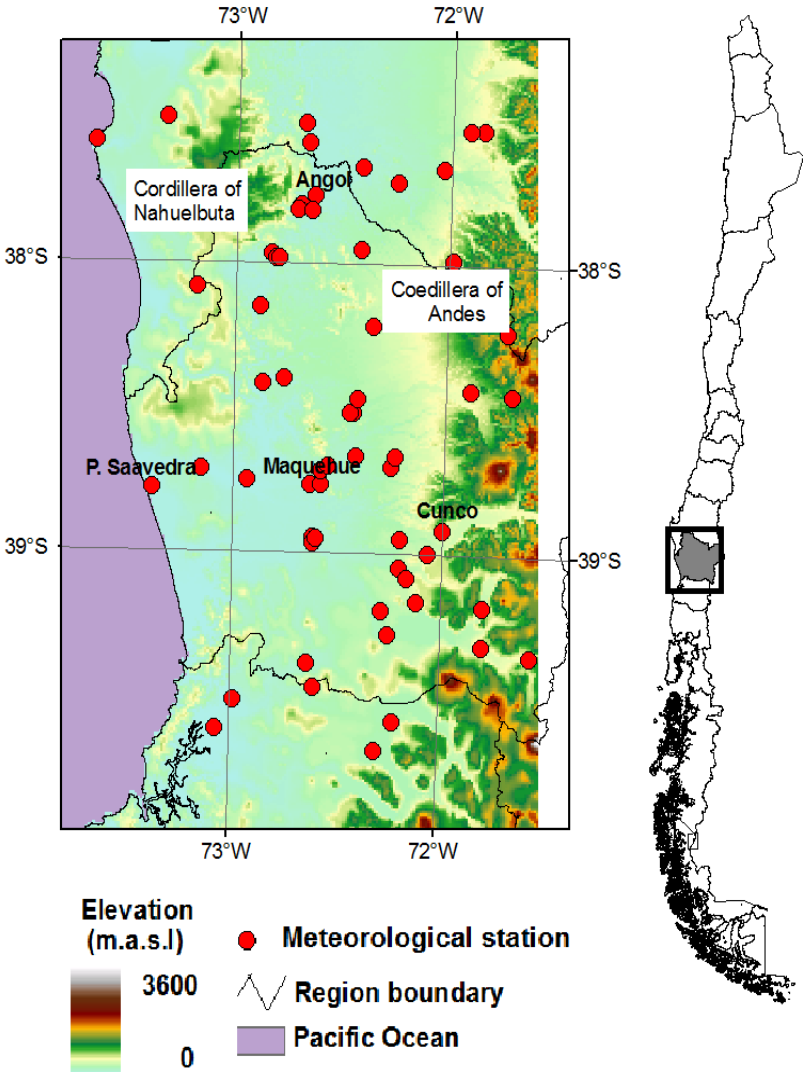

Figure7.1. *Araucanía Region, Chile showing 56 meteorological stations used in the present study.*

6.2.2 *In-situ* Database

We selected 56 meteorological stations located in the Region (Figure6.1) with a complete rainfall records from 1961 to 1991 (see below), whereas a few stations (5) presented other climate records such as photosynthetically active radiation (PAR) and temperature. Using the rule of decade continuous years or 15 years of non-continuous precipitation records between 1961 and 1991, The 10 selected stations were used for calibrating the mesoscale DGF-PRECIS database. These criteria were defined to include the records within one Pacific Decadal Oscillation, which is the main source of climatic variability in the Region (Newman *et al.,* 2003). The remaining 46 stations were used to validate the PCASOA output.

6.2.3 Calibration and validation of DGF-PRECIS database

The mesoscale database was used and it was obtained from PRECIS model applied to the continental Chilean territory between 1961 and 1991 (Fuenzalida *et al.,* 2006). The DGF-PRECIS database was created in 2006 to simulate the impact of climate change from the dynamic downscaling at 25 km grid from HadCM3 model (300 km) (Fuenzalida *et al.*, 2006). DGF-PRECIS database considered 42 climate variables including PAR, temperature, and rainfall. We consider 108 pixels of 25 km from DGF-PRECIS database. The simulated rainfall was validated by comparing the mean of each month with *in-situ* climatology records (1960-1991) for each of the ten selected meteorological stations. The DGF-PRECIS database underestimated the rainfall in winter and autumn, but overestimated this variable in summer and spring. Thus, the database was corrected by computing a monthly ratio between the *in-situ* and the modeled data. The ratio was multiplied by each monthly value of DGF-PRECIS. Therefore, a corrected monthly rainfall was used.Since temperature and solar radiation could not be validated through meteorological records, these variables were used directly from the original database for crop modeling.

6.2.4 Calibration and validation of PCASOA model

The corrected DGF-PRECIS was downscaled from 25 km to 1 km using PCASOA model for projecting the rainfall (Guan *et al.,* 2009). The PCASOA is a statistical model based on multi-regression equation at 1 km of grid resolution (Guan *et al.,* 2009) using topographic significant variables (coordinates, elevation, slope and aspect, see equation4.1).

To run the PCASOA model we used: (i) the corrected DGF-PRECIS database as ASCII list format with UTM projection coordinates and (ii)a DEM model in ASCII grid format and projected in the same geographical area. Detailed knowledge to run PCASOA model was also considered as indicated by Guan *et al* (2009). The DEM was obtained from the Global Topography (GTOPO30) project (Harding *et al*, 1999) for the Araucanía Region. It consists of 30 arc-second (about 1 km) altitude maps obtained from radar satellite records. The PCASOA was calibrated by fitting a multiple regression model using topography characteristics as independent variables with the corrected DGF-PRECIS rainfall grids as dependent variable. We used this model to compute the 1-km rainfall. Only the significant topographical variables (< 0.05) were considered for the parameterization of the equations. The output PCASOA model is the rainfall grid downscaled at 1 km, which is affected by significant topographical variables. Finally, the PCASOA model ran over 125 pixels (25 x 25 km) using the corrected database from DGF-PRECIS given a total of 67,500 fine resolution grid < 1 km *per month*.

The downscaled rainfall records were validated by comparing the climate average of the records in the remaining 46 meteorological stations. The validation showed a positive bias through the year, except for summer season. However, this bias is less than 15% in the growing season (data not shown). This error should be assessed with respect to the crop modeling impact, but it is comparable with other models validated in a similar topography zone (Diaz *et al.,* 2010).

The standard spatial deviation of elevation index (SSDE, Biteuw *et al.,* 2009) was used to divide the studied area in two large homogeneous topographical zones: (i) the flat

topographical zone (FTZ), including intermediate depression valleys and more flat agricultural areas and (ii) the complex topography zone (CTZ), namely hilly-side valleys and both mountain ranges. The SSDE consists of a 12.5 km radius area with SSDE < 100 m.a.s.l. for FTZ and > 100 m.a.s.l. for CTZ. The FTZ covered an area of 21,875 km^2 and the CTZ covered an area of 22,500 km^2 including 21 meteorological stations and 36 meteorological stations respectively. The remaining 23,125 km^2 represented the sea. The selected FTZ were associated with the stations *Maquehue* (38°46' S-72°38' W) at the Experimental Farm Station of Universidad de La Frontera and *Puerto Saavedra* (38°47' S-73°24' W). The CTZ were associated with the stations namely *Angol* (37°58' S -72°50' W) and *Cunco* (38 55'S -72°2' W) (Fig. 6.1).

6.2.5 Validation of crop simulation model

Crop simulation was performed by CERES crop model included in the supported decision system (DSSAT, V.4.0). This is the most used model for estimating the climate change impact on cropping responses (Meza *et al.,* 2008; W*oet al.,* 2013). The model allows changes in several parameters such as CO_2 concentration, fertilization, irrigation schedule, and the use of different varieties. The CERES model requires a daily weather (maximum and minimum temperature, rainfall and PAR radiation), soil database, management conditions, and genetic-crop parameters (Jones *et al.,* 2003). The corrected DGF-PRECIS was downscaled on monthly terms, but we required climate dataset on daily basis. A stochastic weather generator CLIMGEN (Campbell, 1990) was used. To estimate the yield variability, we used the rainfall output dataset from PCASOA model and PAR and temperatures from corrected DGF-PRECIS database. Thus, we produced 50 synthetic years of weather data.

In the present study, the selected variety was generic DSSAT winter wheat defined by seven coefficients: vernalization days (60 days), photoperiod effect (75 days), grain filing duration (500 °C degree days base 10 °C), kernel number (30 units kg^{-1}), kernel average weight under optimum condition (40 mg), stem and spike dry weight at maturity (1.5 g), and phyllochron interval (95 °C degree days base 10 °C). These coefficients correspond to European winter wheat in DSSAT system. The crop model management parameters were defined based on the current values used by the farmers in the Region (sowing in May, 250 plants m^{-2} and row spacing 16 cm). Since the present study focused on determining the effect of climate grid cell resolution based on the simulated grain yield, we fixed soil data obtained from the generic soil default in DSSAT (IB00000002). For the simulation, phosphorous and other nutrients in soils were not limited, except for nitrogen, which has not been considered (Angulo *et al*, 2013; Palusso *et al.,* 2011).

The CERES model output was validated by comparing the observed winter wheat yield in two season years, 2008 and 2009, from experiments carried out across the Region. One experiment was performed at the Experimental Farm Station. In the experiments, winter wheat (*cv. Kumpa*) was seeded under unlimited phosphorous and other nutrients, except for nitrogen. Five levels of nitrogen fertilization (urea), including a control without nitrogen, were applied. Other experiments (1988-2007) of non-nitrogen fertilizer control winter wheat across the region were also regarded (Campillo *et al.,* 2010; Campillo *et al.,* 2007; Rouanet, 1994).

To assess the impact of the scale change of climate variables affected by the topographical conditions on the simulated crop yield, we compared the difference between simulated yield using *in-situ* rainfall records and those obtained from corrected DGF-PRECIS and PCASOA model. The comparisons were performed using a pair-wise sample T-Test computed by using Analysis of Data module contained in Microsoft EXCEL.

6.2.6 Optimal climate grid cells resolution

To estimate OCGR,we used a spatial technique, the semivariogram to compute *h* range distance, where the simulated winter wheat yield variability can be predicted. We simulated the yield on each high resolution cell of 1 km nested within a low resolution cell of 25 km in a typical year as 1970 *i.e.* a year close to the historical average and monthly distribution of rainfall. Although the semivariogram techniques can be computed considering the neighbor in all directions (omnidirectional semivariogram), the directions were selected based on orographic dominance in this study. We considered a longitudinal transect from West to East and latitudinal transect from North to South in the CTZ and FTZ, respectively. Thus, four simulated crop yield semivariograms were computed, two for each FTZ and CTZ using ARC-GIS 9.1 software (Redland California, U.S.A.).

6.3. Results

63.1 Crop model validation and spatial resolution impact

The simulated wheat yield (1961-1991) ranged from 2.8±0.2 Mg ha^{-1} to 3.3±0.2 Mg ha^{-1}, whereas in the field experiments (1988-2007), it ranged from 2.5±0.5 Mg ha^{-1} to 3.5±0.3 Mg ha^{-1} and there was no significant difference (Figure6.2). There were no significant differences in the crop yield mean between FTZ and CTZ.

Figure 6.2. *Average of observed (1988-2007) winter wheat yield field experiments from*

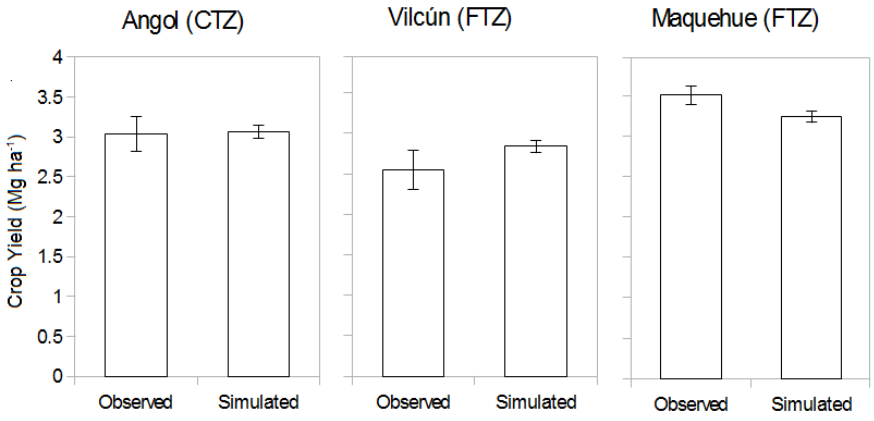

Vilcún (n=6), Maquehue (n=14) and Angol (n= 15) (see Fig 7.1) representing the flat topography zones (FTZ) and complex topography zones (CTZ) in Region of Araucanía as compared with the simulated (DSSAT) winter wheat yield average (1961-1991) in the same locations. Bars represent the standard error of the mean.

There were significant differences between simulated crop yields using PCASOA or DGF-PRECIS database relative to *in-situ* record simulations (error) (Figure6.3). The yield simulation from PCASOA database ranged from -27% to 42 % of the ground simulation, whereas for DGF-PRECIS database it ranged from -72% to 153 %, doubling PCASOA

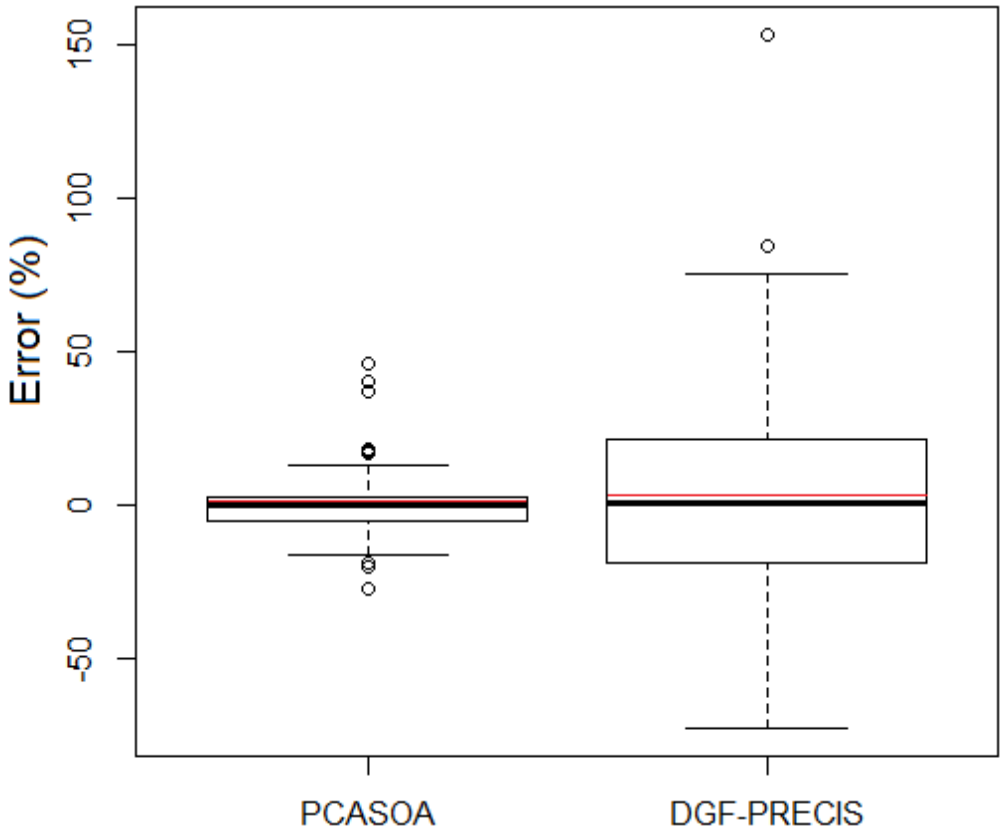

yield errors.

Figure6.3.*Boxplot error of simulated (DSSAT) winter wheat yield of typical* year *1970 (mean and* monthly *precipitation close to the annual values) by PCASOA high resolution (< 1 km) climate output database or DGF-PRECIS low resolution (25 km) climate ouput database relative to in-situ climate records simulation from 46 meteorological stations (1961 and 1991) in Araucanía Region, Chile. Red line shows the mean and black line shows the median.*

The simulated yield in the FTZ and CTZ using PCASOA, DGF-PRECIS and the records data from the stations are presented in Figure6.4. The absolute amount of winter wheat yield was significantly different only in CTZ ($P < 0.05$) (Fig. 4b), but PCASOA showed lesser error than DGF-PRECIS improving the crop simulation in about a 50 % (RSME 0.257 Mg ha^{-1} for PCASOA and 0.719 Mg ha^{-1} for DGF-PRECIS) in both zones. In FTZ, PCASOA simulation showed the lowest variability, whereas DGF-PRECIS showed the highest one. However, the simulated mean yield values were similar among all databases (for PCASOA it was 2.24 Mg ha^{-1}, for DGF-PRECIS it was 2.25 Mg ha^{-1}, and for *in-situ* data it was 2.26 Mg ha^{-1}). In contrast, the simulated yield using *in-situ* and PCASOA

database in CTZ was 1.97 Mg ha^{-1} and 2.09 Mg ha^{-1}, respectively, whereas the variability for DGF-PRECIS in CTZ was the highest value (2.20 Mg ha^{-1}). Comparing the error of PCASOA and DGF-PRECIS database, PCASOA showed lesser error in both zones (-27 to 46 % in FTZ and -8 to 40 % in CTZ compared with DFF-PRECIS (-72 to 75 % and -51 to 153 %) (Figures6.4c and 6.4d).

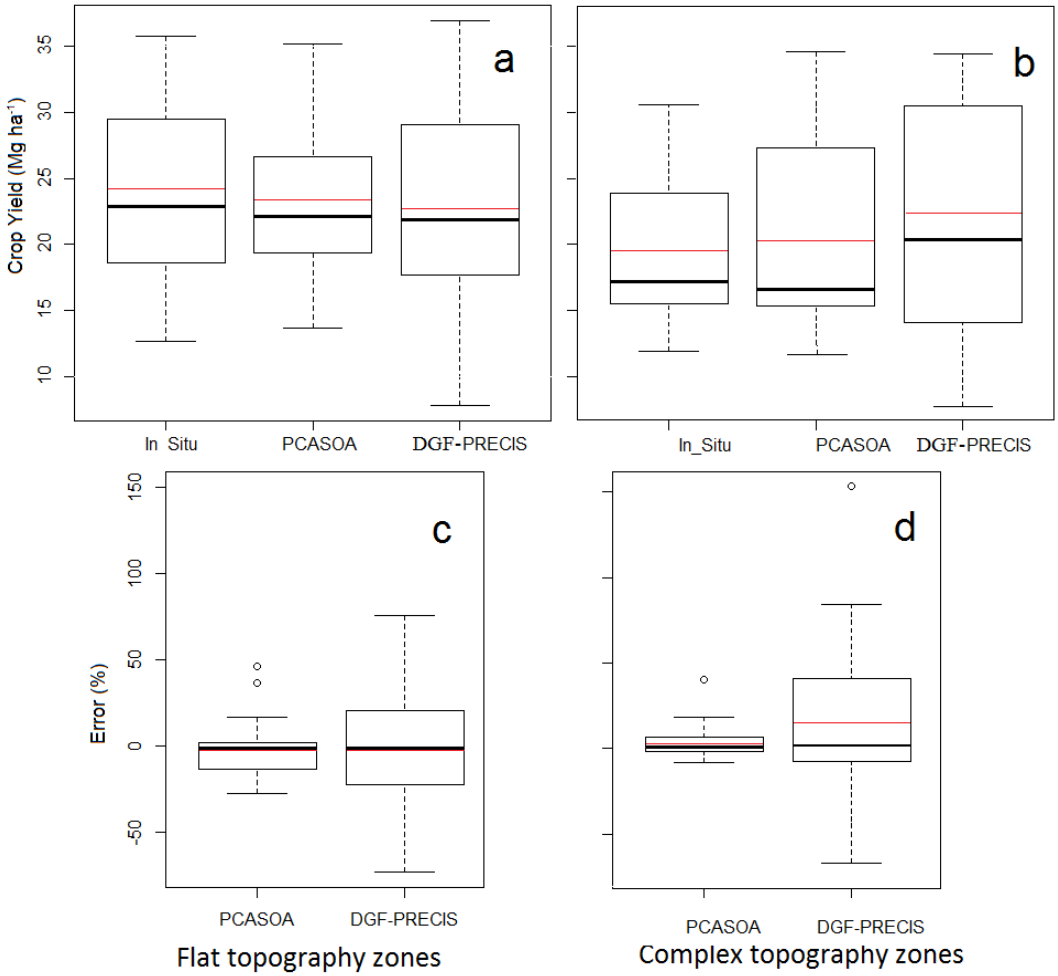

Figure6.4. *Boxplot of (a-b) absolute simulated (DSSAT) winter wheat yield by in-situ climate records from 46 meteorological stations (1961 and 1991) in Araucanía Region and (c-d) relative error of simulated crop yield of typical* year *1970 (mean and* monthly *distribution of mean annual precipitation) by PCASOA high resolution (< 1 km) output database and DGF-PRECIS low resolution (25 km) climate database relative to in-situ climate records. Red lines show the mean and black lines show the median.*

6.3.2 Optimal climate grid cell resolution

The semivariogram of the crop yield variability to estimate the OCGR is shown in Figures7.5 and 7.6. Both, FTZ and CTZ showed a spatial autocorelation, hence spatial

variability could be represented by the semivariograms. In fact, all zones show Moran's indexes close to one which indicates that the database was autorelated. There are no statistical evidences ($P < 0.01$) that the values were non-autocorelated. However, some semivariograms reached a stationary (steady-state) variability showing the maximum distance *h* where the non-sampled neighbors can be predicted. If the non-steady state variability is not reached, we can predict that 25 km of spatial variability cell size can represent the mean yield of the OCGR.

There was no range *h* in the FTZ (Maquehue and P. Saavedra), because the semivariogram either in North-South or East-West directions did not reach a stationary yield within cell, suggesting that the distance, in which OCGR was calculated, is larger than 25 km mesoscale cell (Fig 6.5). In contrast, OCGR in the CTZ in Cunco was estimated from 8 to 25 km, depending on directions North-South or West-East, respectively (Figure6.5). In Angol, *h* was 15 km from North to South and 17 km from West to East (Figure6.6). The last two cases are explained by topography. In Cunco, there is a valley crossing the cell in West-East direction dividing into two hillsides and one valley. This fact implies similar yield on both hillsides, and a different yield in the valley. In Angol, the Nahuelbuta Mountains present an elevation just on the northern zone, which increases rainfall with respect to the southern zones.

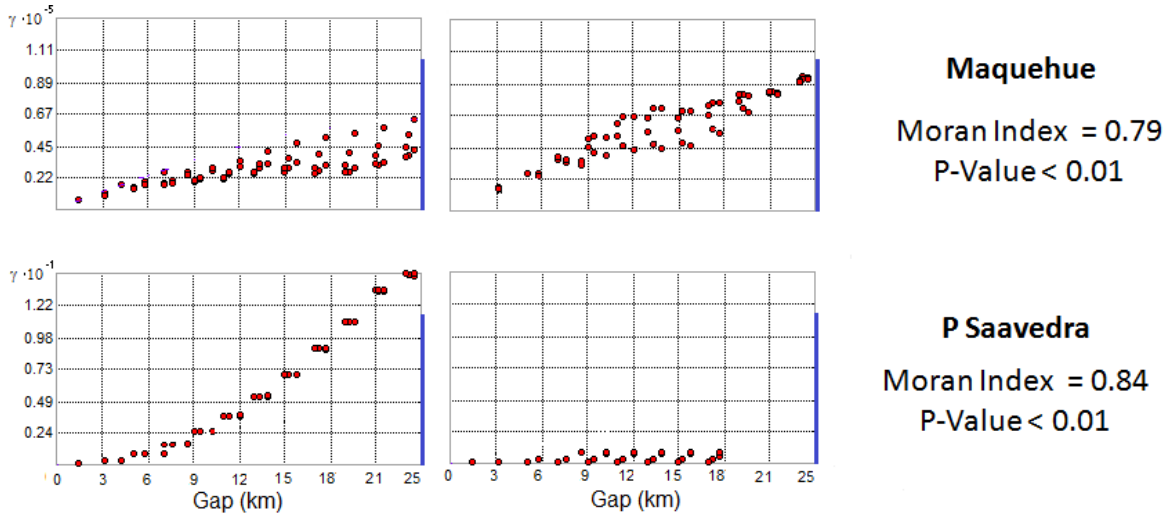

Figure6.5. *Spatial variability of simulated (DSSAT) winter wheat yield estimated representing the flat topography zones (FTZ) in the Araucanía Region. Left semivariogram is North-South direction. Right semivariograms are East-West direction. Moran probability index (0 = non autocorrelation and 1 = full autocorrelation). Vertical line shows range h.*

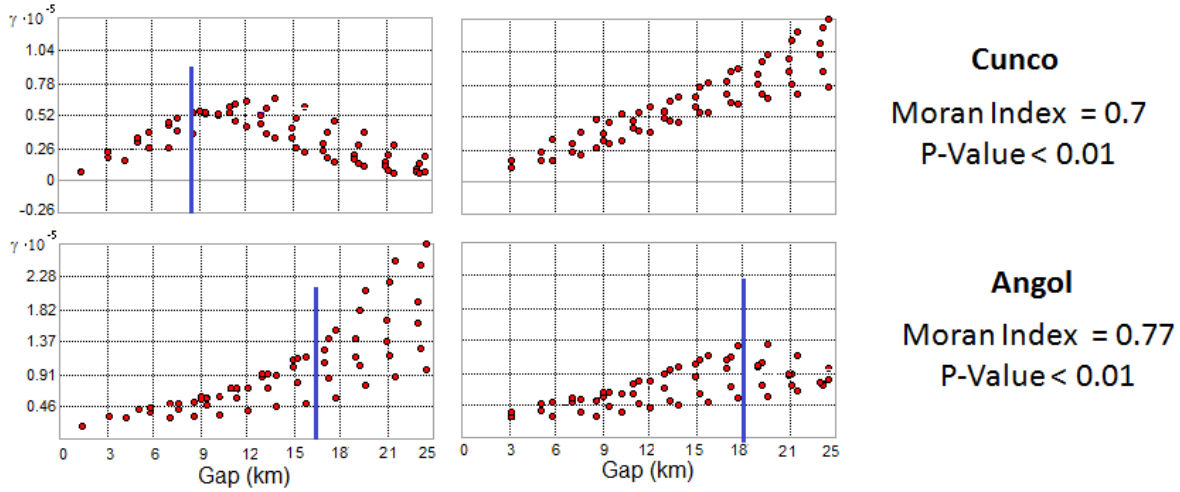

Figure 6.6. Yield directional semivariograms inside the selected low resolution pixels on complex topography areas. Left semivariograms are in North-South direction, and right semivariograms are in East-West direction. Moreover, we show Moran Index and itsprobability equals 0 (non autocorelated). Vertical line shows range h.

6.4. Discussion

In the present study we assumed that downscaling climate low resolution rainfall database for crop model is useful for predicting an OCGR. We hypothesized that the spatial resolution of the simulated crop yield can be computed, which, in turn, represents the optimal grid cell resolution < 1 km database under flat and complex-topography scenarios. For this purpose, we used a semivariogram technique.

As far as we know, there are a few papers which have estimated an OCGR using up-scaling interpolation from the meteorological record dataset (Wong and Asseng, 2006; Olesen *et al.*, 2000) and there are no papers using spatial resolution and topographical features. Therefore, works based on up-scaling are the unique references for analyzing our results. The OCGR estimation was possible because the high resolution climate grid obtained by PCASOA model improved significantly the simulated crop yield introducing the topographical effects. This contrasts with the results obtained by Olesen *et al*. (2000), who reported the spatial crop variability in Denmark at 10 km grid. This effect could not be explained by the climate grid cell resolution, since there was no correlation between climate and yield variability. Angulo *et al*. (2013) studied the spatial crop yield variability in Norway and they reported yield differences of 4 % when the scale resolution changed from *in-situ* data to a 20 km grid. They used several models (including DSSAT) for simulating crop yield and they observed that the resolution scale explained the variability less than the crop model, because the study was performed in the flat agricultural areas. In contrast, the present results indicate a clear relationship between the topographic variables and the impact of climate resolution on crop yield simulation (Fig 6.4).

Although up-scaling is the unique reference for analyzing our results, both approaches have different sources of errors, therefore it is expected that both can present different yield responses. Up-scaling depends on the interpolation method and the climate record density. The spatial resolution technique proposed here depends on climate modeling quality and agriculture feasibility, limited mainly by topographical constraints. Thus, we think that our technique is more suitable than up-scaling from synthetic scenarios based on climate grids (*e.g.* for climate change and climate cycles) or where interpolation methods are unreliable due to lack of data, and/or low spatial autocorrelation.

We observed that there was a poor correlation ($R^2 = 0.30$, $P < 0.01$) between high rainfall *in-situ* record data (> 2000 mm) and crop yield, whereas the opposite was true ($R^2 = 0.71$, $P < 0.01$) at low rainfall (< 2000 mm) (Wong and Asseng, 2006). This could be explained because high rainfall improves the crop growing conditions, reducing the effect of climate variability. In fact, when rainfall exceeds 2000 mm, soil moisture is not a limiting factor for crop growth and precipitation is not related to yield variability (Wong and Aseng, 2006). This result supported the hypothesis of the present study that topography influences OCGR estimation, particularly in CTZ. Therefore, from an operative point of view, OCGR can be well estimated in a dry year to increase the sensitivity of the crop simulation response to climate input.

Finally, downscaling for the study type conducted here should be focused on CTZ, including hilly-side mountains areas where small farmers are located. Climate in this area can be modeled using improved input grids such as OCGR calculated in this research. In addition, our approach can be used for examining the microclimates at high resolution climate dataset.

6.5. Conclusion

In this study we provide an approach for selecting the optimal scale linking climate grids with crop modeling to assess the impact of high resolution downscaling technique on crop simulations of winter wheat in Araucania Region. We showed that downscaling improves the crop model performance in about 50 %. These effects depend on the topographical conditions. In flat topographical zones there are no significant differences in the crop yield simulated with high resolution (< 1 km) or mesoscale resolution (< 25 km) database, whereas in complex topographical (hilly side and mountains) zones these differences were highly significant. In the Araucania Region, the optimal climate grid cell resolution was 25 km in the flat zones, whereas, it was 4 km in complex zones. The optimal climate grid cell resolution estimation was also affected by total rainfall and topography variables (altitude, aspect and slope) providing a clear assessment to a simple estimation of climate grid resolution for optimal crop yield. The broad implication of our findings are: we do not require downscaling from mesoscale models database in flat zones , whereas downscaling to simulate the optimal crop yield is required in hilly-side and complex topography zones.

6.6 Acknowledgements

The original dataset was obtained from Estudio de Variabilidad Climática en Chile para el Siglo XXI project (PBCT ACT-19, http://www.dgf.uchile.cl/PRECIS/), performed by Departamento de Geofísica (DGF) de la Universidad de Chile, and funded by Comisión Nacional de Medio Ambiente (CONAMA). We are highly indebted with Direction General de Aguas (DGA, Chile) and Armada de Chile for the *in-situ* meteorological data. We acknowledge FONDEF DO6I 1100 project. R. Orrego would like to thank CONICYT for the grant that supported doctoral work N°21090443). We also thank the Ph.D program in Science of Natural Resources in Universidad de La Frontera for its support. This research was partially supported by the supercomputing infrastructure of NLHPC (ECM-02) at Centro de Modelación y Computación Científica at Universidad de La Frontera CMCC-UFRO. We acknowledge the two anonymous reviewers for the effort in revising this manuscript.

Chapter 7

General discussions and concluding remarks

7. General discussion

This thesis was focused on projecting the main climate patterns at local scale under climate change scenarios of A2 and B2 from IPCC (2001; 2007) and assessing its impact on crop systems. This analysis considered climate model validation and scale improvement for projecting the impact at high resolution grid (1 km). We use this grid to study the impact of climate change scenarios on wheat crop yield on Araucania Region. In this process, we test the topographical downscaling as methodological steps to improve the climate projections from mesoescale climate model outputs. We also define an optimal climate scale for crop modeling. Our methodology enhances the rainfall and crop projection helping to design mitigation strategies, and it can be extrapolated for any zone and crop. Thus, the novelty of this tesis were: a) to valídate the DGF-PRECIS dataset by comparing with in-situ climate records, identifying its main uncertainties, b) to develop a high resolution projected rainfall dataset (1 km) for the Araucanía region, c) to develop a high resolution crop yield projection (1 km) for the Araucanía región, d) to assess the impact of the downscaling of climate models at high resolution in the crop modeling, and d) to propose a method for identify the optimal climate grid size.

This thesis is compiled in seven chapters. In Chapter 1 a general introduction is presented. In Chapter 2, a compilation of the current theoretical framework of the state of the art on the impact of climate change on crop system is discussed. We hypothesize that the theoretical downscaling techniques must be used for correcting differences of scales between climate models and high resolution crop models (< 1 km grid). This hypothesis was tested in Chapter 6, finding dependence between climate grid resolution and topography. In the same Chapter we computed an optimal climate grid cell size for crop modeling, which was has not been proposed in the literature (Orrego *et al*., 2014).

In Chapter 3, we validated the national dabase projection called DGF-PRECIS for local area (Araucanía Region) using a general validation for the whole Chilean territory to understand the local model biases. DGF-PRECIS database had a good performance to reproduce the rainfall pattern from central to southern Chilean Regions (56-30º S) under neutral ENSO influence. However, in the northern regions (17°-30°S), DGF-PRECIS database showed large errors (>30%). We also found that climate pattern under El Niño and La Niña synoptic condition was not well represented. Althouhg this does not affect the climate projection reliability, ENSO effects could affect the representation of future climate variability. For solving this problem, one strategy should be the use of ENSO phase scenarios.

Although general climate pattern of DGF-PRECIS database are fitted with the observed record in Araucanía region, it projection indicates a drier summer and rainier winter. This was corrected using an empirical coefficient generating a new corrected rainfall dataset. This correction was a critical step to generate a high resolution dataset using a topographic downscaling (Chapter 4), which it was particularly sensitive to the quality of climate grid.

In Chapter 4 we downscaled the corrected DGF-PRECIS in Araucanía Region to obtain high resolution grid (1 km) using a topographical model PCASOA.We added the effect of topography for these simulations, obtaining improvements with respect to both, the original DGF-PRECIS and corrected database. Most important corrections occur precisely during the crop-growing season (spring and summer) impacting the crop modeling (Chapters 5 and 6). Additionally we presented and discussed that high resolution dataset performed better than the climate pattern obtained with mesoescale resolution, such as the orographic rainfall on Nahuelbuta Costal Condillera and the "absolute" dry season located in the North-West of the Araucanía Region. In fact, we project an increase of the Föen effect on Nahuelbuta range, and a later in one month in the dry season under climate change condition. Also, we prove that topographical downscaling is a suitable method in places with a lack of climate records. It is important to say that high resolution do not changes the general trend, but marked the differences.

In Chapter 5, we showed the crop projection made by high resolution climate projection linked with CERES crop model (DSSAT). We obtained positive responses in the crop simulation models by assessing the impact of climate change in Araucanía Region, which can be used for policy makers by simulating crop yield and phenological stages as criteria. This response is explained by higher CO_2 concentration and also by climate condition. The effect of climate condition on the yield is explained by nitrogen lixiviation which would decrease under climate change condition (Chapter 5). Based on our result, it is possible to improve the current policies. Crop modeling assumes that crop genetic coefficient will be constant under climate change condition as well, which is criticized by some authors. Moreover, farmer adaptation is another mitigating effect for projecting the crop yield under climate change conditions. Both ideas are important challenges for improving the crop projection, and they must be considered when our results are used.

Based on all the works mentioned above, in Chapter 6 we performed a spatial analysis for measuring the effect of downscaling on the crop simulation model for an optimal climate grid cell size using the yield response of a crop model. Scale downscaling significantly affected the crop response, but only on complex topography zones. The method proposed here for defining the optimal grid size suggests that mesoscale grids are suitable for representing the crop yield spatial variability on the central valley (flat zones), but fine grids are required for zones located near the Nahuebulta mountain (e.g. Angol) and Andes Mountain (e.g. Cunco). Although the main crop productivity zones are located in flat zones, complex topography zones are more sensitivities to climate change, where the small subsistence farmers are located as well.

7.2. Concluding remarks

- DGF-PRECIS database had a good performance to reproduce the rainfall pattern from central to southern Regions (56-30º S) only under neutral ENSO influence. In fact, climate pattern under El Niño and La Niña rainfall are overestimated. Also, in the northern regions (17°-30°S), DGF-PRECIS database showed large errors

(>30%).This suggest that the interannual dynamic of Pacific Anticyclone is not represented by climate models used in DGF-PRECIS database. The corrected projections showed a decrease in annual precipitation < 458±4 mm *per* year (30%) and 235±9 mm *per* year (15%) under A2 and B2 scenarios.

- Topographic downscaling is a suitable method in places where the lack of climate records is present. This downscaling improved the climate projection, reducing the error in about 20%. Downscaled database showed less error in spring and summer, just the growing crop season. Also, high resolution dataset represent climate pattern which cannot observe at mesoescale resolution. The main effect is the orographic rainfall on Nahuelbuta Costal Condillera and the "absolute" dry season located in the North-West of the region.
- We expected an increase (about 52%) on the crop yield under climate change conditions. This increase is explained for both: higher CO_2 concentration, and better climate condition. We propose earlier seeding date in dry zones and later seeding date in wet zones, and genetic adaptation strategies for winter wheat.
- Optimal climate grid cell size was estimated including the effect of topography in Araucanía Region for winter wheat. It was estimated successfully using variogram technique. We obtained a significant effect of downscaling only on complex topography zones. We computed an optimal climate grid cell < 7 km for complex topography zones, whereas it was > 25 km for flat zones. These values are valid for winter wheat in the Araucanía region, but our method based on semivariograms can be applied to any zone and crops if the rainfall data density is enough to produce such a high resolution climate grid.

7.3. Future prospects

- For solving the climate uncertainties from AOGCM, IPCC has been developing a new projection during the last years considered in the next AR5 report. These new projections include new scenarios, ENSO condition and improvements on linking sub-models (mainly land cover). The uses of these new climate projections for developing high resolution crop projection needs to be locally tested in the near future.
- Topographic downscaling is a suitable method for improve the climate projection. However, computing the maximum resolution to generate good crop response is not an easy task. Theoretically, the maximum resolution depends on elevation, and nowadays high resolution digital elevation model are available (< 100 m). Other factors related to land use must be considered (e.g. water evaporation of crop on close areas, urban heat island) that could affect the climate patterns. To develop downscaling techniques, which included both, topographic and land use, is an interesting challenge for extend our work to other areas and crops where higher resolution are required.
- A promising strategy for climate change adaptation is to project scenarios. The techniques developed in this thesis could be used to improve these projections. In Chile, and in particularly in Araucanía Region, two phenomena show important

effects on climate condition: ENSO and Antarctic Oscillation. The ENSO is widely investigated, but there are no definitive conclusions for the impact on climate change. The International Research Institute for Climate and Society (IRI) has developed seasonal forecast methods based on ocean surface temperature. Antarctic Oscillation is recently investigated because this phenomenon produces important effects on high latitude rainfall. Although these aspects were not included in this thesis, we had improved the season projection for Araucanía Region by making an experimental model, which corrects IRI projection using an Antarctic Oscillation Index. This is an ongoing research where the downscaling techniques applied in this thesis are used to improve these projections for genetic crop strategy on this new climate variability.

- Other challenge is the cropping adaptation strategy to climate change condition. Chile could be an excellent natural laboratory due to its climate variability and geography isolation. On the other hand, an interesting topic is to assess the effect of soil properties as buffer for climate change impact which was not done here. This has not been investigated and could be an interesting prospect to project real crop response under the new climate change condition. On the other hand, the natural crop adaptations are new issues for another research for improving crop projection.
- Our results could be extrapolated to other crops and places located mainly on complex topography zones. If we focus on Chilean crops, the first challenge is to extend this work for others valuables and sensitive agriculture products such as potatoes, fruits and grape-wine. Moreover, our research can also be extrapolated to other research areas, such as forestry and wild life, hydrology, and human health. Since its sensitivity to climate condition and valuable biodiversity, relicts forest (*e.g.* Fray Jorge) could be one of the most important issues to assess its behavior based on high resolution climate projection. However, it is important to assess the optimal grid size estimation. It cans performe by nested simulation, using systematically higher grid resolution to reach a steady state of the modeled crop yield.

8. References

- Aceituno, P., 1998: Climate elements of the South American Altiplano (in Spanish). Rev. Geofisica-IPGH, 44, 37–55.
- Alexandrov, V. A., and G. Hoogenboom. 2000. The impact of climate variability and change on crop yield in Bulgaria. Agricultural and forest meteorology 104,4: 315-327.
- Allen, M., Stott, P., Mitchell, J., Schnur, R., Delworth, T., 2000. Quantifying the uncertainty in forecasts of anthropogenic climate change. Nature 407:617-620.
- Allen, R. L., Erickson, M. C, 2001. AVN-based MOS precipitation type guidance for the United States, NWS Technical Procedures. Bulletin No. 476, NOAA, U.S. Dept. of Commerce, 9p.
- Almazroui, M., 2013. Simulation of present and future climate of Saudi Arabia using a regional climate model (PRECIS). International Journal of Climatology. 33, 9:2247–2259
- American Meteorological Society, cited 2013: "mesoscale " Glossary of Meteorology. Available in the site http://glossary.ametsoc.org/wiki/Main_Page. Last visit 12/11/2013
- American Meteorological Society, cited 2013: "microscale " Glossary of Meteorology. Available in the site http://glossary.ametsoc.org/wiki/Main_Page. Last visit 12/11/2013
- American Meteorological Society, cited 2013: "synoptic " Glossary of Meteorology. Available in the site http://glossary.ametsoc.org/wiki/Main_Page. Last visit 12/11/2013
- Amerine, M. A., and A. J. Winkler. 1974. Composition and quality of musts and wines of California grapes. Hilgardia 5: 493-675.
- Amthor, J., 2001. Effects of atmospheric CO_2 concentration on wheat yield: review of results from experiments using various approaches to control CO_2 concentration. Field Crops Research, 73:1-34.
- Anderson, D., 2003. Coupled Ocean-Atmosphere Models. In Holton, J., Curry, J., Pyle, J.(Ed) Encyclopedia of Atmospheric Science, Elsevier, U.K. pp: 574-582.
- Angulo, C., Rötter, R., Trnka, M., Pirttioja, N., Gaiser, T., Hlavinka, P., Ewert, F. 2013. Characteristic 'fingerprints' of crop model responses to weather input data at different spatial resolutions. European Journal of Agronomy, 49, 104-114.
- Antle JM, Capalbo SM, Elliot ET, Paustian KH. 2004. Adaptation, spatial heterogeneity and the vulnerability of agricultural systems to climate change and CO_2 fertilization: an integrated assessment approach. Climatic Change 64:289–315.

- Anwar, M. R., O'Leary, G., McNeil, D., Hossain, H., Nelson, R., 2007. Climate change impact on rainfed wheat in South-eastern Australia. Field Crops Research, 104,1: 139-147.
- Asseng,S., Ewert, F., Rosenzweig, C., Jones, J.W., Hatfield, J.L., Ruane, A.C., Boote, K.J., Thorburn, P.J., Rötter, R.P., Cammarano, D., Brisson, N., Basso, B., Martre, P. , Aggarwal, P.K., Angulo, C., Bertuzzi, P., Biernath, C., Challinor, A.J., Doltra, J., Gayler, Goldberg, R., Grant, R., Heng, L., Hooker, J., Hunt, L.A., Ingwersen J., Izaurralde, R.C., Kersebaum, K.C., Müller, C., NareshKumar, S., Nendel, C., O'Leary, G., Olesen, J.E., Osborne, T.M., Palosuo, T., Priesack, E., Ripoche, D., Semenov, M.A., Shcherbak, I., Steduto, P., Stöckle, C., Stratonovitch, P., Streck, T., Supit, I., Tao, F., Travasso, M., , Waha, K., Wallach, D., White, J.W., Williams, J.R., Wolf, J., 2013. Uncertainty in simulating wheat yields under climate change. Nature Climate Change
- Augspurger, C., 2009. Spring 2007 warm and frost: phenology, damage and refoliation in a temperate deciduous forest. Functional Ecology 23(6): 1031-1039.
- Baigorria G., Jones, J.W., O'Brien, J. J., 2008. Potential predictability of crop yield using an ensemble climate forecast by a regional circulation model. Agricultural and Forest Meteorology 148: 1353 – 1361.
- Bannayan, M., Hoogenboom, G., 2008. Weather analogue: A tool for real-time prediction of daily weather data realizations based on a modified k-nearest neighbor approach. Environmental Modelling & Software 23: 703-713.
- Baron, C., Sultan, B., Balme, M., Sarr, B., Traore, S., Lebel, T., Janicot, S., Dingkuhn., M., 2005. From GCM grid cell to agricultural plot: scale issues affecting modeling of climate impact. Philosophical Transactions of Royal Society B. 360: 2095–2108.
- Barry, R. G.; Chorley, R. J., 1992. Atmósfera tiempo y clima. Cuarta Edición, Ed Omega, Barcelona. 500 pp
- Batchelor, W. D., Basso, B., Paz, J. O., 2002. Examples of strategies to analyze spatial and temporal yield variability using crop models. European Journal of Agronomy, 18,1: 141-158.
- Bauer, H. S., and V. Wulfmeyer, 2009. Validation of components of the water cycle in the ECHAM4 general circulation model based on the Newtonian relaxation technique: a case study of an intense winter cyclone. Meteorol. Atmos. Phys ,104(3-4), 135-162.
- Benestad, R. 2001. A Comparison Between Two Empirical Downscaling Strategies. International Journal Of Climatology, 21: 1645–1668 (2001)
- Benestad, R. E., Hanssen-Bauer, I., Chen, D., 2008. Empirical-Statistical Downscaling. World Scientific Publishers. 272 p.
- Beniston, M., Stephenson, D., Christensen, O., Ferro, C., Frei, C., Goyette, S., Halsnaes, K., Holt, T., Jylhä ,K . Koffi, B., Palutikof, J., Schöll, R., Semmler, T.,

Woth, K., 2007. Future extreme events in European climate: an exploration of regional climate model projections. Climatic Change, 81:71–95

- Bergström, S., Carlsson, B., Gardelin, M., Lindström, G., Rummukainen, M., 2001. Climate change impacts on runoff Sweden-assessments by global climate models, dynamical downscaling and hydrological modeling. Climate Research 16: 101–112.
- Betts, R., 2005. Integrated approaches to climate-crop modelling: needs and challenges. Philosophical Transactions of Royal Society B. 360: 2049-2065.
- Bindi M., L. Fibbi, B. Gozzini, S. Orlandini, and F. Miglietta. 1996. Modelling the impact of future climate scenarios on yield and yield variability of grapevine. Climate Res. 7: 213-224.
- Bitew, M., Gebremichael, M., Hirpa, F. A.., Gebrewubet, Y. M. ., Seleshi, Y., Girma, Y., 2009. On the local-scale spatial variability of daily summer rainfall in the humid and complex terrain of the Blue Nile: observational evidence. Hydrological Processes 23, 3670–3674.
- Bodwen, P., and C. Edwars. 2003. Ocean Circulation/Surface Wind-Driven Circulation. In: Holton, J., J. Curry, and J. Pyle (eds). Encyclopedia of Atmospheric Science. Elsevier, U.K. pp: 1540-1549.
- Bonan, G., 1996. A land surface model (LSM version 1.0) for ecological, hydrological, and atmospheric studies: technical description and user's guide. NCAR Technical Note NCAR/TN-417+STR National Center for Atmospheric Research. Boulder Colorado. 150 p.
- Boote, K., Jones, J., Pickering, N. 1996, Potential Uses and Limitations of Crop Models. Agronomy Journal. 88, 5: 704-716
- Börgel, R. Geografía de Chile, IX Region de La Araucanía. Santiago de Chile: Instituto Geográfico Militar de Chile, 1986
- Bosilovich, M. G., Schubert, S.D., Rienecker, M., Todling, R., Suarez, M., Bacmeister, J., Gelaro, Kim, G.-K., Stajner, I., Chen, J., 2006: NASA's Modern Era Retrospective-analysis for Research and Applications. U.S. CLIVAR Variations 4(2): 5-8.
- Bosque, J. 1994.Sistemas de información geográfica: prácticas con PC ARC/INFO e IDRISI. RA-MA Ed. 478 pp
- Brisson, N., Gary, C., Justes, E., Roche, R., Mary, B., Ripoche, D., Zimmer, D., Sierra, J., Bertuzzi, P., Burger P., Bussière, Cabidoche F., Cellier, P., Debaeke P., Gaudillère J., Hénault, C., Maraux, F., Seguin, B., Sinoquet, H., 2003. An overview of the crop model STIC. European Journal of Agronomy 18:309-332.
- Brouder, S., Volenec, J., 2008. Impact of climate change on crop nutrient and water use efficiencies. Physiologia Plantarum 133: 705 – 2008.
- Buizza, R. 2003., Weather Prediction / Ensemble Prediction. In Holton, J., Curry, J., Pyle, J.(Ed) Encyclopedia of atmospheric science, Elsevier, U.K. pp 2546-2557.

- Busby, S. J., K. R. Briffa, and T. J. Osborn., 2007. Simulation of ENSO forcings on U.S. drought by the HadCM3 coupled climate model, Journal of Geophysical Research 112, D18112
- Busuioc, A., D., Chen, C., Hellström. Performance of Statistical Downscaling Models in Gcm Validation and Regional Climate Change Estimates: Application for Swedish Precipitation, International Journal of Climatology 21: 557–578 (2001).
- Caldeira, K., and G. Rau, 2000. Accelerating carbonate dissolution to sequester carbon dioxide in the ocean: geochemical implications. Geophys. Res. Lett. , 27 (2), 225-228.
- Campbell, G. S. 1990. ClimGen, climatic data generador. Washington State University. http://www.bsuse.wsu.edu/climgen (consultado 29 abril 2009).
- Campillo, R., Jobet, C., Undurraga, P., 2007. Optimización de la fertilización nitrogenada para trigo de alto potencial de rendimiento en andisoles de la Region de la Araucanía, CHILE. Chilean Journal of Agricultural Research 67,3:281-291
- Cannon, A., 2007. Nonlinear analogy predictor analysis: A coupled neural network/analogy model for climate downscaling. Neural Networks 20: 444-453.
- Castillo, H., Santibañez, F., 1987. Efecto de la Temperatura sobre la fenología del trigo (Cultivar Aurifen). Agricultura Técnica 47, 1.
- Caya D., Laprise, R., 1999. A semi-Lagrangian semi-implicit regional climate model: The Canadian RCM. Monthly Weather Review127, 341–362
- Centritto, M., Lee, H.S.J., Jarvis, P.G., 1999. Increased growth in elevated [CO_2]: an early, short-term response? Global Change Biology 5:623-633.
- Cerri, C., Sparovek, G., Bernoux, M., Easterling W., Melillo, J., Cerri, C., 2007. Tropical agriculture and global warming: impacts and mitigation options. Scientia Agrícola. 64(1):83-99.
- Cess, R., 2005. Water Vapor Feedback in Climate Models. Science, 310, 795-796.
- Chakraborty, S., Newton., A. 2011. Climate change, plant diseases and food security: an overview. Plant Pathology: 60, 2–14
- Challinor, A , Ewert, F., Arnold, S, Simelton, E. Fraser, E, 2009. Crops and climate change: progress, trends, and challenges in simulating impacts and informing adaptation. Journal of Experimental Botany, 1-15.
- Challinor, A., Wheeler, T., 2008. Crop yield reduction in the tropics under climate change: processes and uncertainties. Agricultural and Forest Meteorology 148:343 – 356.
- Chartzoulakis, K., Psarras, G., 2005. Global change effects on crop photosynthesis and production in Mediterranean: the case of Crete, Greece. Agriculture, Ecosystems and Environment 106:147-157.

- Chen, F., Dudhia, J., 1999. Coupling an Advanced Land Surface–Hydrology Model with the Penn State–NCAR MM5 Modeling System. Part I: Model Implementation and Sensitivity. Monthly Weather Review 129: 569-585.
- Christensen J. H., Machenhauer, B., Jones, R. G., Schar, C., Ruti, P., Castro, M., Visconti, G., 1997. Validation of present-day regional climate simulations over Europe: LAM simulations with observed boundary conditions. Climate Dynamic, 13, 489–506.
- Christensen, J., Carter, T., Rummukainen, M., Amanatidis, G., 2007. Evaluating the performance and utility of regional climate models: the PRUDENCE project. Climatic Change , 81:1–6
- CIREN-CORFO. 2002. Descripciones de suelos, materiales y suelos.Estudio agroecológico IX Region. Centro de Información de Recursos Naturales (CIREN). Corporación de Fomento de la Producción (CORFO). Santiago, Chile
- Clark, P., Pisias, N., Stocker, T., Weaver, A., 2002. The role of the thermohaline circulation in abrupt climate change. Nature 415: 863-869.
- Clark, S., and J. Lynch, 2009. The opening of Pandora's Box: climate change impacts on soil fertility and crop nutrition in developing countries. Plant Soil, 335 (1-2), 101-115.
- Cock, M. J., Biesmeijer, J. C., Cannon, R. J., Gerard, P. J., Gillespie, D., Jiménez, J. J., Lavelle, P.M., Raina, S. K., 2013. The implications of climate change for positive contributions of invertebrates to world agriculture.
- Cohen S., 1990. Bringing the global warming issue closer to home: The challenge of regional impact studies. Bulletin of the American Meteorology Society, 71:520-526.
- Collins, M., 2005. El Niño-or La Niña-like climate change?. Climate Dynamics,24,1: 89-104.
- Collins, M., 2007. Ensembles and probabilities: a new era in the prediction of climate change. Philosophical Transactions of Royal Society A, 365: 1957-1970.
- Conde, C., F. Estrada, B. Martínez, O. Sánchez and C. Gay, 2011. Regional climate change scenarios for México. Atmósfera 24, 125-140
- Cooley, H. S., Riley, W. J., Torn, M. S., & He, Y. 2005. Impact of agricultural practice on regional climate in a coupled land surface mesoscale model. Journal of Geophysical Research: Atmospheres (1984–2012), 110.D3
- Cusack, D.F., 1983. Introduction: reviving the Green Revolution. D.F. Cusack (Ed.), Agroclimate Information for Development: Reviving the Green Revolution, Westview Press, Boulder, CO, USA, p 12-16.
- Daly C., Neilson R.P., Phillips D.L., 1994. A statistical–topographic model for mapping climatological precipitation over mountainous terrain. Journal of Applied Meteorology 33: 140–158.

- De Witt, A.J.W., Boogaard, H.L., Van Diepen, C.A., 2005. Spatial resolution of precipitation and radiation: The effect on regional crop yield forecasts. Agricultural and Forest Meteorology 135: 156–168.
- Denis, B., Laprise, R., Caya, D., Côte, J., 2006. Downscaling ability of one-way nested regional climate models: the Big-Brother Experiment. Climate Dynamic 18: 627–646.
- Déqué M., Marquet P., Jones R.G., 1998. Simulation of climate change over Europe using a global variable resolution general circulation model. Climate Dynamic 14:173–189.
- Déqué M., R.G. Jones, M. Wild , F. Giorgi, J. H. Christensen, D. C. Hassell, P.L. Vidale, B. Rockel, D. Jacob, E. Kjellström, M. de Castro, F. Kucharski, and B. Van Den Hurí, 2005. Global high resolution versus Limited Area Model climate change projections over Europe: quantifying confidence level from PRUDENCE results. Climate Dynam., 25, 653–670.
- Déqué, M., Piedelievre, J., 1995. High resolution climate simulation over Europe. Climate Dynamic 11:321-339.
- Di Castry, F., and Hayek, E., 1976. Bioclimatología de Chile. Editorial de la Universidad Católica de Chile, Santiago, 163 pp
- Dibike, Y.B., Coulibaly, P., 2006. Temporal neural networks for downscaling climate variability and extremes. Neural Networks 19:135-144.
- Dijkstra, F. A., Blumenthal, D., Morgan, J. A., Pendall, E., Carrillo, Y., Follett, R. F., 2010. Contrasting effects of elevated CO_2 and warming on nitrogen cycling in a semiarid grassland. New Phytologist, 187,2: 426-437.
- Dirección General de Aguas (DGA), 2012. Red hidrometeorológica. Disponible en la www en el sitio http://www.arcgis.com/apps/OnePane/basicviewer/index.html?appid=d508beb3a88f43d28c17a8ec9fac5ef0. It visited at May 5st of 2012.
- Doherty, R., Mearns, L. A. 1999 Comparison of Simulations of Current Climate from Two Coupled Atmosphere-Ocean Global Climate Models Against Observations and Evaluation of their Future Climates Report to the National Institute for Global Environmental Change. [Online] National Center for Atmospheric Research. Available from: http://www.isse.ucar.edu/doherty/index.html.
- Doherty, R., Mearns, L., Raja Reddy, K., Downton, M., Mcdaniel, L., 2003. Spatial scale effects of climate scenarios on simulated cotton production in the Southeastern U.S.A. Climatic Change 60: 99–129.
- Döscher, R., Willen, U., Jones, C., Rutgersson, A., Meier, H.E.M., Hansson, U., Graham, L.P., 2002. The development of the coupled regional ocean-atmosphere model RCAO. Boreal Environmental Research 7:183–192.

- Drake, B., Gonzalez-Meler, M., Long, S., 1997. More efficient plants: a consequence of rising atmospheric CO_2? Annual Review of Plant Physiology 48:609-639.
- Dzotsi, K. A., Jones, J. W., Adiku, S. G. K., Naab, J. B., Singh, U., Porter, C. H., Gijsman, A. J., 2010. Modeling soil and plant phosphorus within DSSAT. Ecological Modelling, 221,23:2839-2849.
- Easterling, D., 1999. Development of regional climate scenarios using a downscaling approach. Climatic Change 41:615-634.
- Easterling, W.E, Chetri, N, Niu, X., 2003. Improving the realism of modeling agronomic adaptation to climate change: simulating technological substitution. Climate Change 60(1–2):149–173
- Esralew R.A., Baker, R.D., 2008. Determination of baseline periods of record for selected streamflow-gaging stations in New Jersey for determining ecologically relevant hydrologic indices (ERHI). U.S. Geological Survey Scientific Investigations Report, 2008-5077.
- Fangmeier, A., De Temmerman, L., Mortensen, L., Kemp, K., Burke, J., Mitchell, R., Van Oijen, M., Weigel, H.J., 1999. Effects on nutrients and on grain quality in spring wheat crops grown under elevated CO_2 concentrations and stress conditions in the European, multiple-site experiment 'space-wheat'. European Journal of Agronomy 10:215-229.
- FAO (Food and Agriculture Organization), 2010. Agricultura climáticamente inteligente, políticas, prácticas y financiación para la seguridad alimentaria, adaptación y mitigación. FAO press, Roma (Italia). 46 p
- FAO (Food and Agriculture Organization), 2013. FAO statistical yearbook 2013. World, food and agriculture. FAO press, Roma (Italia). 307 p
- Fischer, G., Tubiello, N., Van Velthuizen, H. Wiberg, D., 2007. Climate change impacts on irrigation water requirements: effects of mitigation, 1990-2080 Technological Forecasting & Social Change 74:1083-1107.
- Fischer, M., Dewitte, B., Mâtrepierre, L., 2004. A non-linear statistical downscaling model: El Niño/Southern Oscillation impact on precipitation over New Caledonia. Geophysical Research Letters, 31:L16204. 4p.
- Flato, G., Boer, G., Lee, W., McFarlane, N., Ramsden, D., Reader, M., Weaver, A., 2000. The Canadian Centre for Climate Modelling and Analysis global coupled model and its climate. Climate Dynamics 16: 451-467.
- Foody, G. 2008. Refining predictions of climate change impacts on plant species distribution through the use of local statistics. Ecological Informatics 3: 228-236.
- Fowler, H.J., Blenkinsop, S., Tebaldi, C., 2007. Linking climate change modelling to impacts studies: recent advances in downscaling techniques for hydrological modelling. International Journal of Climatology 27 (12), 1547–1578

- Fraisse, C. W., Breuer, N. E., Zierden, D., Bellow, J. G., Paz, J., Cabrera, V. E., Garcia y Garcia , A., Ingram, K.T., Hatch, U., Hoogeboom, G., Jones, J.W, O'Brien, J. J 2006. AgClimate: A climate forecast information system for agricultural risk management in the southeastern USA. Computers and Electronics in Agriculture 53,1: 13-27.
- Fuenzalida, H., Falvey, M., Rojas, M., Aceituno, P., Garreaud, R., 2006. Estudio de la variabilidad climática en Chile para el siglo XXI. Informe para CONAMA. 71 p.
- Fuhrer, J., 2003. Agroecosystem responses to combinations of elevated CO_2, ozone, and global climate change. Agriculture, Ecosystems and Environment 97:1-20.
- Furevik, T., Bentsen, M., Drange, H., Kindem, I.K.T., Kvamstø, N.G., and Sorteberg, A., 2003. Description and Validation of the Bergen Climate Model: ARPEGE coupled with MICOM. Climate Dynamics 21: 27-51.
- Garreaud, R., Aceituno, P. 2001: Interannual Rainfall Variability over the South American Altiplano. Journal of Climate, 14, 2779–2789.
- Garreaud, R., Vuille, M., Climent, A. 2003. The climate of the Altiplano: observed current conditions and mechanisms of past changes. Palaeogeography, Palaeoclimatology, Palaeoecology 194: 5-22
- Garreaud, R., Vuille, M., Compagnucci, R., Marengo, J., 2009. Present-day South American climate. Palaeogeography, Palaeoclimatology, Palaeoecology 281: 180–195
- Gates, W., 1985. The use of general circulation models in the analysis of the ecosystem impact of climate change. Climate Changes 7:267-284.
- Gbetibouo, G. Hassen, R., 2005. Measuring the economic impact of climate change on major South African field crops: a Ricardian approach. Global and Planetary Change 47:143 – 152
- Gillingham, P. K., Palmer S., Huntley B., Kunin W., Chipperfield, J., Thomas, C. 2012. The relative importance of climate and habitat in determining the distributions of species at different spatial scales: a case study with ground beetles in Great Britain. Ecography 35, 9: 831–838
- Giorgi F., Marinucci, M. R.., Bates, G. T., 1993. Development of a second-generation regional climate model (REGcm2). Part I: Boundary-layer and radiative transfer processes. Monthly Weather Review, 121: 2794–2813.
- Giorgi, F., Mearns, L., 1999. Regional climate modelling revisited: an introduction to the special issue. Journal of Geophysical Research. 104(D6):6335–6352.
- Gitay, H., Brown, S., Easterling,W., Jallow, B., 2001. Ecosystems and their goods and services, in McCarthy *et al*. (eds.), Climate Change 2001: Impacts, Adaptation and Vulnerability, Contribution of Working Group II to the Third Assessment Report of the Intergovernmental Panel on Climate Change, Cambridge University Press, Cambridge, pp. 235-342.

- Gordon, C., Cooper, C., Senior, C., Banks, H., Gregory, J. Johns, T., Mitchell, J., Word, R., 2000. The simulation of SST, sea ice extents and ocean heat transports in a version of the Hadley Centre coupled model without Flux adjustments Climate Dynamics 16:147-168.
- Gordon, C.T., Stern, W.F., 1982. A description of the GFDL global spectral model. Monthly Weather Review 110, 625-644.
- Grimm, A. M., Barros, V. R., Doyle, M.E., 2000 Climate variability in southern South America associated with El Niño and La Niña events." Journal of climate 13,1: 35-58.
- Grimm, A., Natori, A., 2006. Impacts of climate change in South America: mean fields and variability, Proceedings of 8 ICSHMO, Foz do Iguaçu, Brazil, April 24-28, 2006, INPE, pp 269-274.
- Groppelli, B., Bocchiola, D., Rosso, R., 2012. Spatial downscaling of precipitation from GCMs for climate change projections using random cascades: A case study in Italy. Water Resources Research 47, 3:
- Grupta, V., Waymire, E. 1993. A statistical analysis of mesoescala rainfall as a random cascade. Journal of Applied Meteorology 32:251-267.
- Guan, H., Love, A., Simmons, C., Makhnin, O., Kayaalp, A. 2010. Factors influencing chloride deposition in a coastal hilly area and application to chloride deposition mapping. Hydrology and Earth System Science, 14, 801–813.
- Guan, H., Wilson, J.L., Makhnin, O., 2005. Geostatistical mapping of mountain precipitation incorporating autosearched effects of terrain and climatic characteristics. Journal of Hydrometeorology 6 (6), 1018–1031.
- Guan, H., Zhang, X., Makhnin, O., Sun, Z. 2013. Mapping meanmonthly temperatures over a coastal hilly area incorporating terrain aspect effects. Journal of Hydrometeorology, 14(1), 233-250.
- Guan., H. Hsu, H., Makhnin, O., Xie, H., Wilson, J., 2009b. Examination of selected atmospheric and orographic effects on monthly precipitation of Taiwan using the ASOADeK model. 29,8: 1171–1181.
- Guan., H. Wilson, J., Xie, H., 2009. A cluster-optimizing regression-based approach for precipitation spatial downscaling in mountainous terrain. Journal of Hydrology 375 578–588Guerra, L. C., *et al*. 2007 Irrigation water use estimates based on crop simulation models and kriging. Agricultural water management 89,3: 199-207.
- Guevara-Díaz, J. 2008. El ABC de los índices usados en la identificación y definición cuantitativa de El Niño - Oscilación del Sur (ENSO). Terra, 24 (35), 85-140.
- Gupta, S., Banerjee, S., Mondal, S. 2009. Phytotoxicity of fluoride in the germination of paddy (Oryza sativa) and its effect on the physiology and biochemistry of germinated seedlings. Fluoride, 42(2), 142.

- Gupta, V.K., Waymire, E.C., 1993. A statistical-analysis of mesoscale rainfall as a random cascade. Journal of Applied Meteorology 32 (2), 251–267.
- Gutiérrez, J., Pond, M., 2006. Modelización Numérica del cambio climático: Bases científicas, incertidumbres y proyecciones para la península ibérica. Revista de Cuaternario y Geomorfología, 20 (3-4):15-28.
- Hansen J, Challinor AJ, Ines A, Wheeler TR, Moron V. 2006. Translating climate forecasts into agricultural terms: advances and challenges. Climate Research: 33:27-41.
- Hansen, J. W., and J. W. Jones. 2000. Scaling-up crop models for climate variability applications." Agricultural Systems 65,1: 43-72.
- Hansen, J.W. Indeje, M., 2004. Linking dynamic seasonal climate forecasts with crop simulation for maize yield prediction in semi-arid Kenya. Agricultural and Forest Meteorology 125:143–157.
- Hanssen-Bauer, I., Achberger, C., Benestad1, R. E. Chen, D., Førland, E. J., 2005. Statistical downscaling of climate scenarios over Scandinavia. Climate Research 29: 255–268.
- Harding, D., Dean B. Gesch, Claudia C. Carabajal, Scott B. Luthcke, 1999. Application Of The Shuttle Laser Altimeter In An Accuracy Assessment Of Gtopo30, A Global 1-Kilometer Digital Elevation Model. International Archives of Photogrammetry and Remote Sensing32 ((Part 3W14)):81–85.
- Hawkins, E., Sutton, R., 2012. The potential to narrow uncertainty in projections of regional precipitation change. Climate Dynamic, 37:407–418
- Held, I., Soden, B., 2000. Water Vapor Feedback and Global Warming. Annual Review of Energy and the Environmental 25:441-75.
- Hengl, T., 2007. A Practical Guide to Geostatistical Mapping of Environmental Variables. European Community Publication Office, Italy. 165 p
- Hessami, M., Gachon, P., Ouarda, T., St-Hilaire A., 2008. Automated regression-based statistical downscaling tool. Environmental Modelling & Software 23 (6):813-834.
- Hewitson, B., Crane, R., 1996. Climate downscaling: Techniques and application, Climate Research 7: 85-95.
- Hijmans R J, Cameron SE, Parra JL, Jones PG, Jarvis A (2005). Very high resolution interpolated climate surfaces for global land areas. International Journal of Climatology 25: 1965-1978.
- Houghton, J., Meira, L., David, F., Griggs, J., Maskell, K., 1997. Introducción a los modelos climáticos simples utilizados en el Segundo Informe de Evaluación del IPCC. IPCC, 60 p.
- Hu, Q., Weiss, A., Feng, S., Baenziger, P., 2005. Earlier winter wheat heading dates and warmer spring in the U.S. Great Plains. Agricultural and Forest Meteorology 135:284-290.

- Hudson, Gordon, and Hans Wackernagel. 1994. Mapping temperature using kriging with external drift: theory and an example from Scotland. International journal of Climatology 14,1: 77-91.
- Huffman, G., Adler, R., Arkin, P., Chang, A., Ferraro, R., Gruber, A., Janowiak, J., McNab, A., Rudolf, B., Schneider, U., 1997. The Global Precipitation Climatology Project (GPCP) Combined Precipitation Dataset. Bulletin of the American Meteorological Society 78, 1,5:20
- Huntingford, C., Lambert, F., Gash, J., Taylor, C., Challinor, A., 2005. Aspects of climate change prediction relevant to crop productivity. Philosophal Transaction of the Royal Society B, 360, 1999–2009
- Huth R., Kyselý J., Dubrovský M., 2001. Time structure of observed, GCM-simulated, downscaled, and stochastically generated daily temperature series. Journal of Climate, 14, 4047-4061.
- Iizumi, T., Semenov, M., Nishimori, M., Ishigooka, Y., Kuwagata., Y., (2012) ELPIS-JP: a dataset of local-scale daily climate change scenarios for Japan. Philosophy Transaction of Royal Society. A, 370, 1121–1139
- INE (Instituto Nacional de Estadísticas), 2010. InformeEconómico Regional. [Online] Available from: http://www.ine.cl/canales/chile_estadistico/territorio/iner/iner.php.
- Ines, A., Hansen, J., 2006. Bias correction of daily GCM rainfall for crop simulation studies. Agricultural and Forest Meteorology 138: 44-53.
- IPCC (Intergovernmental Panel on Climate Change), 2007. Climate Change 2007: The Physical Science Basis. Contribution of Working Group I to the Fourth Assessment Report of the Intergovernmental Panel on Climate Change. In: Solomon, S., Qin, D., Manning, M., Chen, Z., Marquis, M., Averyt, K.B., Tignor, M., Miller, H.L., (Eds.), Cambridge University Press, Cambridge, United Kingdom and New York, NY, USA, 996 p.
- IPCC (Intergovernmental Panel on Climate Change),Working Goup I, 2001. Climate Change 2001: The scientific basis. Contribution of Working Group I to the Third Assessment Report of the IPCC., Cambridge University Press, Cambridge, UK. 944 pIsaaks, E., Srivastava, E.M. 1989. An introduction to applied geostatistics. U.S.A., Oxford University Press. 592 pp
- Jacob, D., Podzun, R., 1997. Sensitivity Studies with the Regional Climate Model REMO. Meteorology and Atmospheric Physic 63: 119-129.
- Jara, V., Meza, F. J., Zaviezo, T., Chorbadjian, R. 2013. Climate change impacts on invasive potential of pink hibiscus mealybug, Maconellicoccus hirsutus (Green), in Chile. Climatic Change, 117,1-2, 305-317.
- Johns, T., Durman, C., Banks, H., Roberts, M., McLaren, A., Ridley, J., Senior, C., Williams, K., Jones, A., Rickard, G., Cusack, S., Ingram, W., Crucifix, M., Sexton, D., Joshi, M., Dong, B., Spencer, H., Hill, R., Gregory, J., Keen, A., Pardaens, A., Lowe, J., Bodas-Salcedo, A., Stark, S., Searl, Y., 2006. The new Hadley Centre

climate model HadGEM1: Evaluation of coupled simulations. Journal of Climate, 19: 1327-1353.

- Jones, R.G., Noguer M, Hassell D, Hudson D, Wilson S, Jenkins G, Mitchell J. 2004. Generating High Resolution Climate Change Scenarios using PRECIS, report, Met Office Hadley Centre: Exeter, UK.Kiladis, G., Van Loon, H., 1988. The Southern Oscillation. VII - Meteorological anomalies over the Indian and Pacific sectors associated with the extremes of the Oscillation. Monthly Weather Review. Vol. 116, pp. 120-136
- Jones, G. V. 2006. Climate change and wine: Observations, impacts and future implications. Wine Industry J. 21(4): 21-25.
- Jones, G. V., and R. E. Davis. 2000. Climate influences on grapevine phenology, grape composition, and wine production and quality for Bordeaux, France. Am. J.Enology Vitic. 51: 249-261.
- Jones, G. V., M. A. White, O. R. Cooper, and K. H. Storchmann. 2005. Climate change and global wine quality. Climatic Change 73: 319-343.
- Jones, J., Hoogenboom, G., Porter, C., Boote, K., Batchelor, W., Hunt, L, Wilkens, J., Singh, U, Gijsman, A., Ritchie, J., 2003. The DSSAT cropping system model. European Journal of Agronomy 18:235_/265
- Jones, P., Thornton, P., 2003. The potential impacts of climate change on maize production in Africa and Latin America in 2055. Global Environmental Change 13:51-59.
- Juang H.M.H., Hong, S.Y., Kanamitsu, M., 1997: The NCEP regional spectral model: An update. Bulletin of the American Meteorological Society 78, 2125-2143.
- Juang H.M.H., Kanamitsu, M., 1994. The NMC nested regional spectral model. Monthly Weather Review 122, 3-26.
- Kalnay, E., Kanamitsu, M., Kistler, R., Collins, W., Deaven, D., Gandin, L., Iredell, M., Saha, S., White, G. , Woollen, J., Zhu, Y., Leetmaa, A., Reynolds, R., Chelliah, M., Ebisuzaki, W., Higgins, W., Janowiak, J., Mo, K.C., Ropelewski, C., Wang, J., R. Jenne, Joseph, D., 1996. The NCEP/NCAR 40-Year Reanalysis Project. Bulletin of the American Meteorological Society 77: 437–471.
- Karmalkar. A.V., S M. A. Taylor, J. Campbell T. Stephenson, M. New, A. Centella, A. Benzanilla And J. Charlery, 2013. A review of observed and projected changes in climate for the islands in the Caribbean. Atmósfera 26(2), 283-309
- Kim, J., Chang, J., Baken, N., Wilks, D., Gates, W., 1984. The statistical problems of climate inversion: determination of the relationship between local and large-scale climate. Monthly Weather Review 112:2069-2077.
- Kleijnen, J. 1995. Theory and Methodology Verification and validation of simulation models. Eur. J. Oper. Res., 82, 145-162.
- Koe, L., Arellano, A., McGregor, J., 2003. Application of DARLAM to Regional Haze Modeling. Pure and applied Geophysics. 160:189-204.

- Kowalczyk, E., Garratt, J., Krummel, P., 1994. Implementation of a soil-canopy scheme into the CSIRO AOGCM - regional aspects of the model response. CSIRO Atmospheric Research Technical Paper # 32. 59 p.
- Krüger, L, R. da Rocha, M. Reboita, and T. Ambrizzi, 2012. RegCM3 nested in HadAM3 scenarios A2 and B2: projected changes in extratropicalcyclogenesis, temperature and precipitation over the South Atlantic Ocean. Climatic Change, 113:599–621.
- Lamb, P., 1987. On the development of regional climatic scenarios for policy oriented climatic impact assessment. Bulletin of the American Meteorological Society 84:89-95.
- Langensiepen M., Hanus H., Schoop P., Gräsle W. 2008. Validating CERES-Wheat under North-German environmental conditions Agricultural Systems 97:34–47
- Lawlor, D., Michel, R.,1991. The effects of increasing CO_2 on crop photosynthesis and productivity: A review of field studies. Plant, Cells and Environment 14:807-818.
- Lee, J., De Gryze, S., Six, J., Effect of climate change on field crop production in California's Central Valley. Climatic Change 109, Suppl 1:S335–S353
- Legutke, S., Voss, R., 1999. The Hamburg Atmosphere-Ocean Coupled Circulation Model ECHO-G. Technical report, No. 18, German Climate Computer Centre (DKRZ), Hamburg, 62 p.
- Lenderink, G., Van den Hurk, B.J.J.M., Van Meijgaard, E., Van Ulden, A.P., Cuijpers, H., 2003. Simulation of present-day climate in RACMO2: first results and model developments. Technical Report TR-252, Royal Netherlands Meteorological Institute, De Bilt. 24 p.
- Linderson, M.L., Achberger, C., Chen, D., 2004. Statistical downscaling and scenario construction of precipitation in Scania, southern Sweden. Nord Hydrol 35:261–278.
- Liu, B., Henderson, M., Xu, M., 2008. Spatiotemporal change in China's frost days and frost-free season, 1955–2000, Journal of Geophysical Research 113:D12104.
- Lobell, D. 2013. Errors in climate datasets and their effects on statistical crop models. Agricultural and Forest Meteorology. 170:58-66
- Lobell, D. B., Cahill, K. N., Field, C. B., 2007. Historical effects of temperature and precipitation on California crop yields. Climatic Change, 81,2: 187-203.
- Lobell, D., Burke, M., 2008. Why are agricultural impacts of climate change so uncertain? The importance of temperature relative to precipitation. Environmental Research Letters. 034007: 1-8.
- Lobell, D., Field, C., 2007. Global scale climate–crop yield relationships and the impacts of recent warming. Environmental Research Letters 2. 014002: 1-7.

- Lobell, D., Field, C., 2008. Estimation of the carbon dioxide (CO_2) fertilization effect using growth rate anomalies of CO_2 and crop yields since 1961. Global Change Biology 14:39-45.
- Long, S., Ainsworth E., Leakey A., Nosberger J., Ort, D., 2006. Food for thought: lower-than-expected crop yield stimulation with rising CO_2 concentrations. Science 312: 1918–1921.
- Lorenz, D. H., K. W. Eichhorn, H. Blei-Holder, R. Klose, U. Meier, and E. Weber. 1994. Phänologische Entwicklungsstadien der Weinrebe (Vitis vinifera L. ssp. vinifera). Vitic. Enol. Sci. 49: 66-70.
- Lorenz, E.N. 1956. Empirical Orthogonal Functions and Statistical Weather Prediction. Sci. rep. 1. Department of Meteorology, MIT, USA.
- Luebke B. H., 2008. A geographical interpretation of "El Vergel," a fundo of the central valley of Chile. Scottish Geographical Magazine. 52, 6: 361-375
- Lüthi D., Cress, A., Davis, H. C., Frei, C., Shär, C., 1996. Interannual variability and regional climate simulations. Theoretical and Apply Climatology 53: 185-209.
- Mackay, N.G., Chandler, R.E., Onof, C., Wheater, H.S., 2001. Disaggregation of spatial rainfall fields for hydrological modelling. Hydrology and Earth System Sciences 5 (2), 165–173
- Mantua, N. J., Hare, S. R. 2002. The Pacific decadal oscillation. Journal of Oceanography, 58(1), 35-44.
- Marengo, J., Ambrizzi, T., 2006. Use of regional climate models in impacts assessments and adaptations studies from continental to regional and local scales. Proceedings of 8 ICSHMO, Foz do Iguaçu, Brazil, April 24-28, 2006, INPE, p. 291-296.
- Marquis, M., K. B. Averyt, M. Tignor, H. L. Miller (eds). Cambridge University Press, Cambridge, United Kingdom and New York, NY, USA. 996 p.
- Matus, F., Amigo, X., Kristiansen. S.M. 2006. Aluminium stabilization controls organic carbon levels in Chilean volcanic soils. Geoderma, 132: 58–18
- Mearns, L.O., 2001. Issues in the Impacts of Climate Variability and Change on Agriculture. Climatic Change 60: 1–6.
- Mearns, L.O., Carbone, G., Doherty, R.M., Tsvetsinskaya, E., Mccarl, B.A., Adams, R.M., Mcdaniel, L., 2003.The Uncertainty due to Spatial Scale of Climate Scenarios in Integrated Assessments: An Example from U.S. Agricultura. Integrated Assessment 4, 4: 225–235.
- Mearns, L.O., Rosenzweig, C., Golberg, R., 1996. The effect of changes in daily and interannual climatic variability on CERES-Wheat: A sensitivity study. Climate Change 32:257-292.
- Mechoso, C., Arakahua, A., 2003. General Circulation Models. In Holton, J., Curry, J., Pyle, J.(Ed). Encyclopedia of Atmospheric Science, Elsevier, U.K. pp 861-869.

- Meza F., Silva, D., 2009. Dynamic adaptation of maize and wheat production to climate change. Climatic Change 94:143-156.
- Meza, F., Silva, D., Vigil., H., 2008. Climate change impacts on irrigated maize in Mediterranean climates: Evaluation of double cropping as an emerging adaptation Agricultural Systems, 98: 21-30.
- Michelsen, J., 1987. Cross validation in statistical climate forecast models. Bolletin of American Meteorogical Society 26: 1586-1600
- Mielke Jr., P., Berry., K., Landsea, C., Gray., W. 1996., Artificial Skill and Validation in Meteorological Forecasting. Weather and Forecasting. 11: 153-159
- Mirás-Avalos, J., R. Mestas-Valero, P. Sande-Fouz, and A. Paz-González, 2009 Consistencyanalysis of pluviometricinformation in Galicia (NW Spain). Atmos. Res., 94, 629–640.
- Misra, V., Dirmeyer, P., Kirtman, B. 2003. Dynamic Downscaling of Seasonal Simulations over South America. Jurnal of Climate 16:103-117
- Mitchell, P. 1997. Misuse of regression of empirical validation of models. Agr. Syst, 54 (3), 313-326.
- Mitchell, Timothy D., and Philip D. Jones. 2005. An improved method of constructing a database of monthly climate observations and associated high?resolution grids. International Journal of Climatology 25,6: 693-712.
- Montecinos, A., Aceituno, 2003. P. Seasonality of the ENSO-Related Rainfall Variability in Central Chile and Associated Circulation Anomalies. Journal of Climate 16:281-296
- Morgan, J., LeCain, D., Pendall, E., Blumenthal, D., Kimball, B., Carrillo, Y., Williams, D., Jana Heisler-White, J., F., West, M., 2011. C4 grasses prosper as carbon dioxide eliminates desiccation in warmed semi-arid grassland, Nature 476:202-205
- Morse, A., 2007. Climate change impact in the European ENSEMBLES Project. Geophysical Research Abstracts, Vol. 9:11523.
- Murugan , M., Krishnappa Shetty, K., Ravi, R., Anandhi, A., Rajkumar, A., 2012. Climate change and crop yields in the Indian Cardamom Hills, 1978–2007 CE. Climatic Change 110:737–753
- Nanzyo, M., Shoji, S., Dahlgren, R.A., 1993. Physical characteristics of volcanic ash soils. In: S Shoji; M Nanzyo & RA Dahlgren (eds.), Volcanic ash soils. Genesis, properties and utilization. Developments in Soil Science. Elsevier, Amsterdam, pp. 189-207.
- Nemani, R. R., M. A. White, D. R. Cayan, G. V. Jones, S.W. Running, J. C. Coughlan, and D. L. Peterson., 2001. Asymmetric warming over coastal California and its impact on the premium wine industry. Climatic Research 19: 24– 25.

- New, Mark, Mike Hulme, and Phil Jones. Representing twentieth-century space-time climate variability. 1999. Part I: Development of a 1961-90 meanmonthly terrestrial climatology." Journal of Climate 12.3: 829-856.
- Newman, M., Compo, G.P., Alexander, M., 2003. ENSO-forced variability of the Pacific Decadal Oscillation. Journal of Climate 16,23: 3853-3857.
- Olesen, J. E., Carter, T. R., Díaz-Ambrona, C. H., Fronzek, S., Heidmann, T., Hickler, T., Holt, T., Minguez, M. I., Morales, P., Palutikof, J. P., Quemada, M., Ruiz-Ramos, M., Rubæk, G. H., Sau, F., Smith, B., Sykes, M. T., 2007. Uncertainties in projected impacts of climate change on European agriculture and terrestrial ecosystems based on scenarios from regional climate models. Climate Change 81:123-143.
- Olesen, J., Bindi, M., 2002. Consequences of climate change for European agricultural productivity, land use and policy. European Journal of Agronomy 16:239-262.
- Olesen, J., Bøcher, E., Jensen, T. 2000. Comparison of scale of climate and soil data for aggregating simulated yield of winter wheat in Denmark. Agriculture, Ecosystems and Environment 82.1:213-228.
- Onogi, K., Tsutsui, J., Koide, H., Sakamoto, M., Kobayashi, S., Hatsushika, H., Matsumoto, T., Yamazaki, N., Kamahori, H., Takahashi, K., Kadokura, S., Wada, K., Kato, K., Oyama, R., Ose, t., Mannoji, N., Taira, R., 2007: "The JRA-25 Reanalysis". Journal of the Meteorological Society of Japan 85: 369-432.
- Orrego, R., Abarca del Río, R, Ávila, A., Morales, L., 2013. Validation and correction of dynamically-downscaled projections of XXIst century rainfall scenarios for the Araucanía Region, Chile. Sumitted to Atmósfera.
- Orrego, R., Huan, G., Abarca, R., Ávila, A. 2012. High resolution rainfall climate change projection based on Topographical Based Downscaling Model. A high resolution projection. Draf for paper
- Orrego, R., Avila, A., Meza, F., Matus, F. 2014. Using a crop simulation model to select the optimal climate grid cell resolution: A study case in Araucanía Region.Journal of Soil Science and Plant Nutrition, 14,2:407-420
- Ortega-Farías, S., P. Lozano, Y. Moreno, y L. León. 2002. Desarrollo de modelos predictivos de fenología y evolución de madurez en vid para vino cv. Cabernet Sauvignon y Chardonnay. Agric. Téc. 62 (1): 27-37.
- Osterkamp T., Burn, C., 2003. Permafrost. In Holton, J., Curry, J., Pyle, J.(Ed) Encyclopedia of Atmospheric Science, Elsevier, U.K. pp 1717-1729.
- Paaijmans, K., Thomas, M., 2011. The influence of mosquito resting behaviour and associated microclimate for malaria risk. Malaria Journal 2011, 10:183
- Pabico, J.P.., G. Hoogenboom, R.W. McClendon. 1999. Determination of variety coefficients of crop models using a genetic algorithm: a conceptual framework. T. ASAE, 42:223–232

- Palosuo, T., Kersebaum, K. C., Angulo, C., Hlavinka, P., Moriondo, M., Olesen, J. E., Patilf, R., Rugetg, F., Rumbaurc, C., Takáč, J., Trnkad, M., Bindii, M., Çaldağj, B., Ewertc, F., Ferrisee, R., Mirschelb, W., Şaylanj, L., Šiškak, B., Röttera, R., Rötter, R., 2011. Simulation of winter wheat yield and its variability in different climates of Europe: a comparison of eight crop growth models. European Journal of Agronomy, 35,3:103-114.
- Parry, M., Rosenzweig, C., Iglesias, A., Livermore, M., Fischer, G., 2004. Effects of climate change on global food production under SRES emissions and socio-economic scenarios. Global Environmental Change 14:53-67.
- Parry, M., Rosenzweig, C., Livermore, M., 2005. Climate change, global food supply and risk of hunger. Philosophical Transactions of Royal Society 360: 2125-2138.
- Paruelo, J., Salas, O., 1993. Effect of global change on maize production in the Argentinean Pampas. Climate Research: 3:161-167.
- Patz, J., Campbell-Lendrum, D., Holloway, T., Foley, J., 2005. Impact of regional climate change on human health. Nature, Vol 438,17:310-317.
- Peña, O. y H. Romero. 1977. Sistemas en Climatología (Aplicación a una clasificación genética de los climas chilenos). Notas Geográficas (Valparaíso) 8: 7-15.
- Peñuelas, J., and I. Filella. 2001. Responses to a warming world. Science 294: 793-794.
- Pereira de Lucena, A., Szklo, A., Schaeffer, R., Marques Dutra, R. 2010. The vulnerability of wind power to climate change in Brazil. Renewable Energy 35:904–912
- Petrie, P. Sadras, V., 2008. Advancement of grapevine maturity in Australia between 1993 and 2006: putative causes, magnitude of trends and viticultural consequences. Australian Journal of Grape and Wine Research 14:33-45.
- Piechota, T. C., Chiew, F. H., Dracup, J. A., McMahon, T. A. 2001. Development of exceedance probability streamflow forecast. Journal of Hydrologic Engineering, 6(1), 20-28.
- Pielke, R., Coauthors, A. S., 1992. A comprehensive meteorological modelling system-RAMS. Meteorology and Atmospheric Physic 49: 69-91.
- Porter, J., Semenov, M., 2005. Crop responses to climatic variation. Philosophical Transactions of Royal Society 360: 2021-2035.
- Prior, S., Torbert, H., Runion, G., Mullins, G., Rogers, H., Mauney, J., 1998. Effects of carbon dioxide enrichment on cotton nutrient dynamics. Journal of Plant Nutrition 21:1407-1426.
- Priya, S., Shibasaki, R., 2001. National spatial crop yield simulation using GIS-based crop production model. Ecological Modelling 135:113-129.

- Prudhome, C., Reynard, N., Croks, S., 2002. Downscaling of global climate models for flood frequency analysis: Where are now? Hydrological Processes 16:1137-1150.
- Prudhomme, C., Jakob, D., Svensson, C., 2003. Uncertainty and climate change impact on the flood regime of small UK catchments. Journal of Hydrology 277 : 1–23
- Purves, R. S., Hulton, N. R. J., 2000. A climatic-scale precipitation model compared with the UKCIP baseline climate.International Journal of Climatology, 20(14), 1809-1821.
- Qian, B., Corte-Real, J., Xu, H., 2002. Multisite stochastic weather models for impact studies. Int. Journal of Climatology. 22: 1377–1397.
- Racsko, P., Szeidl, L, Semenov, M., 1991. A serial approach to local stochastic weather models. Ecological Modelling 57: 27-41.
- Radu, R., Déqué, M., Somot, S., 2008. Spectral nudging in a spectral regional climate model. Tellus , 60A, 898–910.
- Räisänen, J ., U. Hansson, A. Ullerstig, R. Döcher, L.P. Graham, C. Jones, H.E.M. Meier, P Samuelsson, and U. Willén, 2004. European climate in the late twenty-first century: regional simulations with two driving global models and two forcing scenarios. Climate Dynam. 22: 13–31.
- Räisänen, J., 2007. How reliable are climate models? Tellus 59A: 2–29.
- Reyes-Fox, M., Stelzer,H., Trlica, M., McMaster, G., Andales, A., LeGrain, D., Morgan, J., 2014. Elevated CO2 furter lengthens growing season under warming conditions. Nature
- Richardson, C.W., 1981. Stochastic simulation of daily precipitation, temperature, and solar radiation. Water Resources Research 17: 182-90.
- Rodell, M., Houser, P., Jambor, U., Gottschalck, J., Mitchell, K., Meng, C.J., Arsenault, K., Cosgrove, B., Radakovich, J., Bosilovich, M., Entin, J., Walker, J., Lohmann, D., Toll, D., 2004. The global land data assimilation system. Bulletin of the American Meteorological Society 85(3): 381-394.
- Roeckner, E., Bäuml, G., Bonaventura, L., Brokopf, R., Esch, M., Giorgetta, M., Hagemann, S., Kirchner, I., Kornblueh, L., Manzini, E., Rhodin, A., Schlese, U., Schulzweida, U., Tompkins, A., 2003. The atmospheric general circulation model ECHAM5. Part I: Model description. Max Planck Institute for Meteorology Report 349, 127 p.
- Rosenlof, K. H., Terray, L., Deser, C., Clement, A., Goosse, H., Davis, S., 2013. Changes in Variability Associated with Climate Change. In Climate Science for Serving Society (pp. 249-271). Springer Netherlands.
- Rosenzweig, C., Parry, M., 1994. Potential impacts of climate change on world food supply. Nature 367:133-138.

- Rosenzweig, C., Tubiello, F., Goldberg, R., Mills, E., Bloomfield, J., 2002. Increased crop damage in the US from excess precipitation under climate change. Global Environmental Change 12: 197–202.
- Rouanet, J. 1983. Clasificación agroclimática IX Region. Macroárea I. Investigación y Progreso Agropecuario. INIA Carillanca 2(4): 25-28.
- Rouanet, J. L., 1994. Eficiencia fisiológica de uso de nitrógeno por cultivos anuales en futura agricultura sustentable. Agricultura Técnica. 54, 169-179.
- Rounsevell, M. D. A., Reay, D. S., 2009. Land use and climate change in the UK. Land use policy 26: S160-S169.
- Rummukainen M, Bergstrom S, Persson G, Rodhem J, Tjernstrom M., 2004. The Swedish regional climate modelling programme, SWECLIM: A review. Ambio. 33: 176–182.
- Rummukainen, M. 1997. Methods for statistical downscaling of GCM simulation. SWECLIM report. Norrköping: Rossby Centre, SMHI
- Rupa Kumar, K., Sahai, A., Krhishna Kumar, S., Patwardhan, S., Mishra, P., Revadekar, J., Kamala, K., Pant, G. 2006. High-resolution climate change scenarios for India for the 21st century. Current Science, 90, 3:334-345
- Rupp, D., Licznar, P., Adamowski, W., Lésniewski, M. 2012. Multiplicative cascade models for fine spatial downscaling of rainfall: parameterization with rain gauge data. Hydrology and Earth System Science, 16, 671–684
- Russo, J., Zack. J., 1997. Downscaling AOGCM Output with a Mesoscale Model. Journal of Environmental Management. 49:19–29.
- Rutllant, J. Aspectos de la circulación atmosférica de gran escala asociada al ciclo ENOS 1997-1999 y sus consecuencias en el régimen de precipitación en Chile central. In: El Niño-La Niña 1997-2000. Sus Efectos en Chile (S. Avaria, J. Carrasco, J. Rutllant, E. Yáñez eds.). Valparaíso, Chile, CONA. pp. 61-76, 2004.
- Rutllant, J., Fuenzalida, H., Aceituno, P., 2003. Climate dynamics along the arid northern coast of Chile: the 1997–1998 Dinámica del Clima de la Region de Antofagasta (DICLIMA) experiment. Journal of Geophysical Research 108 (D17), 4538.
- Saavedra, N., Müller, E.P., Foppiano, A.J., 2002. Monthly mean rainfall frecuency model for the central chilean coast:Some climatic inferences. International Journal of Climatology19:1495-1509.
- Sah, R.K. 1987. Tropical economies and weather information. J.S. Fein, P.L. Stephens (Eds.), Monsoons, John Wiley & Sons, New York, pp. 105–119
- Salathe, E. 2005, Downscaling simulations of future global climate with application to hydrologic modelling. Int. J. Climatol. 25: 419-436.
- Salinger, M.J. 1987. Impact of climatic warming on the New Zealand growing sea A Mathematical Approach to Plant and Crop Physiology. Clarendon Press, Oxford, USA. 350 p.

- Sayar, R., Khemira, H., Kameli, A., Mosbahi, M., 2008. Physiological tests as predictive appreciation for drought tolerance in durum wheat (Triticum durum Desf.). Agronomy research 6,1: 79-90.
- Schmidhuber, J., Tubiello, F. 2007. Global food security under climate change. PNAS 104, 50:19703-19708
- Schoof, J., 2012. Scale Issues in the Development of Future Precipitation Scenarios. Journal of Contemporary Water Research & Education,147,1 8-16
- Searcy J.K., and Hardison, C.H. 1960. Double mass curves. US Geological Survey, Water-Supply Paper 1541-B.
- Semenov, M., 2007. Development of high-resolution UKCIP02-based climate change scenarios in the UK. Agricultural and Forest Meteorology 144:127-138.
- Semenov, M., Barrow, E., 1997. Use of a stochastic weather generator in the development of climate change scenarios. Climatic Change 35: 397-414.
- Semenov, M., Donatelli, M., Stratonovitch, P., Chatzidaki, E., Baruth, B., 2010. ELPIS: a dataset of local-scale daily climate scenarios for Europe. Climate Research 44: 3–15
- Semenov, M., Porter, J., 1995. Climatic variability and the modelling of crop yields. Agricultural and Forest Meteorology 73: 265-83.
- Seo, S., Mendelsohn, R. 2008. A Ricardian Analysis of the Impact of Climate Change on South American Farms. Chilean Journal of Agricultural Research 68(1):69-79.
- Seth, A., Rojas, M. 2003. Simulation and Sensitivity in a Nested Modeling System for South America. Part I: Reanalyses Boundary Forcing. Journal of Climate 16,15, 2437-2453
- Skamarock, W. C., Klemp, J. B., Dudhia, J., Gill, D. O., Barker, D. M., Wang, W., Powers, J. G., 2005. A description of the Advanced Research WRF Version 2. NCAR Tech. Note, NCAR/TN-468+STR, 88 p.
- Slingo, J., Challinor, A., Hoskins, B., Wheeler., T., 2005. Introduction: food crops in a changing climate. Philosophal Transaction of the Royal Society B.360, 1983–1989.
- Smit, L., 2003. Predictibilidad and Kaos. In Holton, J., Curry, J., Pyle, J.(Ed) Encyclopedia of Atmospheric Science, Elsevier, U.K. pp 1777-1785.
- Sokal, R. R., Rohlf, F. J. 1995. The principles and practice of statistics in biological research. New York.: Edition 3.
- Solman, S., Nuñez, M., 1999. Local estimates of global climate change: a statistical downscaling approach. International Journal of Climatology 19: 835-861.
- Soussana, J.F., Graux, A.I., Tubiello, F.N., 2010. Improving the use of modelling for projections of climate change impacts on crops and pastures. Journal of Expimental Botanic 61:2217–2228.

- Souvignet, M., Gaese, H., Ribbe, L., Kretschmer, N., Oyarzún, R., 2010. Statistical downscaling of precipitation and temperature in north- central Chile: an assessment of possible climate change impacts in an arid Andean watershed.Hydrological Sciences Journal–Journal des Sciences Hydrologiques, 55,1: 41-57.
- Sparks, T., Croxton, P., Collinson, N. Taylor, P., 2005. Examples of phenological change, past and present, in UK farming. Annals of Applied Biology 146: 531-537.
- SRES (Special Report on Emissions Scenarios) 1997. Nakicenovic, Nebojsa and Swart, Rob (eds.), Cambridge University Press, Cambridge, United Kingdom, 612 p, 2000.
- Steduto, P., Hsiao, T. C., Raes, D., Fereres, E., 2009. AquaCrop—The FAO crop model to simulate yield response to water: I. Concepts and underlying principles. Agronomy Journal, 101(3), 426-437.
- Steppeler, J., Doms, G., Schättler, U., Bitzer, H.W., Gassmann, A., Damrath, U., Gregoric G., 2003. Meso-gamma scale forecasts using the nonhydrostatic model L.M. Meteorology and Atmospheric Physic 82:75–96.
- Stocker T. *et al*., 2010. IPCC Expert meeteng on assessing and Combining Multi Model Climate Projections. Meeteng report.Colorado, USA.
- Survey Laboratory Staff, 1996. Soil survey laboratory methods manual. Soil Survey Investigations Report, vol. 42. USDA SCS, Washington DC, USA
- Sutherst, R., Constable, F., Finlay, K., Harrington, R., Luck, J., Zalucki, M., 2011. Adapting to crop pest and pathogen risks under a changing climate. Wiley Interdisciplinary Reviews: Climate Change 2, 2: 220–237
- Tadross, M., Jack, C., Hewitson, B. 2005. On RCM-based projections of change in southern African summer climate. Geophysical Research Letters, 32: L23713, 4 pp
- Tan, G. y Shibasaki, R., 2003. Global estimation of crop productivity and the impacts of global warming by GIS and EPIC integration. Ecological Modelling 168:357-370.
- Taylor, K., 2001. Summarizing multiple aspects of model performance in a single diagram. Journal of Geophysical Research, 106,7:7183-7192
- Temebl, M., 2005. Downscaling of Temperature and Precipitation in the Alpine Region Hohe Tauern. Scientifc Report No. 5-2005. Wegener Center for Climate and Global Change-University of Graz, Austia 104 p.
- Thimgen M., Rivington, M., Azam-Al, S., Colls, J., 2007 Assessment of the ClimGen stochastic weather generator at Cameroon sites. African Journal of Environmental Science and Technology 1,4:086-092.
- Thomson, A., Brown, R., Rosenber, N., Izaurralde, R. Benson, V., 2005. Climate Change Impacts For The Conterminous USA: An Integrated Assessment Part 3. Dryland Production Of Grain And Forage Crop. Climatic Change 69: 43-65.
- Timbal B., McAvaney, B. J., 2001. An analogue-based method to downscale surface air temperature: application for Australia. Climate Dynamic 17 (12): 947-963.

- Tingem M., Rivington, M., Azam-Al, S., Colls, J. Assessment of the ClimGen stochastic weather generator at Cameroon sites. African Journal of Environmental Science and Technology.1,4:086-092
- Toggweiler, J., Key, R., 2003. Thermohaline Circulation. En Holton, J., Curry, J., Pyle, J.(Ed) Encyclopedia of Atmospheric Science, Elsevier, U.K. 1549-1555.
- Tognetti, R., Sebastiani, L., Vitagliano, C., Raschi, A., Minnocci, A., 2001. Responses of two olive tree (Olea europaea L.) cultivars to elevated CO_2 concentration in the field. Photosynthetica 39:403-410.
- Tonietto, J., Carbonneau, A, 2002. A multicriteria climatic classification system for grape-growing regions worldwide. Agricultural and Forest Meteorology. 124: 81-97.
- Tsvetsinskaya, E. A., Mearns, L. O., Mavromatis, T., Gao, W., Mcdaniel, L., Downton, M. W., 2003. The effect of spatial scale of climatic change scenarios on simulated Maize, Winter Wheat, and Rice production in the Southeastern United Status. Climatic Change 60:37–71.
- Uppala, S.M., Kållberg, P.W., Simmons, A.J., Andrae, U. da Costa Bechtold, V., Fiorino, M., Gibson, J.K., Haseler, J., Hernandez, A., Kelly, G.A., Li, X., Onogi, K., Saarinen, S., Sokka, N., Allan, R.P., Andersson, E., Arpe, K., Balmaseda, M.A., Beljaars, A.C.M., van de Berg, L., Bidlot, J., Bormann, N., Caires, S., Chevallier, F., Dethof, A., Dragosavac, M., Fisher, M., Fuentes, M., Hagemann, S., Hó1m, E., Hoskins, B.J., Isaksen, L., Janssen, P.A.E.M., Jenne, R., McNally, A.P., Mahfouf, J.-F., Morcrette, J.-J., Rayner, N.A., Saunders, R.W., Simon, P., Sterl, A., Trenberth, K.E., Untch, A., Vasiljevic, D., Viterbo, P., Woollen, J., 2005. The ERA-40 re-analysis. Quarterly Journal of the Royal Meteorological Society. 131: 2961-3012.
- Valcke, S., Caubel, A., Vogelsang, R., Declat, D. 2004. OASIS3 Ocean Atmosphere Sea Ice Soil User's Guide Technical Report TR/CMGC/04/68, CERFACS, Toulouse, France. 70 p.
- Van Ittersum, M.K., Leffelaar, P.A., Van Keulen, H., Kropff, M.J., Bastiaans, L. , Goudriaan, J. 2003. On approaches and applications of the Wageningen crop models. European Journal of Agronomi:18 201–234
- Van Vuuren, D.P., Edmonds, J., Thomson, A., Riahi, K., Kainuma, M., Matsui, T., Hurtt, G.C., Lamarque, J.-F, Meinshausen, M., Smith, S., Roose, S., 2011. The representative concentration pathways: an overview. Climatic Change, 109, 1-2:5-31
- Vara-Prasad, V., Boote K. y Allen, L., 2006. Adverse high temperature effects on pollen viability, seed-set, seed yield and harvest index of grain-sorghum Sorghum bicolor (L.) Moench are more severe at elevated carbon dioxide due to higher tissue temperatures. Agricultural and Forest Meteorology 139: 237-251.
- Vellinga, M., Wood, R., 2002. Global climatic impacts of a collapse of the Atlantic thermohaline circulation. Climatic Change 54: 251-267.

- Vidale, P. L., D. Lüthi, C. Frei, S. I. Seneviratne, and C. Schär, Predictability and uncertainty in a regional climate model, Journal Geophysical Reserach, 108(D18), 4586, doi:10.1029/2002JD002810, 2003.
- Villalobos, F. Mateos, L., Orgáz, F., Ferres, E., 2002. Fitotecnia: Bases y tecnologías de la producción agrícola, Ed. Mundiprensa, España. 496 p.
- Von Hardenberg, J., Ferraris, L., Rebora, N., & Provenzale, A. (2007). Meteorological uncertainty and rainfall downscaling. Nonlinear Processes in Geophysics, 14(3), 193-199.
- Von Storch, H. 1999., On the Use of ‘‘Inflation’’ in Statistical Downscaling. Journal of Climate 12:3505-3506.
- Von Storch, H., Langenberg, H., Feser, F. 2000. A Spectral Nudging Technique for Dynamical Downscaling Purposes. Monthly Weather Review 128:364 -3771.
- Warton, D. I., Weber, N. C. 2002. Common slope tests for bivariate errors in variables models. Biometrical Journal 44,2:161-174. Warton, D.I., Wright, i.j., Falster, D.S., Westoby, M., 2006. Bivariate line-fitting methods for allometry.Biological Reviews 81, 2:259-291
- Watson D. F., Philip G. M., 1984. Triangle based interpolation. Mathematical Geology. 16, 8: 779-795. DOI: 10.1007/BF01036704
- Watterson, I.G. 1996, Non-Dimensional Measures Of Climate Model Performance . International Journal of Climatology 16: 379-391 (1996)
- Weaver, A., Zwiers, F., 2000. Uncertainty in climate change. Nature 407:571-572.
- Webb L. B., P. H. Whetton, and E. W. R. Barlow. 2007. Modelled impact of future climate change on the phenology of winegrapes in Australia. Austr. J. Grape Wine Res. 13: 165-175.
- White, J., Hoogenboomb, G., Kimball B., Wall, G. 2011. Methodologies for simulating impacts of climate change on crop production. Field Crops Research 124,3: 357-368.
- Wilby, R. 1998 Statistical downscaling of daily precipitation using daily airflow and seasonal teleconnection indices. Climate Research 10: 163–178, 1998
- Wilby, R. L., Wigley, T. M. L., 1997. Downscaling general circulation model output: A review of methods and limitations, Progress in Physical Geography 214: 530-548.
- Wilby, R. L., Wigley, T. M. L., 2000. Precipitation predictors for downscaling: observed and general circulation model relationships. International Journal of Climatology 20: 641–661
- Wilby, R., 2001. Downscaling summer rainfall in the UK from North Atlantic ocean temperatures. Hydrology and Earth System Sciences, 5(2): 245-257.
- Wilby, R., C.E. Zorita, B. Timbal, P. Whetton, L. Mearns, 2004. Guidelines for use of Climate Scenarios developed from Statistical downscaling Methods. Supporting

Material of the Intergovernmental Panel on Climate Change. Technical Report. The IPCC Data Distribution Centre, Norwich, UK, 27 pp

- Wilby, R., Conway D., Jones., P., 2002. Prospects for downscaling seasonal precipitation variability using conditioned weather generador parameters. Hydrology Processes 16: 1215–1234.
- Wilby, R.L., C.W. Dawson and E.M. Barrow, 2002. SDSM - a decision support tool for the assessment of regional climate change impacts, Environmental Modelliing & Software17: 147–159Wilks, 1992. Adapting stochastic weather generation algorithms for climate change studies. Climatic Change 22, 1: 67-84
- Wilks, D. S., Wilby, R. L. 1999. The weather generation game: a review of stochastic weather models. Progress in Physical Geography 23,3:329-357.
- Wilks, D., 2006. Statistical Methods in Atmospheric Science. Second Editions, Elsevier. U.S.A. 634 pp
- Wille, C., L. Kutzbach, T. Sachs, D. Wagner, and E. Pfeiffer. 2008. Methane emission from Siberian arctic polygonal tundra: eddy covariance measurements and modeling. Glob. Change Biol. 14: 1395-1408.
- Williams, D. W., H. L. Andris, R. H. Beede, D. A. Luvisi, M. V. K. Norton, and L. E. Williams. 1985. Validation of a model for the growth and development of the Thompson Seedless grapevine. II. Phenology. Am. J. Enol. Vitic. 36: 283-289.
- Wolfe, D., Schwartz, M., Lakso, A., Otsuki, Y., Pool, R., Shaulis, N., 2005. Climate change and shifts in spring phenology of three horticultural woody perennials in northeastern USA. International Journal of Biometeorology 49: 303-309.
- Wong, M. T. F., Asseng, S. 2000. Determining the causes of spatial and temporal variability of wheat yields at sub-field scale using a new method of upscaling a crop model. Plant and Soil 283, 1,2: 203-215.
- Wood, G., M. A. Oliver, and R. Webster. 1990. Estimating soil salinity by disjunctive kriging. Soil Use and Management 6,3: 97-104
- Wu, Chunlei, Ruediger Anlauf, and Youhua Ma, 2013. Application of the DSSAT Model to Simulate Wheat Growth in Eastern China. Journal of Agricultural Science. 5,2:98-208
- Xiong W., Conway, D., Lin, E., Colman, I., 2009. Potential impacts of climate change and climate variability on China's rice yield and production. Climate Research 40: 23–35.
- Yamamura K., Yokozawa, M., Nishimori, M., Ueda, Y., Yokosuka, T., 2006. How to analyze long-term insect population dynamics under climate change: 50-year data of three insect pests in paddy fields, Population Ecology. 48:31-48.
- Yarnal, B., Comrie, A., Frakes, B.,Brown, D., 2001. Developments and prospects in synoptic climatology, International Journal of Climatology 21:1923-1950.
- Yuval, Hsieh, W., 2003. An Adaptive Nonlinear MOS Scheme for Precipitation Forecasts Using Neural Networks. Weather and Forecasting 18:303-310.

- Zagar, M., Pristov1, N., Rakovec, J. A., 2004. Diagnostic method for high-resolution precipitation prediction using dynamically adapted vertical velocities. Meteorology and Atmospheric Physics. 85:187–204.
- Zhang, Q., H. Liu, H. Chen, Q. Li, and Z. Zhang, 2008. A Precise and Adaptive Algorithm for Interharmonics Measurement Based on Iterative DFT. Power Delivery IEEE Transac. 23 (4), 1728 – 1735
- Zhang, T., Zhu, J., Yang, X., 2008. Non-stationary thermal time accumulation reduces the predictability of climate change effects on agriculture. Agricultural and Forest Meteorology 148:1412 – 1418.Zhang, X., 2005. Spatial downscaling of global climate model output for site-specific assessment of crop production and soil erosion. Agricultural and Forest Meteorology 135: 215-229.
- Zhang, Y., Xu, Y., Dong, W., Cao, L., Sparrow, M., 2006, A future climate scenario of regional changes in extreme climate events over China using the PRECIS climate model, Geophysical Research Letter, 33, L24702
- Ziska, L., Bunce, J., 2007. Predicting the impact of changing CO_2 on crop yields: some thoughts on food. New Phytologist 175: 607-618.
- Zorita, E., 2000. Predicción global y regional del clima. Revista de la Real Academia de Ciencias, Madrid. 38 p.
- Zorita, E., Von Storch, H., 1999. The Analogue Method as a Simple Statistical Downscaling Technique: Comparison with More Complicated Methods. Journal of Climate 12: 2475-2489.